International Atomic Energy Agency

INDC(CCP)-42/U

INDC INTERNATIONAL NUCLEAR DATA COMMITTEE

USSR State Committee on the Utilization of Atomic Energy

Nuclear Data Centre

# NUCLEAR CONSTANTS

NO. 9

Translated by

the International Atomic Energy Agency

Vienna, August 1974

IAEA NUCLEAR DATA SECTION, KÄRNTNER RING 11, A-1010 VIENNA

INDC(CCP)-42/U

USSR State Committee on the Utilization of Atomic Energy

Nuclear Data Centre

# NUCLEAR CONSTANTS

NO. 9

Translated by

the International Atomic Energy Agency

Vienna, August 1974

## Foreword

This translation of the 9th Issue of "Nuclear Constants" contains only those articles which are directly pertinent to nuclear data measurements. Articles 9 to 14 are not planned to be translated by the IAEA. The first article of this report has been translated earlier and was released as INDC(CCP)-26/U in September 1972.

Contents Page

Chapter I. Nuclear physics constants



---

* The first article of this report has been translated earlier and released as INDC(CCP)-26/U in September 1972.

(Vol. 9, pp 34-43)

# RE-EVALUATED NUCLEAR CONSTANTS FOR THE ENERGY 0.0253 eV

G.B. Morogovsky

In 1970-71 two programmes for processing nuclear data (SIGMA and NYPF) were written in FORTRAN at the Nuclear Energy Institute (NEI) of the Byelorussian SSR Academy of Sciences and run on a Minsk-22 digital computer. The first programme was designed for obtaining recommended values of the standard parameters $\sigma_f$, $\sigma_a$, $\sigma_\gamma$, $\eta$, $\nu$ and $\alpha$ for a fissionable nucleus and the second for calculating standard values for the four nuclei $^{233}U$, $^{235}U$, $^{239}Pu$ and $^{252}Cf$ simultaneously using the correlations between them. The results of the calculations performed with the two programmes are presented in Tables 1 and 2.

Table 1 contains nuclear parameter values obtained with the SIGMA programme on the basis of initial data presented by Hanna in Ref. [1], and deviations from the values suggested by him. The observed deviations of the calculated values from Hanna's results indicate a correlation between the parameters of the different nuclei.

Table 2 contains the results of calculations performed with the NYPF programme and values of $\nu$ recommended by other authors. The calculated values are lower than the recommended ones, which is in line with the way in which fission yield values (number of neutrons per fission) are tending to change.

Table 1

Results obtained with the SIGMA programme on the basis of Hanna's initial data

| | $U^{233}$ | $U^{235}$ | $Pu^{239}$ | $Pu^{241}$ |
|---|---|---|---|---|
| I | 2 | 3 | 4 | 5 |
| $\eta$ | 2,289±0,0079 (+0,23%)* | 2,0738±0,0078 (±0,09%) | 2,1102±0,0089 (±0,08%) | 2,1513±0,0130 (±0,11%) |
| $\nu$ | 2,4958±0,0086 (±0,37%) | 2,4266±0,0091 (±0,15%) | 2,8704±0,0127 (-0,33%) | 2,9438±0,0250 (±0,33%) |
| $\sigma_f$ | 529,15±2,48 (-0,27%) | 580,98±1,90 (±0,13%) | 742,97±3,07 (±0,18%) | 1010,3±3,2 (±0,30%) |

* Percentage deviation from Hanna's final data ($\frac{\text{NEI-Hanna}}{\text{Hanna}} \times \%$).

Table 1 (continued)

| I | 2 | 3 | 4 | 5 |
|---|---|---|---|---|
| $\sigma_a$ | 576,78±2,69 (-0,14%) | 679,82±2,21 (+0,19%) | 1010,31±4,17 (-0,23%) | 1382,5±3,2 (+0,52%) |
| $\alpha$ | 0,09002±0,00036 (+1,72%) | 0,17012±0,00052 (+0,43%) | 0,36022±0,00610 (-1,55%) | 0,3684±0,0096 (+0,82%) |
| $\sigma_\gamma$ | 47,64±0,31 (±1,36%) | 98,83±0,45 (±0,54%) | 267,64±1,93 (-1,35%) | 372,19±2,6 (±1,11%) |

Table 2

Comparison of the results of NYPF calculations with values recommended by other authors

| $\nu(U^{233})$ | $\nu(U^{235})$ | $(Pu^{239})\nu$ | $(Cf^{252})\nu$ | |
|---|---|---|---|---|
| 2,505 ± 0,012 | 2,438 ± 0,011 | 2,901±0,018 | | [2] |
| 2,502 ± 0,014 | 2,434 ± 0,019 | 2,89 ±0,05 | | [3] |
| 2,504 ± 0,008 | 2,442 ± 0,006 | 2,898±0,011 | 3,779±0,010 | [4] |
| 2,494 ± 0,009 | 2,430 ± 0,008 | 2,871±0,014 | 3,772±0,015 | [5] |
| 2,4866± 0,0069 | 2,4229±0,0066 | 2,8799±0,0090 | 3,765±0,012 | [1] |
| 2,4544± 0,0026 | 2,4093±0,0019 | 2,8590±0,0027 | 3,7333±0,0038 | *) |

*) The present work (1971).

REFERENCES


[1] HANNA, G.C., et al., Atom. Energy Rev. 7 (1969) 4.

[2] SJOSTRAND, N.G., STORY, J.S., Neutron Data for Reactor Design, Ch. 4, U.K.A.E.A., rep. AEEW-M 125 (1961).

[3] LEONARD, B.R., Neutron Physics (YEATER, M.L., Ed.), Academic Press (1962).

[4] SHER, R., FELBERBAUM, J., Least Squares Analysis, USAEC rep. BNL-918 (1965).

[5] WESTCOTT, C.H., et al., Atom. Energy Rev. 3 (1965) 2.

# ABSOLUTE MEASUREMENTS OF α FOR $^{235}U$ and $^{239}Pu$ IN THE NEUTRON ENERGY RANGE 10 keV-1 MeV

V.N. Kononov, E.D. Poletaev, Yu.S. Prokopets
A.A. Metlev, Yu.Ya. Stavissky

The ratio of the radiative capture and fission cross-sections of $^{235}U$ and $^{239}Pu$ was measured using a pulsed Van-de-Graaff accelerator and the time-of-flight method in the neutron energy range 10 keV-1 MeV. The capture and fission events were recorded by a liquid scintillation detector with a volume of 400 litres. The capture and fission events were identified by recording fission neutrons after slowing-down and absorption in cadmium. In the neutron energy range 10-80 keV, the experiment was performed on the basis of the continuous spectrum of neutrons from the reaction $^{7}Li(p,n)^{7}Be$, the energy of the neutrons being measured by the time-of-flight method. At higher energies, the experiment was performed using mono-energetic neutrons. The method used for measuring the values of α is an absolute one. In the experiments, metallic $^{239}Pu$ samples with a thickness of $2.9 \times 10^{21}$ nuclei/cm$^2$ and $^{235}U_3O_8$ samples with a thickness of $4.1 \times 10^{21}$ $^{235}U$ nuclei/cm$^2$ were used.

The main experimental results relating to the value of α for $^{235}U$ and $^{239}Pu$ are presented in Tables 1 and 2. The tables also contain the mean-square error of the energy dependence of α (including only the statistical error) and the total mean-square error in the values of α.

Table 1

Values of α for $^{235}U$ obtained in the present work

| $E_n$ (keV) | α | $\sigma_\alpha$ (due to curve shape) | $\sigma_\alpha$ (total error) |
|---|---|---|---|
| 12,4 ± 0,7 | 0,549 | 0,043 | 0,057 |
| 13,4 ± 0,8 | 0,476 | 0,061 | 0,069 |
| 14,3 ± 0,8 | 0,457 | 0,040 | 0,051 |
| 15,4 ± 0,9 | 0,531 | 0,032 | 0,048 |
| 15,9 ± 1,0 | 0,452 | 0,030 | 0,043 |
| 16,4 ± 1,0 | 0,424 | 0,031 | 0,042 |
| 16,9 ± 1,1 | 0,365 | 0,032 | 0,041 |
| 17,4 ± 1,1 | 0,350 | 0,026 | 0,036 |
| 17,9 ± 1,2 | 0,394 | 0,033 | 0,043 |
| 18,5 ± 1,2 | 0,398 | 0,024 | 0,036 |
| 19,1 ± 1,3 | 0,370 | 0,020 | 0,033 |
| 19,8 ± 1,4 | 0,338 | 0,029 | 0,038 |
| 20,4 ± 1,4 | 0,317 | 0,024 | 0,033 |
| 21,1 ± 1,5 | 0,307 | 0,020 | 0,030 |
| 21,9 ± 1,6 | 0,337 | 0,034 | 0,042 |
| 22,7 ± 1,7 | 0,339 | 0,021 | 0,031 |
| 23,5 ± 1,8 | 0,344 | 0,021 | 0,032 |
| 24,3 ± 1,9 | 0,336 | 0,013 | 0,030 |
| 25,3 ± 2,0 | 0,283 | 0,017 | 0,026 |
| 26,2 ± 2,0 | 0,268 | 0,019 | 0,027 |
| 27,3 ± 2,2 | 0,292 | 0,014 | 0,025 |
| 28,4 ± 2,4 | 0,312 | 0,016 | 0,027 |
| 29,5 ± 2,5 | 0,333 | 0,017 | 0,029 |
| 30,7 ± 2,7 | 0,346 | 0,019 | 0,031 |
| 32,1 ± 2,8 | 0,350 | 0,019 | 0,031 |
| 33,4 ± 3,0 | 0,342 | 0,018 | 0,030 |
| 34,9 ± 3,2 | 0,350 | 0,017 | 0,030 |
| 36,5 ± 3,4 | 0,340 | 0,020 | 0,031 |
| 38,2 ± 3,7 | 0,346 | 0,019 | 0,031 |
| 40,0 ± 3,9 | 0,332 | 0,019 | 0,030 |
| 42,0 ± 4,2 | 0,335 | 0,019 | 0,030 |
| 44,1 ± 4,6 | 0,308 | 0,011 | 0,025 |
| 46,3 ± 4,9 | 0,307 | 0,016 | 0,027 |

Table 1 (continued)

| $E_n$ (keV) | α | $\sigma_\alpha$ (due to curve shape) | $\sigma_\alpha$ (total error) |
|---|---|---|---|
| 48,8 ± 5,3 | 0,030 | 0,017 | 0,027 |
| 51,4 ± 5,7 | 0,285 | 0,016 | 0,026 |
| 54,3 ± 6,2 | 0,288 | 0,018 | 0,027 |
| 57,4 ± 6,8 | 0,277 | 0,015 | 0,025 |
| 60,8 ± 7,4 | 0,292 | 0,013 | 0,025 |
| 90 ± 15 | 0,307 | 0,020 | 0,030 |
| 135 ± 25 | 0,247 | 0,015 | 0,024 |
| 185 ± 15 | 0,218 | 0,010 | 0,019 |
| 300 ± 10 | 0,181 | 0,011 | 0,018 |
| 400 ± 10 | 0,183 | 0,010 | 0,018 |
| 500 ± 10 | 0,150 | 0,006 | 0,014 |
| 750 ± 30 | 0,127 | 0,011 | 0,012 |
| 900 ± 30 | 0,101 | 0,010 | 0,014 |
| 1100 ± 30 | 0,077 | 0,009 | 0,013 |

Table 2

Values of α for $^{239}$Pu obtained in the present work

| $E_n$ (keV) | α | $\sigma_\alpha$ (due to curve shape) | $\sigma_\alpha$ (total error) |
|---|---|---|---|
| 9,4 ± 0,5 | 0,502 | 0,079 | 0,085 |
| 10,4 ± 0,5 | 0,508 | 0,058 | 0,067 |
| 11,3 ± 0,6 | 0,572 | 0,041 | 0,055 |
| 12,2 ± 0,7 | 0,517 | 0,068 | 0,076 |
| 13,1 ± 0,7 | 0,538 | 0,077 | 0,084 |
| 14,2 ± 0,8 | 0,478 | 0,037 | 0,048 |
| 15,2 ± 0,9 | 0,418 | 0,054 | 0,061 |
| 15,9 ± 1,0 | 0,366 | 0,038 | 0,045 |
| 16,4 ± 1,0 | 0,342 | 0,042 | 0,049 |
| 16,8 ± 1,1 | 0,331 | 0,032 | 0,040 |
| 17,3 ± 1,1 | 0,325 | 0,028 | 0,037 |
| 17,9 ± 1,2 | 0,329 | 0,030 | 0,038 |
| 18,4 ± 1,2 | 0,316 | 0,026 | 0,035 |
| 19,2 ± 1,3 | 0,328 | 0,031 | 0,039 |
| 19,6 ± 1,4 | 0,340 | 0,025 | 0,034 |
| 20,3 ± 1,4 | 0,352 | 0,032 | 0,040 |
| 20,9 ± 1,5 | 0,346 | 0,021 | 0,032 |

Table 2 (continued)

| $E_n$ (keV) | $\alpha$ | $\sigma_\alpha$ (due to curve shape) | $\sigma_\alpha$ (total error) |
|---|---|---|---|
| 21,6 ± 1,6 | 0,369 | 0,018 | 0,030 |
| 22,4 ± 1,7 | 0,348 | 0,015 | 0,029 |
| 23,2 ± 1,7 | 0,346 | 0,022 | 0,033 |
| 24,0 ± 1,8 | 0,320 | 0,018 | 0,029 |
| 24,8 ± 1,9 | 0,316 | 0,015 | 0,027 |
| 25,8 ± 2,0 | 0,330 | 0,022 | 0,032 |
| 26,7 ± 2,2 | 0,302 | 0,017 | 0,027 |
| 27,8 ± 2,3 | 0,293 | 0,015 | 0,026 |
| 28,8 ± 2,4 | 0,282 | 0,021 | 0,030 |
| 30,0 ± 2,6 | 0,247 | 0,011 | 0,022 |
| 31,2 ± 2,7 | 0,258 | 0,011 | 0,022 |
| 32,5 ± 2,9 | 0,272 | 0,012 | 0,024 |
| 33,9 ± 3,1 | 0,286 | 0,016 | 0,026 |
| 35,3 ± 3,3 | 0,260 | 0,015 | 0,025 |
| 36,9 ± 3,5 | 0,260 | 0,009 | 0,022 |
| 38,6 ± 3,4 | 0,243 | 0,011 | 0,022 |
| 40,4 ± 4,0 | 0,247 | 0,014 | 0,024 |
| 42,3 ± 4,3 | 0,240 | 0,010 | 0,021 |
| 44,3 ± 4,6 | 0,225 | 0,007 | 0,020 |
| 46,5 ± 4,9 | 0,213 | 0,006 | 0,019 |
| 48,9 ± 5,3 | 0,207 | 0,009 | 0,020 |
| 51,4 ± 5,7 | 0,193 | 0,007 | 0,018 |
| 54,2 ± 6,2 | 0,176 | 0,008 | 0,018 |
| 57,2 ± 6,7 | 0,174 | 0,007 | 0,018 |
| 60,4 ± 7,3 | 0,170 | 0,005 | 0,017 |
| 64 ± 8,0 | 0,172 | 0,006 | 0,017 |
| 110 ± 20 | 0,149 | 0,007 | 0,015 |
| 150 ± 25 | 0,115 | 0,010 | 0,016 |
| 185 ± 15 | 0,090 | 0,009 | 0,015 |
| 300 ± 10 | 0,103 | 0,012 | 0,018 |
| 400 ± 10 | 0,075 | 0,009 | 0,015 |
| 500 ± 10 | 0,082 | 0,010 | 0,015 |
| 750 ± 30 | 0,071 | 0,009 | 0,015 |
| 900 ± 30 | 0,032 | 0,006 | 0,012 |
| 1000 ± 30 | 0,008 | 0,013 | 0,017 |

# RELATIVE YIELDS OF DELAYED NEUTRONS FROM URANIUM-238 FISSION BY NEUTRONS WITH ENERGIES IN THE RANGE 3.9-5.1 MeV

B.P. Maksyutenko, Yu.F. Balakshev, G.I. Volkova

After a metallic $^{238}U$ sample weighing 30 g had been irradiated for 300 seconds, the decay curves of the delayed neutrons were recorded for 1024 seconds with a channel width of one second. The neutrons were obtained by the reaction $D(d,n)^3He$ from a titanium-deuterium target (thickness 1 mg/cm$^2$; diameter 45 mm) using a KG-2.5 accelerator.

A series of 30 measurements was summed over the channels so as to obtain one decay curve for a given energy of the fission-inducing neutrons. For each energy two such decay curves were obtained, each being treated separately. The decay curves were expanded by the least-squares method for specified half-life values [1].

Table 1 contains the relative yields of groups of delayed neutrons together with the mean-square errors obtained from the scatter of the curves for the two series. Fig. 1 shows the variation in the ratio of the group yields with changes in the energy of the neutrons inducing fission. The figures above each curve are the numbers of the groups whose yield ratio is described by the curve in question. The lines drawn through the points are arbitrary, for no rule has been established for the variation in yields and the yield of any group except the first one is the sum of the contributions of many precursors. It can be seen that the variations amount to ~ 20-30% and exceed the experimental errors.

## REFERENCE

[1] KEEPIN, J.R., Physics of nuclear kinetics (1965).

Table 1

Relative yields of delayed neutrons from $^{238}U$ fission by fast neutrons

| Group number | $E_n$ / $T_{I/2}$ | Relative yields | | | | |
|---|---|---|---|---|---|---|
| | | 3,9 MeV | 4,2 MeV | 4,5 MeV | 4,8 MeV | 5,I MeV |
| I. | 52,38 | I,0 | I,0 | I,0 | I,0 | I,0 |
| 2. | 2I,58 | 9,24 ± 0,I4 | 8,72 ± 0,06 | 9,29 ± 0,32 | I0,48 ± 0,06 | 8,0 ± 0,2 |
| 3. | 5,00 | I4,37 ± 0,7I | I2,23 ± 0,23 | I2,50 ± 0,47 | I4,5 ± 0,I | II,4 ± 0,9 |
| 4. | I,93 | 43,0 ± 3,7 | 38,6 ± 4,8 | 3I,6 ± 4,6 | 44,53 ± 0,05 | 37,4 ± 4,8 |

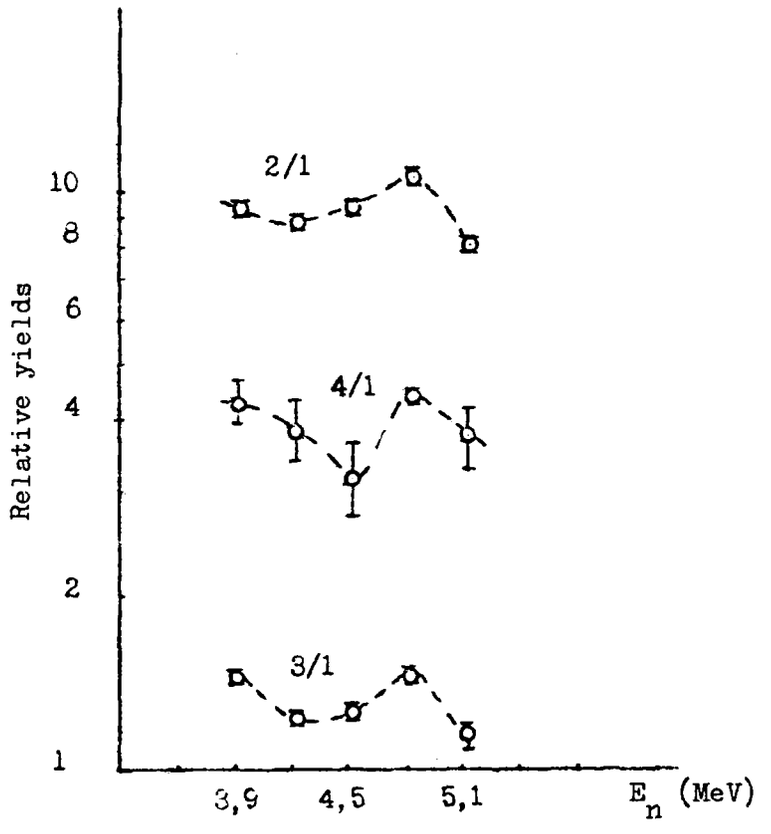


Fig. 1. Relative yields of delayed neutrons.

# EXPERIMENTAL CROSS-SECTIONS FOR NUCLEAR REACTIONS INVOLVING NEUTRONS WITH ENERGIES OF ABOUT 14 MeV

G.N. Maslov, F. Nasyrov, N.F. Pashkin

The authors present the results of measurements - performed for various isotopes - of cross-sections for (n,n') and (n,2n) reactions and for reactions accompanied by the escape of charged particles. In the case of nitrogen and oxygen, the total cross-sections for the reactions were found.

Most of the cross-sections were measured by a relative method, the reaction $^{65}Cu(n,2n)^{64}Cu$ being used as a standard; cross-sections of 920 $\pm$ 20 mbarn and 960 $\pm$ 20 mbarn were assumed for this reaction in the case of neutrons with energies of 14.2 MeV and 14.6 MeV respectively [1, 2]. The reactions were recorded by the activation method.

The activated materials were of natural isotopic composition (metal foils or thin pellets made from powder). The activity of the irradiated materials was determined by using a gamma spectrometer with a single NaI(Tl) crystal 80 x 80 mm in diameter to measure the intensity of the gamma radiation in the photopeaks. The sensitivity of the spectrometer to gamma photons of different energies was determined using gamma sources of known strength.

The measurement results are presented in Table 1, which also shows the gamma yields assumed in the experiments. For the standard reaction, a yield of 38% was assumed for gamma photons with an energy of 0.51 MeV [3]. The cross-section for the Pb(n,2n) reaction for a natural mixture of isotopes was determined by measuring neutron transmission through spherical lead envelopes.

Some reactions led to the formation of isomeric pairs with isomeric transitions to the ground state, which was determined by the half-life of the isotope whose yield was being studied. In all cases the activities were recorded over a period sufficiently long for transition of the nuclei from the metastable to the ground state. The authors thus measured the cumulative cross-section for the formation of nuclei in the ground state.

Total cross-sections for reactions in air, nitrogen and oxygen were measured using neutrons with an energy of 14.1 ± 0.1 MeV:

1638 ± 35 mbarn (dry air);

1614 ± 40 mbarn (nitrogen);

1696 ± 50 mbarn (oxygen).

The cross-sections were found from the attenuation of the neutron flux by the gaseous medium. The measurements were performed in a "good" geometry using a collimated neutron beam. Attenuation of the neutron flux was recorded by activation detectors based on the reactions $^{63}Cu(n,2n)^{62}Cu$ and $^{65}Cu(n,2n)^{64}Cu$.

REFERENCES

[1] Neutron Cross-Sections, BNL-325, Vol. II A, Second Edition, Supplement No. 2, 1966.

[2] GUZZOOREA, P., PERILLE, E., NOTARRIGO, S., Best-fits for some standard neutron-induced reaction cross-sections around 14 MeV, INFN/BE-67/13, 1967. Instituto Nazionale di Fisica Nucleare.

[3] LEDERER, C. Michael, HOLLANDER, J.M., Table of Isotopes, Sixth Edition, 1968.

Table 1

Experimental cross-sections for nuclear reactions involving neutrons with energies of 14.2 ± 0.2 MeV and 14.6 ± 0.2 MeV

| Reaction | $T_{1/2}$ | $E_\gamma$ (MeV) | Gamma yield (%) | σ (mbarn) | |
|---|---|---|---|---|---|
| | | | | 14,2 MeV | 14,6 MeV |
| 1 | 2 | 3 | 4 | 5 | 6 |
| $Na^{23}(n,2n)Na^{22}$ | 2,62 г | 1,275 | 100 | 21,1±2,2 | 37,4±4,0 |
| | | 0,51 | 180 | | |
| $Ti^{46}(n,2n)Ti^{45}$ | 3,09 ч | 0,51 | 170 | 12,7±1,3 | - |
| $Cr^{52}(n,2n)Cr^{51}$ | 27,8 д | 0,332 | 9 | 347±30 | 543±50 |
| $Mn^{55}(n,2n)Mn^{54}$ | 303 д | 0,835 | 100 | - | 866±65 |
| $Fe^{54}(n,\alpha)Cr^{51}$ | 27,8 д | 0,32 | 9 | - | 106±7 |
| $Co^{59}(n,p)Fe^{59}$ | 45,6 д | 1,095 | 56 | - | 64±7 |
| | | 1,292 | 44 | | |
| $Ni^{58}(n,p)Co^{58}$ | 71,3 д | 0,810 | 99 | - | 382,27 |
| $Ni^{58}(n,np)+$ $(n,d)Co^{57}$ | 270 д | 0,122 | 87 | 658±55 | 812±57 |
| | | 0,136 | 11 | | |
| $Ni^{60}(n,p)Co^{60}$ | 5,263 г | 1,173 | 100 | 179±20 | - |
| | | 1,332 | 100 | | |
| $Ni^{61}(n,p)Co^{61}$ | 99 м | 0,067 | 89 | - | 144±15 |
| $Ni^{62}(n,p)Co^{62}$ | 13,9м | 1,17 | 180 | 12,5±1,5 | 13,5±1,4 |
| $Cu^{65}(n,\alpha)Co^{60}$ | 5,263 г | 1,173 | 100 | - | 53,5 ±6,0 |
| | | 1,332 | 100 | | |
| $Cu^{65}(n,p)Ni^{65}$ | 2,564 ч | 1,115 | 16 | 29,2±3,0 | 31,2±3,2 |
| | | 1,481 | 25 | | |
| $Mo^{92}(n,2n)Mo^{91}$ | 15,49 м | 0,51 | 188 | 152 ±16 | - |
| $Mo^{100}(n,2n)Mo^{99}$ | 66,7 ч | 0,140 | 90 | 1920±140 | - |
| $J^{127}(n,2n)J^{126}$ | 12,8 д | 0,386 | 34 | 1950±200 | - |
| | | 0,667 | 33 | | |
| $Cs^{133}(n,2n)Cs^{132}$ | 6,59 д | 0,668 | 99 | 1755±180 | - |
| $W^{182}(n,2n)W^{181}$ | 140 д | рентген Та | 100 | 2050±400 | - |
| $Au^{197}(n,2n)Au^{196}$ | 6,18 д | 0,333 | 25 | 2243±160 | - |
| | | 0,356 | 94 | | |
| $Pb^{204}(n,n')Pb^{204m}$ | 66,9 м | 0,90 | 189 | 84,8±9,0 | 76,2±8,0 |
| $Pb^{204}(n,2n)Pb^{203}$ | 52,1 ч | 0,279 | 81 | 1950±140 | 2130 ±150 |
| $Pb^{206}(n,\alpha)Hg^{203}$ | 46,9 д | 0,279 | 77 | 0,527±0,070 | 0,673±0,070 |
| $Pb^{208}(n,p)Tl^{208}$ | 3,10 м | 2,614 | 100 | - | 1,26 ±0,20 |
| Pb (n,2n) | — | — | — | 2240 ±170 | - |

Key

| | | | | | |
|---|---|---|---|---|---|
| г | = | years | ч | = | hours |
| д | = | days | м | = | min. |

# EXCITATION FUNCTIONS FOR THE REACTIONS $^{27}Al(n,\alpha)^{24}Na$ AND $^{27}Al(n,p)^{27}Mg$

Yu.A. Nemilov, Yu.N. Trofimov

The literature contains many accounts of work in which cross-sections for reactions induced by 14 MeV neutrons were measured with fair accuracy. However, comparatively few cross-section determinations have been made at other neutron energies, and the results of different authors often diverge considerably [2, 1]. In view of the importance of knowing these cross-sections for fast reactor calculations, the authors measured the cross-sections for the reactions $^{27}Al(n,\alpha)^{24}Na$ and $^{27}Al(n,p)^{27}Mg$ by the activation method in the neutron energy range 7.7-9.3 MeV.

Mono-energetic neutrons from the reaction $^{2}H(d,n)^{3}He$ were obtained using the Radium Institute's cyclotron, which accelerates deuterons to 6.6 MeV. Thin layers of deuterium-saturated zirconium or titanium were used as targets. The neutron energies were varied by varying the angles of exposure of the samples. The aluminium targets were in the shape of discs 10 mm in diameter and 100 μm thick. The samples were placed at a distance of 45 mm from the centre of the neutron source.

The irradiation time varied within the range 0.5-1.5 hours. The beam current was 1-2 μA. By a system of diaphragms, the deuterons were collimated to a spot 3 mm in diameter. The non-uniformity of the neutron energies - due to slowing-down of the deuterons in the zirconium layer and to differences in the neutron escape angles caused by the finite dimensions of the source and target - was about 0.3 MeV.

The induced beta activity was measured in a $4\pi$ proportional, methane-filled flow counter. Particular attention was paid to the purity of the target, which was controlled by checking that activities with other half-lives were not present. Specific activity determinations were performed by irradiating aluminium samples of different thicknesses simultaneously. The specific activity was determined by extrapolation to zero thickness.

The fast neutron flux was measured using an ionization fission chamber with a $^{238}U$ layer. The amount of uranium in the chamber was found by alpha-counting.

In determining the neutron flux, we introduced a correction for the neutron background. For this purpose, a tungsten target with a zirconium layer not saturated with deuterium was introduced into the beam. The correction varied between 10% and 60%, depending on the angle of exposure of the sample. The neutrons from the break-up of deuterons by deuterons - the reaction $^{2}H(d,np)^{2}H$ - could not be taken into account in these measurements, so that the corresponding correction had to be made by computational means. The neutrons from this reaction are distributed over the energy range 1-3 MeV and do not participate in the reaction $^{27}Al(n,\alpha)^{24}Na$, the threshold of which is 3.25 MeV. In this energy region, the cross-sections for the reaction $^{27}Al(n,p)^{27}Mg$ (threshold 1.87 MeV) are less than or of the order of 1 mbarn [4]. As - at the energies in question - the number of neutrons from the deuterium break-up reaction is only 5% of the total number, it is safe to say that these neutrons do not make an appreciable contribution to the activity of $^{27}Mg$. When estimating the neutron flux, however, it is necessary to introduce a correction for these neutrons. The number of $^{238}U$ fission events is proportional to the product of the fission cross-section and the neutron intensity. The cross-section for fission by the break-up neutrons has the following appearance:

$$\bar{\sigma}_f = \frac{\int^{E_{max}} \sigma_f \cdot \sigma H^2(d,np) H^2 \cdot dE}{\int^{E_{max}} \sigma H^2(d,np) H^2 \cdot dE}$$

The correction to the fission event count to allow for the break-up neutrons is found from the relation

$$\varepsilon = \frac{\bar{\sigma}_f \int^{E_{max}} \sigma H^2(d,np) H^2 \cdot dE \cdot 100}{\bar{\sigma}_f \int^{E_{max}} \sigma H^2(d,np) H^2 \cdot dE + \sigma_f \cdot \sigma H^2(d,p) He^3} \quad \text{(in \%)}$$

Using the results of Granberg et al. [5], we find that the correction was $5 \pm 1\%$ in the case under consideration. The overall mean expected error is made up of the following measurement errors:

| | | |
|---|---|---|
| 1. | The inaccuracy in determining the weight of the $^{238}U$ | 1.5% |
| 2. | The uncertainty in the $^{238}U$ cross-section value | 3% |
| 3. | The statistical error in the fission event count | 2% |
| 4. | The inaccuracy in determining the efficiency of counting the activity of the $^{24}Na$ and $^{27}Mg$ in the aluminium target | 3% |

5. The error introduced by the inaccuracy in determining the neutron background 3%

6. The statistical error in determining the sample count rate 1%

7. Errors associated with inaccuracies in taking into account the geometric conditions of the experiment 1%

The mean square error is estimated by us at 6%; in certain less favourable cases it is as high as 10%.

The measurement results, together with the corresponding errors, are presented in Table 1. The excitation function curves obtained by us and those known from the literature are shown in Figs 1 and 2. Our results for the reaction $^{27}Al(n,p)^{27}Mg$ are in good agreement with the measurement results reported in Ref. [4]. For the reaction $^{27}Al(n,\alpha)^{24}Na$, the cross-section values found by us are close to the results of Butler et al. [3] and somewhat higher than those of Lisken et al. [1] and Grundl et al. [6].

Table 1

| $E_n$ | $\sigma_{n\alpha}$ $^{27}Al(n,\alpha)^{24}Na$ | $\sigma_{np}(n,p)^{27}Mg$ |
|---|---|---|
| (MeV) | (mbarn) | (mbarn) |
| 9.3 | 82 ± 6 | 92 ± 8 |
| 9.05 | 78 ± 7 | 98 ± 9 |
| 8.6 | 77 ± 8 | 92 ± 10 |
| 8.0 | - | 75 ± 8 |
| 7.7 | 43 ± 5 | - |

REFERENCES

[1] LISKEN, H., PAULSEN, A., "Compilation of cross-sections for some neutron-induced threshold reactions" EURATOM, 1961.

[2] ABAGYAN, L.P., ZAKHAROVA, S.M., Cross-sections for neutron reactions accompanied by the escape of charged particles (in Russian), Bulletin of the Information Centre for Nuclear Data, Issue 2, Atomizdat (1965).

[3] BUTLER, J.P., SANTRY, D.C., Can. J. Phys. 41, 372 (1963).

[4] Neutron Cross-sections, BNL-325, 1958.

[5] GRANBERG, L., ARMSTRONG, A.H., HENKEL, R.L., Phys. Rev. 104, 1639 (1956).

[6] GRUNDL, J.A., HENKEL, R.L., PERKINS, B.L., Phys. Rev. 109, 425 (1958).

[7] SCHMITT, H.W., HALPERIN, Y., Phys. Rev. 121, 827 (1961).

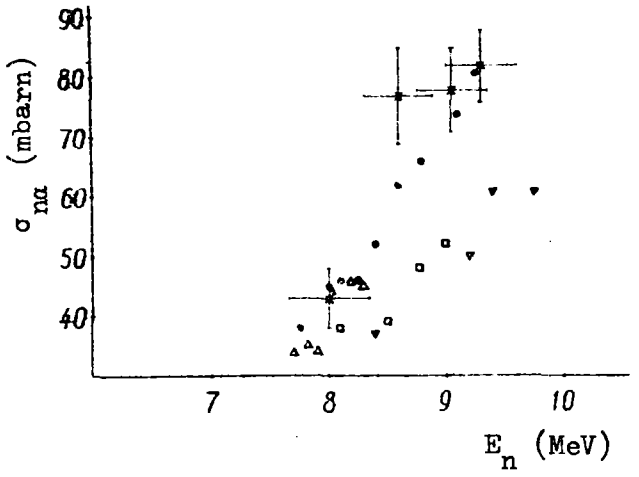


Fig. 1 Reaction excitation function

- Present paper
- Ref. [3]
- Ref. [6]
- Ref. [7]
- Ref. [1]

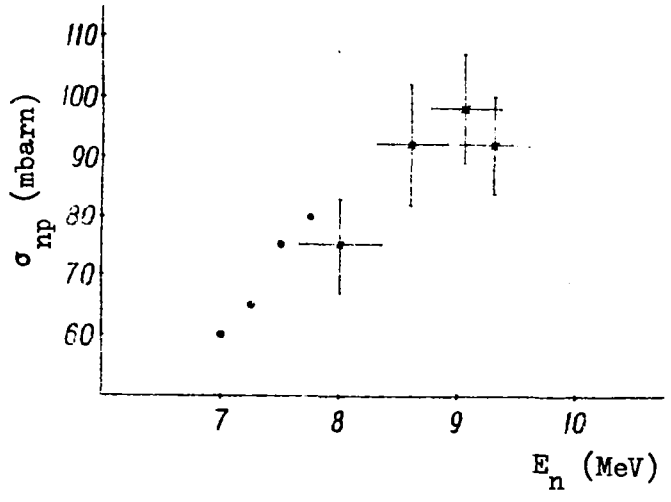


Fig. 2 Reaction excitation function

- Present paper
- Ref. [4]

# POLARIZATION AND ANGULAR DISTRIBUTION OF RESONANT NEUTRONS

E.M. Saprykin, A.A. Lukyanov

## 1. Introduction

The polarization, or a definite orientation, of the spin of a neutron relative to its direction of motion occurs in nuclear reactions as a result of a strong dependence of the interaction potential on the spin state of the colliding particles. Neutron polarization in nuclear reactions is usually associated with the presence of a spin–orbital interaction. In this case, the differential cross-section for the reaction depends on the orientation of the spin vector relative to the orbital momentum vector, which leads to polarization of the reaction products, for neutrons with one spin direction scatter more readily through certain angles while those with another spin direction scatter more readily through other angles.

In principle, study of the interaction of polarized particles with oriented nuclei enables one to determine the corresponding nuclear reaction parameters which characterize the interaction potential for the different spin states of the colliding particles (or the reaction products), whereas the use of unpolarized particles gives only averages over every kind of spin state.

Let us define the problem more precisely. A given bombarding particle a' and a nucleus A' form an overall system in one of its possible states $\alpha'$. It is assumed that the disintegration of this system leaves a particle a and a residual nucleus A in one of the possible states $\alpha$. For the sake of definiteness we shall assume that in both cases the small letters denote the lighter particles. The entire discussion will be conducted in the non-relativistic approximation, although many conclusions can be applied without modification to the relativistic case. This approximation is a valid one when the kinetic energy of the particles is less than a few per cent of their potential energy.

Actual calculations are best performed for a fixed energy; accordingly, the steady-state formalism of scattering theory is used. It is also assumed that the law of parity conservation holds.

Having made these assumptions, let us consider the following problem. If the polarizations of the particles a' and A' are given, what will be the polarizations of the particles a and A? The usual formulation of a nuclear reaction

problem consists in a comparison of the parameters characterizing the colliding particles before the reaction with the corresponding parameters for the reaction products. In classical mechanics, these parameters include the co-ordinates and momenta of the particles before and after collision and certain variables characterizing the internal state of the particles. In a quantum-mechanical description, the states of a system of particles before and after interaction are specified by corresponding sets of quantum numbers. In the steady-state consideration of a reaction involving only two particles in the initial and final states, the intensity of (or cross-section for) the reaction is characterized by the amplitude of the probability of transition from an initial state (entrance channel) with a definite set of quantum numbers to some final state (reaction channel) with corresponding quantum numbers. It is assumed that for any pair of nuclei there is some final distance $r_o$ between the nuclei constituting the pair such that with greater distances neither nucleus is affected by any polarized potential fields produced by the other nucleus. We shall apply the word "channel" to every kind of two-particle system state characterized by a definite set of quantum numbers in a situation where the particles are separated by a distance exceeding $r_o$. What quantum numbers define a channel?

There are two ways of describing the relative motion of particles. One is to use a representation in which states are represented by plane waves, each of which propagates in a definite direction, usually characterized by the wave vector $\vec{K}$. In this case, the quantum numbers characterizing the relative motion of the particles are the vector modulus $\vec{K}, |\vec{K}| = K$ (which is associated with the energy of relative motion of the particles and is therefore included in the assembly of quantum numbers denoted by the single subscript $\alpha$) and a unit vector in the direction of propagation - $\vec{n}_K = \vec{K}/K$.

A plane wave contains all the moments of momentum of relative motion. This representation is therefore more convenient when a large number of partial waves, corresponding to specific moments of momentum of relative motion, play a part in reactions in which only a small range of angles around the direction of an incident beam is involved.

The other way is to use a representation in which a state has a specific moment of relative motion $\ell$ and its projection $m_\ell$, but covers the entire range of angles.

The first representation is normally used to describe the relative motion of particles in the entrance channel of a reaction. Actually, experiments usually

involve particles of fixed energy which, moving along some axis from the source, hit a target. Thus, the momentum of the particles is known, whereas the orbital momentum is not determined.

The second representation is convenient for describing the relative motion of particles in reaction channels, for only a small number of angular momenta contribute to the reaction cross-section if the energies of the incident particles are relatively low.

If the colliding particles have non-zero spin (for example, particle a' has spin i' and projection $m_i'$, while particle A' has spin I' and projection $m_I'$), the spin state of such a system of particles can be characterized by a wave function dependent on i', I', $m_i'$ and $m_I'$. It is sometimes convenient to use another representation. Instead of i', I', $m_i'$ and $m_I'$, the channel spin s' and its projection $m_s'$ are introduced, so that the spin state of the system is characterized in the new representation by wave functions dependent on s' and $m_s'$. The channel spin s is a vector sum of the spins i' and I'. $\vec{s} = \vec{i}' + \vec{I}'$ and can assume values $(I'-i') \leqslant s' \leqslant I' + i'$. We shall use both these representations.

Thus, the entrance channels can be characterized by, for example, the following subscripts:

$\alpha'$ - the type of particles in a pair and their internal state,

$\ell'$ - the magnitude of the vector of the orbital momentum of relative particle motion,

s' - the magnitude of the channel spin,

$m_\ell'$ and $m_s'$ - the projections of the corresponding momenta on the z axis.

For a reaction channel we use a set of subscripts without primes:

$$c \equiv \{\alpha \ell s m_\ell m_s\} \quad \text{or} \quad \{\alpha \ell i I m_i m_I\}$$

Besides these quantum numbers, the system of colliding particles is characterized, both in the entrance channel and in the exit channel of a reaction, by those quantities which are conserved in the reaction (integrals of motion). They are the total momentum of the system $J = (\vec{J}) = (\vec{\ell}' + \vec{s}') = (\vec{\ell} + \vec{s})$, its projection M, parity $\pi$, the total energy E and the total linear momentum $\vec{P}$ of the system*/.

---

*/ In some applications, isotopic spin is also used as an integral of motion.

Further discussion will be conducted in the centre-of-mass system. Thus, the total linear momentum of the system is excluded from consideration as it is by definition equal to zero in this system.

The cross-section for the process $\alpha' \ell' s' \to \alpha \ell s$ for given values of the integrals of motion $J, \pi$ and E is characterized by elements of the scattering matrix $S_{\alpha \ell s}(J, \pi, E)$, the general properties of which - symmetry and unitarity - follow from basic physical principles (conservation of the probability flux, time reversibility and causality)*/.

A matrix element of the $S(J, \pi, E)$ matrix can be represented in the form [1]:

$$S_{c'c} = e^{-i\varphi_{c'}} \left( \delta_{c'c} + i \sum_{\lambda} \frac{\Gamma_{\lambda c'}^{1/2} \Gamma_{\lambda c}^{1/2}}{E_\lambda + \Delta_\lambda - E - i\Gamma_\lambda/2} \right) e^{-i\varphi_c}, \qquad (1.1)$$

where the parameters of the formalism are: $\varphi_{c'}$ and $\varphi_c$ the phases of potential scattering; $\Gamma_{\lambda c'}$ and $\Gamma_{\lambda c}$ - the widths of the $\lambda$ level for the $\{\alpha' \ell' s'\}$ and $\{\alpha \ell s\}$ channels respectively; $\Gamma_\lambda$ - the total width of the $\lambda$ level; $E_\lambda$ - the energy of the $\lambda$ level; and $\Delta_\lambda$ - the displacement of the $\lambda$ level (the sum over $\lambda$ includes levels only of a given set of J and $\pi$).

Another relation for the S-matrix elements is given by the R-matrix theory of Wigner and Eisenbud [24];

$$S_{c'c}(J, \pi, E) = e^{-i\varphi_{c'}} \left\{ \delta_{c'c} + 2i P_{c'}^{1/2} \left[ (1 - RL)^{-1} R \right]_{c'c} P_c^{1/2} \right\} e^{-i\varphi_c}, \qquad (1.2)$$

where

$$R_{c'c}(J, \pi, E) = \sum_{\lambda(J,\pi)} \frac{\gamma_{\lambda c'} \gamma_{\lambda c}}{E_\lambda - E} \qquad (1.3)$$

Here, $2P_c \gamma_{\lambda c}^2$ is the partial width of decay of the $\lambda$ level in a channel with $(\alpha \ell s)$, $P_c$ is the penetrability, $L_c = S_c - b_c + iP_c$, and $S_c - b_c$ is the displacement factor for the boundary condition $b_c$.

---

*/ The S-matrix elements are a quantitive characteristic of the reaction intensity and do not depend on the projections of the momenta; otherwise, their magnitude would change when the system of co-ordinates was rotated.

In the single-channel case, by representing $R(J,\pi,E)$ in the form of the sum $R = R_0 + R_1$ (where $R_0$ includes the non-resonance part of the R-matrix and $R_1$ includes the resonantly energy-dependent part), the function $S(J,\pi,E)$ can be reduced to the form:

$$S(J,\pi,E) = e^{-2i\delta(J,\pi,E)} \times \frac{1 - R_1(J,\pi,E)\bar{L}^*}{1 - R_1(J,\pi,E)\bar{L}} \qquad (1.4)$$

where

$$\delta(J,\pi,E) = \varphi_c(E) - \operatorname{arc\,tg} \frac{P_c R_0(J,\pi,E)}{1 - (S_c - B_c) R_0(J,\pi,E)}$$

$$\bar{L}_c = L_c (1 - R_0 L_c)^{-1}.$$

The general approach to analysing the polarization and the angular distribution of reaction products consists primarily in expressing the corresponding cross-sections in terms of S-matrix elements, without specifying their explicit form; only in application to specific examples does the need arise to use a parametric representation for the S-matrix. This one-to-one link between cross-sections and S-matrix elements characterizes the kinematics of a nuclear reaction.

## 2. Wave functions in the external region

The wave function of a system of nucleons satisfies the Schrödinger equation. For a definite channel "C", the total wave function can be written as the product of four wave functions:

$$\Phi_{\alpha i I m_i m_I}(\vec{r}) = \varphi_\alpha \psi_\alpha(\vec{r}) \chi_{i m_i} \chi_{I m_I} , \qquad (2.1)$$

where

$\varphi_\alpha$ is a wave function describing the internal state and the type of the colliding particles (internal variable particles),

$\psi_\alpha(\vec{r})$ is a wave function describing the relative motion of particles in the centre-of-mass system,

$\chi_{i m_i}$ and $\chi_{I m_I}$ are wave functions describing the spin states of the particles a and A respectively.

The functions introduced above are orthonormalized. The orthonormality of the $\Phi_\alpha$ functions with respect to the subscripts $\alpha$ and $\alpha'$ in the event that these subscripts correspond to different particle types is a consequence of the spatial non-overlapping of the corresponding functions. When, on the other hand, the subscripts $\alpha$ and $\alpha'$ correspond to different excited states of the same particles, orthonormality is then a consequence of the usual orthonormality of wave functions corresponding to different energy states of a specified system. The $\chi_{im_i}$ wave functions are eigenfunctions of the operators $\hat{i}^2$ and $\hat{i}_z$. They are column matrices containing $(2i + 1)$ elements and satisfy the following orthonormality relation:

$$\chi^{+}_{im_i}\,\chi_{im'_i} = \delta_{m_i m'_i} \,. \tag{2.2}$$

The same applies to the $\chi_{Im_I}$ functions.

2.1. Channel spin wave functions

In the channel C, the particle interaction potential is by definition independent of the relative orientation of spins i and I of particles a and A, so that there is degeneration with respect to their projections. For the same reason it is possible to take a linear combination of the products of wave functions describing the spin state of particles a and A as the wave function describing the spin state of the channel. Such linear combinations are selected in such a way that the wave function has a specified channel spin value as quantum number:

$$\chi_{Sm_s} = \sum_{m_i m_I} (i\,I\,m_i\,m_I \,|\, S\,m_s)\,\chi_{im_i}\,\chi_{Im_I} \,. \tag{2.3}$$

The coefficients $(iIm_i m_I \,|\, sm_s)$ are Clebsch-Gordan coefficients (vector sum coefficients; see Annex 1). The channel spin wave functions are orthonormalized:

$$\chi^{+}_{s'm'_s}\,\chi_{sm_s} = \delta_{s's}\,\delta_{m'_s m_s} \,, \tag{2.4}$$

This is a consequence of the unitarity of the vector sum coefficients (see expression A.1.5). It should also be noted that, as there are no polarized potentials in the channel, the channel spin s is an integral of motion in the channel.

Under time reversal conditions, the wave functions considered by us behave as follows:

$$\hat{K}\,\chi_{sm_s} = (-1)^{s-m_s}\,\chi_{s-m_s}\,. \qquad (2.5)$$

The operator $\hat{K}$ is a time reversal operator [23]. The reversal property (2.5) follows from expression (2.3) if $\chi_{im_i}$ and $\chi_{Im_I}$ behave in the same way as $\chi_{sm_s}$ under time reversal conditions.

2.2. Wave functions of relative motion

As the interaction in a channel is described only by central potentials (the Coulomb potential plus the centrifugal potential), the orbital momentum $\ell$ is an integral of motion in the channel $\{a\ell s\}$. Thus, the angular dependence of the wave functions of relative motion is factorized in the form of the functions $i^{\ell}Y_{\ell m_\ell}$, which are eigenfunctions of the operators of the orbital momentum and of its projection $m_\ell$. The $Y_{\ell m_\ell}$ functions are ordinary normalized spherical functions satisfying the relation:

$$Y^{*}_{\ell m_\ell} = (-1)^{m_\ell}\,Y_{\ell\,-m_\ell}\,. \qquad (2.6)$$

Under time reversal conditions, the functions $i^{\ell}Y_{\ell m}$ behave like the $\chi_{sm_s}$ functions:

$$\hat{K}\left(i^{\ell}Y_{\ell m_\ell}\right) = (-1)^{\ell-m_\ell}\,Y_{\ell\,-m_\ell}\,i^{\ell}\,. \qquad (2.7)$$

The total wave functions of relative motion can be represented in the form:

$$\Psi^{\ell}_{\alpha}(\vec{r}) = \frac{1}{r}\,U_{\alpha\ell}(r)\,(i^{\ell}Y_{\ell m}),$$

where the functions $U_{a\ell}$ are a solution of Schrödinger's radial equation. The solutions of Schrödinger's radial equation in the central potential, corresponding to converging and diverging waves, have the form [24]:

$$\begin{aligned} I_{a\ell} &= (G_{a\ell} - iF_{a\ell})\exp i\omega_{a\ell} \\ O_{a\ell} &= (G_{a\ell} + iF_{a\ell})\exp -i\omega_{a\ell} \end{aligned} \qquad (2.8)$$

where $F_{a\ell}$ and $G_{a\ell}$ are respectively the regular and singular solutions of Schrödinger's radial equation. Here and below we use the following notation:

E - energy of relative motion of the particles constituting a pair,

$m_\alpha = m_a m_A/(m_a + m_A)$ - reduced mass,

$k_\alpha = \sqrt{2m_\alpha}|E|/\hbar^2$ - wave number,

$v_\alpha = \hbar k_\alpha/m_\alpha$ - relative velocity,

$\eta_\alpha = Z_a Z_A e^2/\hbar v_\alpha$ - Coulomb field parameter,

$\sigma_{\alpha\ell} = \arg\Gamma(1 + \ell + i\eta_{\alpha\ell})$ - Coulomb phase shift,

$\rho_\alpha = k_\alpha r$, $\omega_{\alpha\ell} = \sigma_{\alpha\ell} - \sigma_{\alpha 0} = \sum_{n=1}^{\ell} \operatorname{arc\,tg}(\eta_\alpha/n)$.

When there is no Coulomb field ($\eta_\alpha = 0$),

$$F_{\alpha\ell} = \left(\frac{\pi\rho_\alpha}{2}\right)^{1/2} J_{\ell+1/2}(\rho_\alpha), \quad G_{\alpha\ell} = \left(\frac{\pi\rho_\alpha}{2}\right)^{1/2} J_{-\ell-1/2}(\rho_\alpha) \tag{2.9}$$

the asymptotic form of the functions $I_{\alpha\ell}$ and $O_{\alpha\ell}$ corresponding to converging and diverging spherical waves when $\rho_\alpha \gg 1$ [24]:

$$I_{\alpha\ell} \sim \exp[-i(\rho_\alpha - \pi\ell/2)], \quad O_{\alpha\ell} \sim \exp i(\rho_\alpha - \pi\ell/2). \tag{2.10}$$

## 3. Amplitude of the reaction

In experiments, particles of a particular kind and with a fixed energy usually hit the target as they move along the z axis. Thus the momentum of a particle is assumed to be known. In view of the finite size of the source, it is impossible to attribute a fixed orbital momentum to a particle. Consequently, in the entrance channel it is best to select a wave function of relative motion in the form of a plane wave. If the system of co-ordinates is selected in this way, the scattering angles coincide with the angles determining the direction of propagation of the scattered beam. To simplify the notation, when characterizing the entrance and exit channels we shall omit $\vec{h}_{K'}$ and $\vec{h}_{K'}$, remembering, however, that it is they which define the scattering angles. We represent the total wave function in the entrance channel $\alpha's'$ in the form:

$$\Phi_{\alpha's'} = \varphi_{\alpha'} e^{iK'_\alpha z} \chi_{s'm_{s'}} \tag{3.1}$$

It should be noted that for the channel $\alpha's'$ it is possible to introduce one particular spin orientation $m_{s'}$, although all other orientations are possible for the incoming particle. This can be done because different values give

independent non-coherent contributions to the cross-sections. The plane wave $e^{ik'_\alpha z}$ can be series-expanded in the $Y_{\ell_0}$ functions. The asymptotic form of this expansion (for $\rho_{\alpha'} \gg 1$) has the form [2]:

$$e^{ik'_\alpha z} \simeq \frac{\sqrt{\pi}}{\rho_{\alpha'}} \sum_{\ell'=0}^{\infty} i^{\ell'+1}(2\ell'+1)^{1/2}\left[e^{-i(\rho_{\alpha'}-\ell'\pi/2)} - e^{+i(\rho_{\alpha'}+\ell'\pi/2)}\right]Y_{\ell 0}(\vec{r}') \qquad (3.2)$$

where the exponential terms correspond to converging and diverging spherical waves. As already mentioned, the total momentum J of the system, its projection on the direction of the incident beam, and parity $\pi$ are conserved in the reaction. When characterizing a reaction by the value of the total momentum J, it is therefore convenient to go over to the operator eigenfunctions $\hat{J}^2$ and $\hat{J}_z$, which have the sense of generalized spherical functions:

$$\mathcal{G}_{\ell s J M} = \sum_{m_\ell m_s} (\ell s m_\ell m_s | J M)(i^\ell Y_{\ell m_\ell})\chi_{s m_s}, \qquad (3.3)$$

where $(\ell s m_\ell m_s \mid JM)$ are vector sum coefficients. By virtue of the orthogonality of these coefficients:

$$i^\ell Y_{\ell m_\ell}\chi_{s m_s} = \sum_{JM} (\ell s m_\ell m_s | JM)\mathcal{G}_{\ell s J M}, \qquad (3.4)$$

or, in our case,

$$i^{\ell'} Y_{\ell' 0}\chi_{s' m_{s'}} = \sum_J (\ell' s' 0 m_{s'} | J m_{s'})\mathcal{G}_{\ell' s' J m_{s'}}. \qquad (3.5)$$

The sum over M has vanished, for the coefficient $(\ell' s' 0 m_{s'} \mid JM)$ is non-zero only when $m_{s'} = M$. The wave function of the initial state in the channel can, with allowance for expression (3.5), be reduced to the form:

$$\Phi_{\alpha' s'} = \varphi_{\alpha'} \frac{\sqrt{\pi}}{\rho_{\alpha'}} \sum_{\ell'=0}^{\infty} \sum_{J=|\ell'-s'|}^{\ell'+s'} i^{\ell'}(2\ell'+1)^{1/2}(\ell' s' 0 m_{s'} | J m_{s'}) \times \qquad (3.6)$$
$$\times \mathcal{G}_{\ell' s' J m_{s'}}\left[e^{-i(\rho_{\alpha'}-\ell'\pi/2)} - e^{i(\rho_{\alpha'}+\ell'\pi/2)}\right]$$

For some definite set $J, M, \pi$ (in our case $M = m_{s'}$), the fullest representation of the wave function in the exit channel $\alpha s$ can be written in the form of an expansion in the functions $\mathcal{G}_{\ell s J m_s}$:

$$\Phi_{\alpha s}^{J m_s' \pi} = \varphi_\alpha \frac{1}{r} \sum_{\ell=|J-s|}^{J+s} G_{\ell s J m_s'} \left\{ A_{\alpha \ell s}^{J m_s' \pi} e^{-i(\delta_\alpha - \pi\ell/2)} - B_{\alpha \ell s}^{J m_s' \pi} e^{i(\delta_\alpha + \pi\ell/2)} \right\}, \tag{3.7}$$

where the amplitudes of the converging and diverging waves are linked through the scattering matrix

$$B_{\alpha \ell s}^{J m_s' \pi} = \sum_{\alpha' \ell' s'} S_{\alpha \ell s, \alpha' \ell' s'}^{J \pi} A_{\alpha' \ell' s'}^{J m_s' \pi} . \tag{3.8}$$

When the wave function is determined in this way, the coefficients A and B correspond to the probability amplitudes in respect of the particle flux. It should also be noted that the coefficients $S_{\alpha \ell s, \alpha' \ell' s'}^{J\pi}$ are independent of the projection of the total momentum $m_s$, [2].

Comparing the standard form of the wave function representation (3.7) with the plane wave expansion (3.6), we determine the amplitude of the converging wave:

$$A_{\alpha' \ell' s'}^{J m_s' \pi} = i \frac{\sqrt{\pi}}{k_{\alpha'}} (2\ell'+1)^{1/2} (\ell' s' 0 m_s' | J m_s') \delta_{\alpha \alpha'} \delta_{\ell \ell'} \delta_{s s'} \tag{3.9}$$

It should be noted that A is determined by expression (3.9) for the entrance channels ($\alpha' s' \ell'$). For the remaining channels ($\alpha \ell s$), A = 0. Thus, by substituting expression (3.9) into expression (3.8), we obtain:

$$B_{\alpha \ell s}^{J m_s' \pi} = i \frac{\sqrt{\pi}}{k_{\alpha'}} \sum_{\ell'=|J-s'|}^{J+s'} (\ell' s' 0 m_s' | J m_s') (2\ell'+1)^{1/2} S_{\alpha \ell s, \alpha' \ell' s'}^{J \pi} . \tag{3.10}$$

The asymptotic part of the wave function $\Phi_{\alpha s}(\vartheta, \varphi)$, which is connected with the diverging wave, is investigated experimentally. In order to obtain it, one must separate out of $\Phi_{\alpha s}$ the part which corresponds to the initial state:

$$\Phi_{\alpha s} = \sum_J \Phi_{\alpha s}^{J m_s \pi} = \Phi_{\text{inc.}} + \Phi_{\text{reac.}} \tag{3.11}$$

where $\Phi_{\text{inc}}$ is the incident plane wave (3.6). Thus, we obtain the asymptotic form $\Phi_{\text{reac.}}$ in reaction channel $\alpha s$ in the form:

$$\Phi_{reac}(\alpha s) = i\frac{\sqrt{\pi}\,\varphi_\alpha}{k_\alpha r}\sum_{Jee'}(\ell' s' 0 m_{s'}|J m_{s'})(2\ell'+1)^{1/2}\cdot \tag{3.12}$$
$$\times \exp i(\delta_\alpha - \ell\pi/2)\left[\delta_{\alpha\alpha'}\delta_{ee'}\delta_{ss'} - S^{J\pi}_{\alpha e s,\alpha' e' s'}\right] G_{esJm_{s'}}.$$

Expression (3.11) is a convenient one when the detector selects particles with total momentum J and its projection $m_{s'}$. However, it is usually particles moving at an angle $(\vartheta,\varphi)$ to the incident beam, the channel spin s and its projection $m_s$ which are recorded. In this case, the following form is more convenient:

$$\Phi_{reac}(\alpha s) = i\frac{\exp i\delta_\alpha}{r}\varphi_\alpha\sum_{m_s=-s}^{s} F^{\alpha' s' m_{s'}}_{\alpha s m_s}\chi_{s m_s}, \tag{3.13}$$

where

$$F^{\alpha' s' m_{s'}}_{\alpha s m_s} = \frac{\sqrt{\pi}}{k_\alpha}\sum_{J=0}^{\infty}\sum_{\ell=|J-s|}^{J+s}\sum_{\ell'=|J-s'|}^{J+s'}(2\ell'+1)^{1/2}(\ell' s' 0 m_{s'}|J m_{s'})\times \tag{3.14}$$
$$\times(\ell s m_\ell m_s|J m_{s'})\left[\delta_{\alpha\alpha'}\delta_{ee'}\delta_{ss'} - S^{J\pi}_{\alpha e s,\alpha' e' s'}\right] Y_{\ell m_\ell}(\vartheta,\varphi).$$

The square of the wave function (3.13) gives the flux of particles with given $(\alpha,s)$; the wave function in the entrance channel is normalized to unit flux. Thus, the reaction cross-section is:

$$d\sigma_{\alpha' s' m_{s'}\to\alpha s} = \left|\Phi_{reac}(\alpha s)\right|^2 r^2\, d\Omega\, dg \tag{3.15}$$

where g represents internal variables of the particles.

Using expression (3.13) and taking into account the orthogonality of the functions $\varphi_\alpha(g)$ and $\chi_{sm_s}$, we obtain:

$$d\sigma_{\alpha' s' m_{s'}\to\alpha s} = \sum_{m_s}\left|F^{\alpha' s' m_{s'}}_{\alpha s m_s}\right|^2 d\Omega. \tag{3.16}$$

As terms with different $m_s$ values make independent contributions to the cross-section, the quantity $F^{\alpha' s' m_{s'}}_{\alpha s m_s}$ - expression (3.14) - may be termed the "amplitude" of the reaction $\alpha' s' m_{s'} \to \alpha s m_s$. The cross-section for the reaction $\alpha' s' m_{s'} \to \alpha s m_s$ can be written in the form:

$$d\sigma_{\alpha' s' m_{s'} \to \alpha s m_s} = \left| F_{\alpha s m_s}^{\alpha' s' m_{s'}} \right|^2 d\Omega \qquad (3.17)$$

The reaction amplitude F, and consequently the reaction cross-section, depends on the angle $\varphi$, since the $m_{s'}$ and $m_s$ directions are fixed. The cross-section for the reaction $\alpha' s' \to \alpha s$ is obtained, without allowance for polarization, by averaging over the initial spin directions $m_{s'}$, and summing over the final spin directions $m_s$:

$$d\sigma_{\alpha' s' \to \alpha s} = \frac{1}{2s'+1} \sum_{m_s m_{s'}} d\sigma_{\alpha' s' m_{s'} \to \alpha s m_s}. \qquad (3.18)$$

Obviously, the same result can be obtained by averaging over $m_{s'}$ in expression (3.16). Lastly, the cross-section for the reaction $\alpha' \to \alpha$ can be obtained, without allowance for channel spin, by averaging over all possible s' states and summing over all possible s states:

$$d\sigma_{\alpha' \to \alpha} = \sum_{ss'} \frac{2s'+1}{(2I'+1)(2i'+1)} d\sigma_{\alpha' s' \to \alpha s}, \qquad (3.19)$$

where I'(I) and i'(i) are the spins of the nucleus and the particle before and after the reaction, and (2s' + 1) is the statistical weight of the channel.

The values of $F_{\alpha s m_s}^{\alpha' s' m_{s'}}$ for fixed $\alpha$ and $\alpha'$ constitute the matrix in the channel spin representation

$$F = \left\{ (s m_s | \hat{F} | s' m_{s'}) \right\} \qquad (3.20)$$

Taking expression (3.20) into account, one can write the cross-section (3.19) in the form:

$$d\sigma_{\alpha' \to \alpha} = \frac{1}{(2I'+1)(2i'+1)} Sp(FF^+) \, d\Omega, \qquad (3.21)$$

where $Sp(FF^+)$ is the sum of the diagonal elements of the matrix $(FF^+)$. In concluding this section, we would point out that the reaction amplitude may be regarded as some operator converting the wave function of the initial state into the wave function of the final state.

## 4. Scattering of partially polarized nucleons unpolarized nuclei

We shall therefore consider the scattering of particles with a spin of $\frac{1}{2}$ by nuclei with a spin of 1. The problem includes obtaining the differential cross-section for the process and the polarization of the scattered particles if the polarization of the incident particles is specified.

The mean value of the spin operator is termed "polarization by definition". It is obviously a vector quantity. If the wave function $\psi$ describing a given particle state is known, the polarization in this state can be calculated as

$$\langle \vec{\sigma} \rangle = \langle \psi | \vec{\sigma} | \psi \rangle \qquad (4.1)$$

In a real situation, however, an experimentally prepared beam cannot always be described by a definite wave function. In fact, when conducting experiments one does not usually know the spin projection of each particle or quantum numbers such as the channel spin and its projection. The quantum numbers for particles in an experimentally obtained beam are distributed with some probability. Moreover, the initial system may consist of several non-coherent sub-beams which are represented in the beam with certain weights.

In this case, it is possible to introduce a $\rho$-matrix such that the mean value of any physical quantity f acting in the spin space of the system, in a state corresponding to a mixed ensemble, is given by the expression

$$\langle f \rangle = \frac{Sp\, \rho \hat{f}}{Sp\, \rho} . \qquad (4.2)$$

1. It should be noted that the sum of the diagonal elements of the density matrix gives the intensity of the particle beam. Assuming that the intensity of the incident beam is unity, we obtain

$$Sp\, \rho_{inc} = 1 \qquad (4.3)$$

for the density matrix of the incident beam. The density matrix corresponding to the reaction products does not have a unit spur, for the intensity of the diverging beam is not unity. In this case, the spur of the density matrix gives the differential cross-section for the reaction:

$$S_p \rho_{out.} = d\sigma / d\Omega . \qquad (4.4)$$

2. It should also be noted that, when there is no coherence between particle spin states, the total density matrix of the system can be represented in the form of the product of the density matrixes for incident particles and target nuclei. The structure of the density matrix becomes clearest if it is expanded in base matrixes of spin space satisfying the following orthogonality and normalization condition:

$$S_p \omega^n \omega^m = \delta_{nm} (2J+1) \qquad (4.5)$$

In the case of particles with a spin of $\frac{1}{2}$, the system of base matrixes consists of a unit matrix and the Pauli two-dimensional matrixes $\omega_1 = 1$, $\omega_2 = \sigma_x$, $\omega_3 = \sigma_y$, $\omega_4 = \sigma_z$:

$$\rho = \sum_{n=1}^{4} A_n \omega^n , \qquad (4.6)$$

where the coefficients $A_M$ are defined as

$$A_n = \frac{1}{2J+1} S_p \rho \omega^n . \qquad (4.7)$$

As a result, we have

$$\rho = \frac{S_p \rho}{2J+1} \sum_n \langle \omega^n \rangle \omega^n , \qquad (4.8)$$

where

$$\langle \omega^n \rangle = \frac{S_p \rho \omega^n}{S_p \rho} \qquad (4.9)$$

Thus, the density matrix is expressed directly in terms of the experimentally measured mean values $\langle \omega^m \rangle$ of the base matrixes.

Accordingly, for particles with a spin of $\frac{1}{2}$

$$\rho = \frac{1}{2} S_p \rho \left(1 + \langle \vec{\sigma} \rangle \vec{\sigma}\right), \tag{4.10}$$

where

$$\langle \vec{\sigma} \rangle \equiv \frac{S_p \rho \vec{\sigma}}{S_p \rho} = \vec{P} \tag{4.11}$$

$\vec{P}$ being the "polarization vector".

We would point out that $Sp\rho = 1$ for incident particles, so that knowledge of the polarization vector completely determines the density matrix of the incident particles:

$$\rho = \frac{1}{2} \left(1 + \vec{p} \vec{\sigma}\right). \tag{4.12}$$

The density matrix for the unpolarized nuclei of the target is

$$\rho' = \frac{1}{2I+1} I_I, \tag{4.13}$$

Thus, the total density matrix of the system in the initial state is the product

$$\rho = \frac{1}{2(2I+1)} \left(1 + \vec{p} \vec{\sigma}\right) I_I. \tag{4.14}$$

As noted in section 2, for fixed $\alpha'$ and $\alpha$ the reaction amplitude $F^{\alpha' s' m_{s'}}_{\alpha s m_s}$ may be regarded as an operator converting the pure spin state $(s' m_{s'})$ of the entrance channel to the pure spin state $(s m_s)$ of the exit channel. The quantity $F \rho_{inc} F^+$ can then be identified with the density matrix of the spin states of the scattered beam:

$$\rho_{out} = F \rho_{inc} F^+. \tag{4.15}$$

The differential cross-section (4.4) is equal to

$$\frac{d\sigma}{d\Omega} = S_p \rho_{out} = S_p \left(F \rho_{inc} F^+\right) = \frac{1}{2(2I+1)} \left\{ S_p F F^+ + \vec{P}_{inc} S_p F \vec{\sigma} F^+ \right\} \tag{4.16}$$

In the case of an unpolarized beam of incident nucleons, $\vec{P}_{inc} = 0$,

$$\left(\frac{d\sigma}{d\Omega}\right)^{unpol.} = \frac{1}{2(2I+1)} S_p F F^+ \qquad (4.17)$$

Thus, expression (4.16) may be rewritten in the form

$$\frac{d\sigma}{d\Omega} = \left(\frac{d\sigma}{d\Omega}\right)^{unpol.} \left\{ 1 + \vec{P}_{inc} \frac{S_p (F \vec{\sigma} F^+)}{S_p F F^+} \right\} \qquad (4.18)$$

The mean value of the polarization vector in the exit channel is determined in accordance with expression (4.2) by the formula

$$\vec{P}_{out} = \langle \vec{\sigma} \rangle = \frac{S_p (\vec{\sigma} F F^+) + S_p \vec{\sigma} F \vec{P}_{inc} \vec{\sigma} F^+}{S_p F F^+ + S_p F \vec{P}_{inc} \vec{\sigma} F^+} . \qquad (4.19)$$

In the case of unpolarized incident nucleons

$$\left(\vec{P}_{out}\right)^{unpol.} = \frac{S_p (\vec{\sigma} F F^+)}{S_p F F^+} . \qquad (4.20)$$

The polarization vector $(\vec{P}_{out})^{unpol.}$ of the scattered unpolarized nucleons is a pseudovector (the mean value of the Pauli vector matrix). In the case of the scattering of an unpolarized beam of nucleons by unpolarized nuclei, this vector may be only a function of the relative momenta in the entrance ($\vec{k}'$) and exit ($\vec{k}$) channels. One can therefore write

$$\left(\vec{P}_{out}\right)^{unpol.} = \left|\left(\vec{P}_{out}\right)^{unpol.}\right| \vec{n} , \qquad (4.21)$$

where

$$\vec{n} = \frac{[\vec{k}' \times \vec{k}]}{|[\vec{k}' \times \vec{k}]|} \qquad (4.22)$$

Thus, with unpolarized nucleon scattering by unpolarized nuclei, the polarization vector is always non-perpendicular to the scattering plane.

Wolfenstein and Ashkin [25] have shown that, in the case of the elastic scattering of nucleons by unpolarized nuclei, owing to the invariance of

the scattering amplitude with respect to time reversal the following equality is satisfied:

$$S_p F \vec{\sigma} F^+ = S_p \vec{\sigma} F F^+ \qquad (4.23)$$

Taking into account expressions (4.23) and (4.20), it is possible to represent the differential cross-section expression (4.18) in the form

$$\frac{d\sigma}{d\Omega} = \left(\frac{d\sigma}{d\Omega}\right)^{\text{unpol.}} \left(1 + \vec{P}_{out}^{\,\text{unpol.}} \vec{P}_{inc}\right) \qquad (4.24)$$

From this it can be seen that the differential cross-section for the scattering of polarized particles depends on the angle $\varphi$. The coefficient determining the aximuthal asymmetry is $|\vec{P}_{out}^{\,\text{unpol.}} \vec{P}_{inc}| \leq 1$.

When calculating the matrix elements of the matrixes $F\vec{\sigma}F^+$, $F\vec{P}_{inc}\vec{\sigma}F^+$ and $\vec{\sigma}F\vec{P}_{inc}\vec{\sigma}F^+$ entering into expressions (4.16) and (4.19) for the polarization vector and differential cross-section respectively, it is convenient to switch to quantities defined as follows:

$$T(00) = S_p \rho$$
$$T(1\nu) = \frac{2}{\sqrt{3}} \langle \sigma_\nu \rangle S_p \rho, \qquad (4.25)$$

where $\sigma_\nu$ represents unreduced operators of the spin vector for particles with a spin of $\frac{1}{2}$:

$$\sigma_0 = \sigma_z, \quad \sigma_{\pm 1} = \mp (\sigma_x \pm i\sigma_y)/2 .$$

It can be seen from expression (4.25) that the quantities $T(q\ \nu)$ - $q = 0, 1$ and $\nu = -1, 0, 1$ - can be used for describing the differential cross-section and the polarization in nuclear reactions. Using the expression for $F^{\alpha' s' m_{s'}}_{\alpha s m_s}$, and also the fact that

$$\chi_{s m_s} = \sum_{m_i m_I} (1/2 I m_i m_I | s m_s)\, \chi_{1/2\, m_i}\, \chi_{I m_I}; \qquad (4.26)$$

$$\left(\chi_{1/2\, m} (\sigma_x + i\sigma_y) \chi_{1/2\, m'}\right) = \sqrt{\left(\tfrac{1}{2} + m\right)\left(\tfrac{1}{2} - m + 1\right)}\ \delta_{m', m-1}; \qquad (4.26)$$

$$\left(\chi_{1/2\, m} (\sigma_x - i\sigma_y) \chi_{1/2\, m'}\right) = \sqrt{\left(\tfrac{1}{2} - m\right)\left(\tfrac{1}{2} + m + 1\right)}\ \delta_{m'-1, m}; \quad (\chi_{1/2\, m} \sigma_z \chi_{1/2\, m'}) = m \delta_{m m'};$$

it is possible to obtain a general formula combining expressions (4.18) and (4.19) and giving for the $T(q\ \nu)$ value of the scattered beam an expression in terms of $T(q'\ \nu')$ for the incident beam [29]:

$$T(q\nu) = \sum (\tfrac{1}{2} q m_1 \nu | \tfrac{1}{2} m_1)(\tfrac{1}{2} I m_1 M_1 | S_1 \mu_1)(\tfrac{1}{2} I m_2 M_2 | S_2 \mu_2)(\tfrac{1}{2} I' m_1' M_1' | S_1' \mu_1') \times$$
$$\times (\tfrac{1}{2} I' m_2' M_2' | S_2' \mu_2') \frac{\sqrt{\pi}}{K'} \sqrt{2\ell_1'+1}\, (\ell_1' S_1' m_{\ell_1}' \mu_1' | J_1 M_{J_1})(\ell_1 S_1 m_{\ell_1} \mu_1 | J_1 M_{J_1}) \times$$
$$\times U^{J_1\pi_1}_{\alpha\ell_1 s_1, \alpha'\ell_1' s_1'} Y_{\ell_1 m_{\ell_1}} \delta_{m_{\ell_1}' 0} \times \frac{\sqrt{\pi}}{K'} \sqrt{2\ell_2'+1}\, (\ell_2' S_2' m_{\ell_2}' \mu_2' | J_2 M_{J_2})(\ell_2 S_2 m_{\ell_2} \mu_2 | J_2 M_{J_2}) \times \quad (4.27)$$
$$\times U^{J_2\pi_2}_{\alpha\ell_2 s_2, \alpha'\ell_2' s_2'} Y_{\ell_2 m_{\ell_2}} \delta_{m_{\ell_2}' 0} \frac{2q'+1}{2(2I+1)} (\tfrac{1}{2} q' m_1' \nu' | \tfrac{1}{2} m_1')\, T(q'\nu'),$$

where

$$U^{J\pi}_{\alpha\ell s, \alpha'\ell' s'} \equiv \delta_{\alpha\alpha'} \delta_{\ell\ell'} \delta_{ss'} - S^{J\pi}_{\alpha\ell s, \alpha'\ell' s'}, \quad (4.28)$$

Here, summation is over $m_1$, $m_2$, $M_1$, $M_2$, $m_1'$, $m_2'$, $M_1'$, $M_2'$, $s_1$, $s_2$, $s_1'$, $s_2'$, $\mu_1$, $\mu_2$, $\mu_1'$, $\mu_2'$, $J_1$, $\ell_1$, $\ell_1'$, $M_J$, $m_{\ell_1}$, $m_{\ell_1'}$, $J_2$, $\ell_2$, $\ell_2'$, $M_{J_2}$, $m_{\ell_2}$, $m_{\ell_2'}$, $q'$ and $\nu'$.

It is more convenient to calculate the final tensor moments with respect to the axes, which are oriented in a simple manner relative to the final direction. We select a new z axis along the $\vec{k}$ direction and a new y axis along the $[\vec{k}' \times \vec{k}]$ direction, where $\vec{k}'$ and $\vec{k}$ are the initial and final linear momenta respectively. The Euler angles for rotation of the co-ordinate axes will be $(\varphi, \vartheta, 0)$, where $\vartheta$ is the polar and $\varphi$ the azimuthal angle of scattering.

According to the definition (4.25), the $T(q\ \nu)$ quantities are transformed whenever the system is rotated by means of the Wigner matrixes $D^{q}_{m'm}$ [26]. Thus, $T(q\ \nu)$ in the new axes is associated with $T(q\ \nu)$ in the old axes by the relation

$$T(q\nu) = \sum_{\rho} \mathcal{D}^{q}_{\rho\nu}\, T(q\rho). \quad (4.29)$$

The spherical harmonics entering into expression (4.27) should henceforth be described in terms of Wigner D functions:

$$Y_{\ell m}(\theta,\varphi) = (-1)^m \left[\frac{4\pi}{2\ell+1}\right]^{-1/2} \mathcal{D}^{\ell}_{-m0}(\varphi,\theta,0),$$
$$\left(Y^{*}_{\ell m}(\theta,\varphi) = \left[\frac{4\pi}{2\ell+1}\right]^{-1/2} \mathcal{D}^{\ell}_{m0}(\varphi,\theta,0)\right),$$
$$\mathcal{D}_{0m}(\varphi,\theta,0) = \left[\frac{4\pi}{2\ell+1}\right]^{1/2} (-1)^m Y_{\ell m}(\theta,\varphi) = \left[\frac{4\pi}{2\ell+1}\right]^{1/2} Y^{*}_{\ell -m}(\theta,\varphi), \quad (4.30)$$
$$\left[\frac{4\pi}{2\ell+1}\right]^{1/2} Y_{\ell m}(\theta,\varphi) = i^{|m|+m} \left[(\ell-|m|)!\right]^{1/2} \left[(\ell+|m|)!\right]^{1/2} P_{\ell}^{|m|}(\cos\theta)\, e^{im\varphi}.$$

In this system of co-ordinates, expression (4.25) can be reduced to the form

$$T(qv) = (2k')^{-2} \sum_{q'v'} A(qv, q'v', \theta, \varphi) T(q'v') \qquad (4.31)$$

where

$$A(qv, q'v', \theta\varphi) = \sum B(l, s_1, l_2 s_2 qv; l' s_1' l_2' s_2' q'v'; L m_L m_L' J, J_z) \times \times U^{J,\pi_1}(\alpha l_1 s_1, \alpha' l_1' s_1') U^{*J_2\pi_2}(\alpha l_2 s_2 \alpha' l_2' s_2') \mathcal{D}^{L}_{m_L' m_L}, \qquad (4.32)$$

$$B = [(2q+1)2(2I'+1)]^{-1} \sum [4(2q+1)(2q'+1)]^{1/2} (-1)^{I+I'-i-i'-s_2-s_2'} \times$$

$$\times W(\tfrac{1}{2} s_1 \tfrac{1}{2} s_2; Iq) W(\tfrac{1}{2} s_1' \tfrac{1}{2} s_2'; I'q') \times \qquad (4.33)$$

$$\times G_v(J, l_1 s_1, L q J_2 l_2 s_2) G_{v'}(J, l_1' s_1', L q' J_2 l_2' s_2')$$

Here, the $G_v$ function is given by the expression

$$G_v(J, l_1 s_1, L q J_2 l_2 s_2) = [(2J_1+1)(2J_2+1)(2l_1+1)(2l_2+1)(2q+1)]^{1/2} \times$$

$$\times (-1)^{l_1} \sum_{l} (2l+1)(l_1 l_2 00|l0)(lq0v|Lv) X \begin{pmatrix} l & s & J_1 \\ l_2 & q & L \\ l_2 & s_2 & J_2 \end{pmatrix}. \qquad (4.34)$$

The coefficients of B contain a series summed over the magnetic quantum numbers. It should be noted that the T quantities contain all the information about the spin directions before and after the reaction, the B quantities introduce all the geometric information relating to the entire multiplicity of intermediate moments, and the A quantities yield all the information about the dynamics of the problem which is contained in the elements of the V-matrices. This convention was first used by Blatt and Biedenharn [2] to describe the angular distributions when unpolarized targets are bombarded by an unpolarized beam.

The resulting relations - relations (4.33) and (4.34) - contain the main results of Simon [4] with allowance for all the recognized phase and normalization errors. For the particular case q = 0, we obtain

$$G_0(J, l_1 s_1, L 0 J_2 l_2 s_2) = [(2J_1+1)(2J_2+1)(2l_1+1)(2s_1+1)]^{1/2} (-1)^{L+s_1-J_2} \delta_{s_1 s_2} \times$$

$$\times (l_1 l_2 00|L0) W(l_1 J_1 l_2 J_2; s_1 L) = (2s_1+1)^{1/2} \delta_{s_1 s_2} (-1)^{L+s_1-J_2} \times \qquad (4.35)$$

$$\times i^{-L+l_2-l_1} Z(l_1 J_1 l_2 J_2; s L).$$

For this case, the Racah coefficients entering into expression (4.33) have the form

$$W(\tfrac{1}{2} s_1 \tfrac{1}{2} s_2 I 0) = (-1)^{i-I+s_1} [2(2s_1+1)]^{-1/2} \delta_{s_1 s_2}. \qquad (4.36)$$

For the case q' = 0 (unpolarized entrance beam), we obtain

$$T(qv) = (2K)^{-2}\,[2(2I'+1)]\,[2/(2q+1)]^{1/2} \sum_{L} (-1)^{I-i+S_1'-S_2-J_2+L}\; i^{-L+\ell_1-\ell_2} \times$$
$$\times Z(\ell_1' J_1 \ell_2' J_2 S_1' L)\, W(\tfrac{1}{2} S_1 \tfrac{1}{2} S_2, I q)\, G_v(J \ell_1 S_1 L q J_2 \ell_2 S_2) \times \qquad (4.37)$$
$$\times \tfrac{1}{2}\left[U_1^* U_2 + (-1)^q U_1 U_2^*\right] \mathcal{D}^L_{0v}(\varphi, \theta, 0),$$

where the $D^L_{0\nu}$ quantities are expressed in terms of the spherical harmonics (4.30).

For the case q = 0, the general relation (4.31) has the form

$$T(00) \equiv \frac{d\sigma}{d\Omega} = (2K')^{-2}\,[2(2I'+1)] \sum_{L} (-1)^{I'-1/2+S_1-S_2'-J_2+L}\; i^{-L+\ell_1'-\ell_2'}$$
$$[2(2q'+1)]^{1/2}\, Z(\ell_1 J_1 \ell_2 J_2 S L)\, W(\tfrac{1}{2} S_1' \tfrac{1}{2} S_2' I q) \times \qquad (4.38)$$
$$\times G_v(J \ell_1' S_1' L q' J_2 \ell_2' S_2') \times \tfrac{1}{2}\left[U_1^* U_2 + (-1)^{q'} U_1 U_2^*\right] \mathcal{D}^L_{v'0}(\varphi, \theta, 0)\, T(q'v'),$$

and in the case q = q' = 0 (unpolarized entrance and exit beams) it has the form

$$T(00) = \frac{d\sigma}{d\Omega} = (2K')^{-2}\,[2\cdot(2I'+1)]^{-1} \sum (-1)^{S-S'}\; i^{\ell_1'-\ell_1+\ell_2-\ell_2'} \times \qquad (4.39)$$
$$\times Z(\ell_1 J_1 \ell_2 J_2 S L)\, Z(\ell_1' J_1 \ell_2' J_2 S' L)\, \tfrac{1}{2}\left[U_1^* U_2 + U_1 U_2^*\right] P_L(\cos\theta).$$

(For the sake of simplicity, whenever $s_1 = s_2$ or $s_1' = s_2'$, they are replaced by s or s').

Let us consider the case q = 1, q' = 0:

$$T(10) = (2K')^{-2} \frac{1}{2(2I'+1)} \sum (-1)^{I-1/2+S'-S_2-J_2-L}\; i^{-\ell_1'+\ell_2'-L} \times$$
$$\sqrt{2/3} \cdot Z(\ell_1' J_1 \ell_2' J_2 S' L)\, W(\tfrac{1}{2} S_1 \tfrac{1}{2} S_2 I 1)\, G_0(J \ell_1 S_1 L 1 J_2 \ell_2 S_2) \times \qquad (4.40)$$
$$\times \tfrac{1}{2}\left(U_1^* U_2 - U_1 U_2^*\right) P_L(\cos\theta)$$

As the definition of $G_\nu$ contains $(\ell q 0\nu / L\nu)$, it follows that

$$G_{-v}(J \ell_1 S_1 L q J_2 \ell_2 S_2) = (-1)^{\ell-L+q}\, G_v(J \ell_1 S_1 L q J_2 \ell_2 S_2),$$
$$\ell = \ell_1 + \ell_2 + 2n \;\rightarrow\; [(\ell_1 \ell_2 00 | L 0)]$$
$$\ell_1' + \ell_2' = L + 2n \;\rightarrow\; [Z(\ell_1' J_1 \ell_2' J_2 S' L)] \qquad (4.41)$$
$$\ell_1' + \ell_2' + \ell_1 + \ell_2 = 2n \;\rightarrow\; (\pi)$$

The multiplier in expression (4.41) is therefore $(-1)^q$ and

$$G_0(J \ell_1 S_1 L 1 J_2 \ell_2 S_2) = -G_0(J \ell_1 S_1 L 1 J_2 \ell_2 S_2) \equiv 0, \qquad (4.42)$$

Thus, T(10), which is determined by expression (4.40), is identically equal to zero. This means that, provided that the law of parity conservation is satisfied, there is no polarization along the direction of propagation of the scattered beam if the initial beam was not polarized.

Let us consider T(11) and T(1-1), which - in accordance with expression (4.25) - determine the "spiral polarization" of particles with a spin of $\frac{1}{2}$:

$$T(11)=T(1-1)=i(2k')^{-2}[2(2I'+1)]^{-1}\sum(-1)^{I-1/2+S'-S_2-J_2+L+\ell_1}$$
$$3^{-1/2}[6(2\ell_1+1)(2\ell_2+1)(2\ell_1'+1)(2\ell_2'+1)(2S_1+1)(2S_2+1)]^{1/2}$$
$$(2J_1+1)(2J_2+1)(2\ell+1)^{1/2}(\ell_1'\ell_2'00|L0)(\ell_1\ell_2 00|\ell 0)(\ell 101|L1)\times \qquad (4.43)$$
$$\times W(\ell_1'J_1\ell_2'J_2S'L)W(\tfrac{1}{2}S_1\tfrac{1}{2}S_2I1)\chi(\ell_1S_1J_1;\ell_1L;\ell_2S_2J_2)J_m U_1U_2^*[L(L+1)]^{1/2}P_L^1(\cos\theta)$$

It should be noted that $\ell$ can assume the values $\ell = L + 1$, L and L - 1. However, it follows from the condition for non-zero values of the coefficient $(\ell_1'\ell_2'00|L0)$ and from the law of parity conservation that $\ell_1' + \ell_2' + L$ is even and $\ell_1' + \ell_2' + \ell_1 + \ell_2$ is even. From the condition for non-zero values of $(\ell_1\ell_2 00|\ell 0)$ it follows that $\ell_1 + \ell_2 + \ell$ is even. Then, $\ell + L$ is even. Consequently, $\ell = L$. Thus,

$$T(11)=T(1-1)=(2k')^{-2}\frac{1}{\sqrt{2}(2I'+1)}\sum(-1)^{I-1/2+S'-S_1+\ell_1+J_2}\,i\,I_m U_1U_2^*\times$$
$$\times(2J_1+1)(2J_2+1)[(2\ell_1+1)(2\ell_2+1)(2\ell_1'+1)(2\ell_2'+1)(2S_1+1)(2S_2+1)]^{-2}(\ell_1\ell_2 00|L0)\times \qquad (4.44)$$
$$\times(\ell_1'\ell_2'00|L0)W(\ell_1'J_1\ell_2'J_2S'L)W(\tfrac{1}{2}S_1\tfrac{1}{2}S_2I1)\chi(J_1\ell_1S_1,J_2\ell_2S_2,LL1)\left(\frac{2L+1}{L(L+1)}\right)^{1/2}P_L^1(\cos\theta).$$

In accordance with expression (4.25),

$$T(1J)=\frac{2}{\sqrt{3}}\langle\sigma_y\rangle\frac{d\sigma}{d\Omega}, \qquad (4.45)$$

and, in order to obtain agreement with the preceding formulas, we determine the degree of polarization as follows:

$$P(\theta)=2\left[|\langle\sigma_x\rangle|^2+|\langle\sigma_y\rangle|^2+|\langle\sigma_z\rangle|^2\right]^{1/2}. \qquad (4.46)$$

Accordingly, a beam corresponding to a pure magnetic sub-state with a maximum projection in some direction will have P = 1. It is now possible to write

$$\langle \sigma_z \rangle \frac{d\sigma}{d\Omega} = \frac{\sqrt{3}}{2} T(10) = 0 \qquad (4.47a)$$

$$\langle \sigma_x \rangle \frac{d\sigma}{d\Omega} = -\frac{3}{2\sqrt{2}} [T(11) - T(1-1)] = 0 \qquad (4.47b)$$

$$\langle \sigma_y \rangle \frac{d\sigma}{d\Omega} = \frac{3}{2\sqrt{2}} [T(11) + T(1-1)] . \qquad (4.47c)$$

It can be seen from expression (4.47) that the scattered beam is polarized along the y axis - i.e. along the vector $\vec{n} = [\vec{k}'\vec{k}]/|[\vec{k}'\vec{k}]|$ . Thus, we finally obtain

$$P(\theta) \frac{d\sigma}{d\Omega} = -J_m \sqrt{6}\, T(11) \qquad (4.48)$$

Expressions (4.44) and (4.47) have interesting implications:

1. If, in the initial or the final state, only the s wave is effective, then T(11) = 0.

Actually, in this case either $\ell' = \ell_2' = 0$ or $\ell_1 = \ell_2 = 0$. One of the coefficients $(\ell_1' \ell_2' 00 | L0)$ or $(\ell_1 \ell_2 00 | L0)$ then gives L = 0, from which it follows that the coefficient $(L101 | L1)$ is equal to zero, for L must be greater than or equal to unity;

2. If only those levels of the compound nucleus are significant which have $J = \frac{1}{2}$ and a definite parity or J = 0 with any parity, then T(11) = 0.

Actually, if follows from the properties of $\chi\begin{pmatrix} J_1 \ell_1 s_1 \\ J_2 \ell_2 s_2 \\ L L 1 \end{pmatrix}$ that L = 0 when $J_1 = J_2 = 0$, which gives T(11) = 0. For $J_1 = J_2 = \frac{1}{2}$, L = 0 or 1. However, if the levels possess the same parity, $\ell_1 + \ell_2$ is even and it follows from the requirement that the coefficient $(\ell_1 \ell_2 00 | L0)$ be non-zero (which consists in $\ell_1 + \ell_2 = L$ being even) that L = 0. It should be noted that, as follows from expression (4.39), the differential cross-section for the reaction is isotropic in both these cases;

3. If, in the final state, only one channel with s = 0 is open, then T(11) = 0.

Actually, in this case the triangle rule does not hold in the last column of the function $\chi\begin{pmatrix} J_1 \ell_1 s_1 \\ J_2 \ell_2 s_2 \\ L L 1 \end{pmatrix}$.

4. When there is no spin-orbit interaction, there is also no polarization of the scattered beam.

This result is obtained if - using the fact that, when there is no spin–orbit interaction, the V–matrix does not depend on the total momentum J - summation is carried out over $J_1$ and $J_2$ in expression (4.44).

5. As follows from expression (4.47a), there is no polarization of the scattered beam along the direction of propagation.

6. As follows from expression (4.47c), if the choice of direction of the y axis is taken into account, the incident beam polarization vector is normal to the scattering plane.

7. The angular distribution of the polarization is characterized by $P_L^1(\cos\vartheta)$, while $L^{max} \leq 2\ell_{max}, 2\ell'_{max}, 2J_{max}$ - as can be seen from expression (4.44). In many nuclear reactions, only the s–and p–waves are significant, so that the angular dependence of the polarization will be determined by $P_1^1(\cos\vartheta)$ and $P_2^1(\cos\vartheta)$. In this case, therefore, maximum polarization is to be expected at 15° and 135° in the centre–of–mass system.

8. The V–matrix enters into expression (4.44) in the form $V_1^*V_2 - V_1V_2^*$, so that a severe limitation is imposed on the conditions under which it is possible to achieve polarization. For example, if all the matrix elements of the V–matrix have the same phase or if they are real (as they are in the Born approximation), then polarization does not occur.

Polarization occurs in the following very simple cases:

1. The reaction passes with appreciable intensity through two compound states with different J and $\pi$;

2. A contribution to the reaction is made by one resonance and by the interfering amplitudes of potential scattering with other J and $\pi$ (this case is limited to elastic scattering);

3. A contribution to the reaction is made by one resonance with several possible initial and final spins or orbital momenta. Unfortunately, this mechanism is very often suppressed owing to the great difference in penetrability. The behaviour of the differential cross–section and the polarization near the resonance is considered for cases 2 and 3 in section 5.

## 5. Scattering of partially polarized nucleons by nuclei with zero spin

### General relations

Let us consider in greater detail the case of elastic scattering of particles with a spin of $\frac{1}{2}$ by particles with zero spin. In this case, the spin of the entrance and exit channels is $\frac{1}{2}$. As parity and the total momentum $|\vec{J}| = |\vec{z}' + \vec{1}/2| = |\vec{\ell} + \vec{1}/2|$ are conserved during the reaction, it is obvious that in this case the orbital momentum is also the integral of motion $|\ell = \ell'|$. As already mentioned, for fixed $\alpha'$ and $\alpha$, the reaction amplitude is a matrix in the channel spin representation:

$$\hat{F} = \{(Sm_s|F|S'm_{s'})\} = \begin{pmatrix} (1/2\ 1/2|F|1/2\ 1/2)(1/2\ 1/2|F|1/2\ -1/2) \\ (1/2\ -1/2|F|1/2\ 1/2)(1/2\ -1/2|F|1/2\ -1/2) \end{pmatrix} \quad (5.1)$$

Using the reaction amplitude definition (3.14), it is possible to write the scattering matrix in the form

$$\hat{F} = \frac{\pi^{1/2}}{K'} \sum_{J\ell} (2\ell+1)^{1/2} U_\ell^J \begin{pmatrix} (\ell\ 1/2\ 0\ 1/2|J\ 1/2)^2 Y_{\ell 0} & (\ell\ 1/2\ 0\ -1/2|J\ -1/2)(\ell\ 1/2\ -1\ 1/2|J\ -1/2) Y_{\ell-1} \\ (\ell\ 1/2\ 0\ 1/2|J\ 1/2)(\ell\ 1/2\ 1\ -1/2|J\ 1/2) Y_{\ell 1} & (\ell\ 1/2\ 0\ -1/2|J\ -1/2)^2 Y_{\ell 0} \end{pmatrix}. \quad (5.2)$$

In the case under consideration, two values of J correspond to any non-zero value of $\ell$: $J = \ell + \frac{1}{2}$ and $J = \ell - \frac{1}{2}$. Thus, it is possible to rewrite expression (5.2) as a sum only over $\ell$:

$$\hat{F} = \frac{\sqrt{\pi}}{K'} \sum_\ell (2\ell+1)^{-1/2} \left[ U_\ell^{\ell+1/2} \begin{pmatrix} (\ell+1) Y_{\ell 0} & \sqrt{\ell(\ell+1)}\, Y_{\ell-1} \\ \sqrt{\ell(\ell+1)}\, Y_{\ell 1} & (\ell+1) Y_{\ell 0} \end{pmatrix} + U_\ell^{\ell-1/2} \begin{pmatrix} \ell Y_{\ell 0} & -\sqrt{\ell(\ell+1)}\, Y_{\ell-1} \\ \sqrt{\ell(\ell+1)}\, Y_{\ell 1} & \ell Y_{\ell 0} \end{pmatrix} \right]. \quad (5.3)$$

Here, we use

$$\begin{aligned} (\ell\tfrac{1}{2}\,0\tfrac{1}{2}|\ell+\tfrac{1}{2}\,\tfrac{1}{2}) &= (\ell\tfrac{1}{2}\,0\,-\tfrac{1}{2}|\ell+\tfrac{1}{2}\,-\tfrac{1}{2}) = [(\ell+1)/(2\ell+1)]^{1/2}, \\ (\ell\tfrac{1}{2}\,1\,-\tfrac{1}{2}|\ell+\tfrac{1}{2}\,\tfrac{1}{2}) &= (\ell\tfrac{1}{2}\,-1\,\tfrac{1}{2}|\ell+\tfrac{1}{2}\,-\tfrac{1}{2}) = [\ell/(2\ell+1)]^{1/2}, \\ (\ell\tfrac{1}{2}\,0\tfrac{1}{2}|\ell-\tfrac{1}{2}\,\tfrac{1}{2}) &= -(\ell\tfrac{1}{2}\,0\,-\tfrac{1}{2}|\ell-\tfrac{1}{2}\,-\tfrac{1}{2}) = -[\ell/(2\ell+1)]^{1/2}, \\ (\ell\tfrac{1}{2}\,1\,-\tfrac{1}{2}|\ell-\tfrac{1}{2}\,\tfrac{1}{2}) &= -(\ell\tfrac{1}{2}\,-1\,\tfrac{1}{2}|\ell-\tfrac{1}{2}\,-\tfrac{1}{2}) = [(\ell+1)/(2\ell+1)]^{1/2}. \end{aligned}$$

Let us present the part of expression (5.3) which is in square brackets in the form of an expansion in the linearly independent matrices $1, \sigma_x, \sigma_y, \sigma_z$, where $1 = \begin{pmatrix} 1 & 0 \\ 0 & 1 \end{pmatrix}$ is a unit matrix and $\sigma_x = \begin{pmatrix} 0 & 1 \\ 1 & 0 \end{pmatrix}$, $\sigma_y = \begin{pmatrix} 0 & -i \\ i & 0 \end{pmatrix}$ and $\sigma_z = \begin{pmatrix} 1 & 0 \\ 0 & -1 \end{pmatrix}$ are Pauli matrices:

$$U_\ell^{\ell+1/2}\begin{pmatrix}(\ell+1)Y_{\ell 0} & \sqrt{\ell(\ell+1)}\,Y_{\ell-1}\\ \sqrt{\ell(\ell+1)}\,Y_{\ell 1} & (\ell+1)Y_{\ell 0}\end{pmatrix}+U_\ell^{\ell-1/2}\begin{pmatrix}\ell Y_{\ell 0} & -\sqrt{\ell(\ell+1)}\,Y_{\ell-1}\\ -\sqrt{\ell(\ell+1)}\,Y_{\ell 1} & \ell Y_{\ell 0}\end{pmatrix}=a1+b_x\sigma_x+b_y\sigma_y+b_z\sigma_z, \quad (5.4)$$

where

$$\begin{aligned} a &= [(\ell+1)U_\ell^{\ell+1/2}+\ell U_\ell^{\ell-1/2}]Y_{\ell 0}(\theta\varphi);\quad b_z=0;\\ b_x-ib_y &= -[U_\ell^{\ell+1/2}-U_\ell^{\ell-1/2}]\sqrt{\ell(\ell+1)}\,Y_{\ell-1}(\theta,\varphi);\\ b_x+ib_y &= -[U_\ell^{\ell+1/2}-U_\ell^{\ell-1/2}]\sqrt{\ell(\ell+1)}\,Y_{\ell 1}(\theta,\varphi). \end{aligned} \quad (5.5)$$

Solving the system of equations for $b_x$ and $b_y$, we obtain

$$b_x=-i[U_\ell^{\ell+1/2}-U_\ell^{\ell-1/2}]P_\ell'(\theta)\sin\varphi\sqrt{(2\ell+1)/4\pi},$$
$$b_y=i[U_\ell^{\ell+1/2}-U_\ell^{\ell-1/2}]P_\ell'(\theta)\cos\varphi\sqrt{(2\ell+1)/4\pi}$$

As $\vartheta$ and $\varphi$ are scattering angles, the right-hand side of expression (5.4) can be written in the form

$$a1+b(\vec{\sigma}\vec{n}) \quad (5.6)$$

where

$$b=i[U_\ell^{\ell+1/2}-U_\ell^{\ell-1/2}]P_\ell'(\theta)\sqrt{(2\ell+1)/4\pi}, \quad (5.7)$$

and the unit vector $\vec{n}$ is determined by the equality

$$\vec{n}=[\vec{k}'\times\vec{k}]/|[\vec{k}'\times\vec{k}]|. \quad (5.8)$$

Taking into account expressions (5.5) and (5.7), we obtain an expression for the reaction amplitude:

$$\hat{F}=A(\theta)1+B(\theta)(\vec{\sigma}\vec{n}), \quad (5.9)$$

where

$$A(\theta)=\frac{1}{2k}\sum_\ell[(\ell+1)U_\ell^{\ell+1/2}+\ell U_\ell^{\ell-1/2}]P_\ell(\cos\theta), \quad (5.10)$$

$$B(\theta)=\frac{i}{2k}\sum_\ell[U_\ell^{\ell+1/2}-U_\ell^{\ell-1/2}]P_\ell^1(\cos\theta). \quad (5.11)$$

Using expression (5.9), one can reduce the differential scattering cross-section (4.16) to the form

$$\frac{d\sigma}{d\Omega}=(|A|^2+|B|^2)\left[1+\frac{2R_e AB^*}{|A|^2+|B|^2}(\vec{P}_{inc}\vec{n})\right], \quad (5.12)$$

where $\vec{P}_{inc}$ is the incident particle polarization vector. If the incident particles are unpolarized, then the differential cross-section is

$$\left(\frac{d\sigma}{d\Omega}\right)^{unpol.} = |A|^2 + |B|^2. \tag{5.13}$$

In accordance with definition (4.19), the scattered particle polarization vector can be obtained in the following form using the amplitude (5.9):

$$\vec{P}_{out} = \frac{2 Re\, AB^* \vec{n} + (|A|^2 - |B|^2)\vec{P}_{inc} + 2|B|^2 (\vec{n}\vec{P}_{inc})\vec{n} + 2 Im\, AB^* [\vec{n}\vec{P}_{inc}]}{|A|^2 + |B|^2 + 2 Re\, AB^* (\vec{n}\vec{P}_{inc})}. \tag{5.14}$$

If the incident particles are unpolarized, then the scattered particle polarization vector is equal to

$$\left(\vec{P}_{out}\right)^{unpol.} = \frac{2 Re\, AB^*}{|A|^2 + |B|^2}\vec{n}. \tag{5.15}$$

Taking into account expressions (5.12) and (5.15), we obtain for the differential cross-section for polarized neutron scattering

$$\frac{d\sigma}{d\Omega} = \left(\frac{d\sigma}{d\Omega}\right)^{unpol.} \left[1 + \left(\vec{P}_{inc}\vec{P}_{out}^{unpol.}\right)\right]. \tag{5.16}$$

Another useful relation for the value of the polarization vector can be obtained using expressions (5.14) and (5.15):

$$\left|\vec{P}_{out}\right| = \frac{\sqrt{\left[1 + \left(\vec{P}_{inc}\vec{P}_{out}^{unpol.}\right)\right]^2 - \left[1 - \left(P_{out}^{unpol.}\right)^2\right]\left[1 - (P_{inc})^2\right]}}{1 + \left(\vec{P}_{inc}\vec{P}_{out}^{unpol.}\right)} \tag{5.17}$$

As can be seen from this formula, $|\vec{P}_{out}| = 1$ if $P_{inc} = 1$ or $P_{out}^{unpol.} = 1$.

## 6. Scattering of neutrons by $^7$Li nuclei

In the total neutron cross-section of the $^7$Li isotope there is a strong p-resonance at $E_n$ = 225 keV; this corresponds to the 2.26 MeV level in the $^8$Li compound nucleus, which is characterized by $J^\pi = 3^+$. As the ground state of $^7$Li has a spin of $\frac{3}{2}$, the reaction through the $3^+$ resonance occurs with a channel spin of 2. Elwyn and Lane [11] have pointed out that s scattering occurs also with a channel spin of 2. This means that there is a broad s-resonance $J^\pi = 2^-$ at an energy of somewhat higher than 2.26 MeV.

In all further calculations, it is assumed that there is a $^{8}$Li level at 2.26 MeV with $J^{\pi} = 3^{+}$ and some level with $J^{\pi} = 2^{-}$ at a higher energy ($E_{\lambda} \approx 3$ MeV). In the energy region around the 2.26 MeV resonance, it is sufficient to consider these two levels in order to describe the existing experimental data on the differential cross-section and the polarization. In the energy region $E_n \geq 0.5$ MeV, no sharp resonances are observed. Little is known about the $^{8}$Li level structure in this region, so that additional postulated levels are introduced for the purpose of describing the differential cross-section and the polarization in this energy region.

It is assumed that the postulated levels are broad and give only a slightly varying phase shift, for the differential cross-section and the polarization are almost constant in this region.

The following assumptions are made:

1. At the energy in question, only one level with defined J and $\pi$ is significant. This makes it possible to use the single-level approximation for the scattering matrix;
2. The terms corresponding to incoming and outgoing particles with $\ell > 2$ are negligible. As the ground state of $^{7}$Li is characterized by $J^{\pi} = \frac{3}{2}^{-}$, in the reaction involving the $3^{+}$ and $2^{-}$ levels the channel spin is conserved: $s' = s = 2$.

The single-level approximation is based on the fact that there are usually no overlapping levels in light nuclei and interference phenomena are not observed in the total cross-section. The resonance parameters must be chosen in such a way that one obtains:

1. The true non-resonance background below 0.5 MeV;
2. The correct energy dependence of the differential cross-section and the polarization around the $3^{+}$ resonance ($E_n = 0.255$ MeV);
3. A smooth variation of the differential cross-section and the polarization above the $3^{+}$ resonance.

As has been shown experimentally, in the energy region $E_n \sim 0.5$ MeV the polarization is determined mainly by an angular dependence of the form const x sin $2\vartheta$; this leads to predominance of the coefficient $C_2$ in the polarization expression $P(\vartheta)d\sigma/d\Omega = \Sigma c_L P_L^1$. As can be seen from

formula (4.44), the terms corresponding to even values of L occur as a result of the interference of partial waves of the same parity. Such terms may therefore be expected to occur in this energy range either as a result of interference of p waves or as a result of interference of s and d waves. At such energies, the d wave is not at all pronounced, so that the interference of the d waves is negligible by comparison with that of the s and d waves. In the first case, one can postulate levels with $J^{\pi} = 0^+, 1^+, 2^+, 3^+$. The sets of levels $1^+$, $2^+$ (case A) and $0^+$, $2^+$ (case B) are introduced here. Other sets give worse results.

The second case - i.e. the interference of s and d waves - may come about owing to the presence of $0^-$, $1^-$, $2^-$, $3^-$ or $4^-$ levels. Only in the case of the level with $J^{\pi} = 3^-$ is there reasonable agreement with experiment. It should be noted that in this case only the process of transition from a state with a channel spin of 2 to a state with a channel spin of 1 contributes to the polarization. A process which occurs without spin mixing of the channels does not contribute to the polarization, for the X coefficients entering into formula (4.44) vanish for the quantum numbers under consideration. The $3^-$ level must be extremely broad in order to give a smoothly varying differential cross-section and polarization in the region under consideration.

Lane [12] has suggested describing the contribution of the $J^{\pi} = 3^-$ level by means of a two-channel scattering matrix:

$$S_{c'c} = \exp i \left(a_{c'c} + i\, b_{c'c}\right). \tag{6.1}$$

From an analysis of the angular distribution, the same author obtained the phases $a_{c'c}$ and $b_{c'c}$ presented in Fig. 3.

The subscripts c' and c relate to the s = 1 and s = 2 channels. Thus, calculations of the differential cross-section and the polarization were performed using formulas (4.39) and (4.44) and the following three sets of resonance parameters. The interaction radius is assumed to be 4f. The sign of the $(\Gamma_{x\ell s})^{\frac{1}{2}}$ quantities entering into the scattering matrix is assumed to be positive.

| | $E_n$(MeV; lab.) | $J^\pi$ | $\ell$ | S | $\gamma^2$ (MeV) S = I | $\gamma^2$ (MeV) S = 2 | E(MeV; c.m.s.) |
|---|---|---|---|---|---|---|---|
| A | 0,25 | $3^+$ | I | 2 | 0 | 0,307 | - 0,043 |
| | 3,4 | $2^-$ | 0 | 2 | 0 | 2,28 | 3,0 |
| | I,5 | $I^+$ | I | I,2 | I,5 | I,5 | 0,2 |
| | 3,0 | $2^+$ | I | I | 3,0 | 0 | I,55 |
| B | 0,25 | $3^+$ | I | 2 | 0 | 0,307 | - 0,043 |
| | 3,4 | $2^-$ | 0 | 2 | 0 | 2,28 | 3,0 |
| | I,0 | $0^+$ | I | I | 3,0 | 0 | - 0,7 |
| | 3,0 | $2^+$ | I | I | 3,0 | 0 | I,55 |
| C | 0,25 | $3^+$ | I | 2 | 0 | 0,307 | - 0,043 |
| | 3,4 | $2^-$ | 0 | 2 | 0 | 2,28 | 3,0 |
| | 3,4 | $3^-$ | 2 | I,2 | Phase shift (Fig. 8) | | |

The results of the calculations together with experimental data from Ref. [12] are presented in Figs 9-13. In Figs 9 and 10, we present the coefficients of the expansion of the differential cross-section and the polarization in Legendre polynomials:

$$\frac{d\sigma}{d\Omega} = \sum_L B_L P_L(\cos\theta) \tag{6.2}$$

$$P(\theta)\frac{d\sigma}{d\Omega} = \sum_L C_L P_L^1(\cos\theta). \tag{6.3}$$

The dotted, dashed and continuous lines represent the results of calculations based on sets A, B and C respectively.

In Figs 11-13, we present the angular dependence of the differential cross-section and the polarization in the energy region 0.226-2 MeV, which is calculated on the basis of resonance parameter set C.

We would point out in conclusion that the data on neutron scattering by $^7$Li nuclei in the energy region $E_n \approx 0.25$ MeV can be described fairly well by considering the $J^\pi = 3^+$ resonance which is formed by the p wave and the $J^\pi = 2^-$ resonance which is formed by the s wave and which lies at a lower energy and gives a constant background.

When calculating the polarization in the energy region 0.5-2 MeV it is necessary to take into account the additional levels. The best agreement with experiment is observed if one includes the $J^\pi = 3^-$ level with the phase shift indicated. One of the most difficult problems at higher energies is associated with the fact that the differential cross-section and the polarization vary slowly with energy - i.e. there are no predominant resonance like, for example, the resonance at $E_n = 0.25$ MeV. This situation can be ascribed to the presence of a large number of overlapping resonances in this region.

## 7. The reaction $^{7}Li(p,n)^{7}Be$

From data on the total cross-section for the reaction $^{7}Li(p,n)^{7}Be$, Macklin and Gibbons [13] found that $^{8}Be$ has two resonances in the energy range extending from the reaction threshold ($E_p$ = 1.88 MeV) to 2.3 MeV: an s-resonance with $J^\pi = 2^-$ at $E_p$ = 1.9 MeV and a p-resonance with $J^\pi = 3^+$ at 2.25 MeV. From the fact that the ground state of the $^{7}Li$ nucleus is characterized by $J^\pi = 3/2^-$ it is clear that the reaction $^{7}Li(p,n)^{7}Be$ through the s and p levels of the $^{8}Be$ compound nucleus (with $J^\pi = 2^-$ and $J^\pi = 3^+$ respectively) occurs with a channel spin of 2. Austin et al. [14] tried to interpret differential cross-section and polarization data using the set of levels proposed in Ref. [13]. It was found that the calculations based on this set of levels were in poor agreement with the observed angular distributions and polarization. Level schemes of $^{8}Be$ are given in Refs [15] and [16]. It can be seen from the schemes that the levels corresponding to $l < 2$ (a reaction involving a channel spin of 2) are the levels with $J^\pi = 1^+$ and $J^\pi = 2^+$ at $E_p$ = 3.0 MeV*/.

In this section we attempt to interpret data on the differential cross-section and the polarization in the energy region extending from the threshold to 3 MeV using the levels with $J^\pi = 2^-$, $3^+$ and $2^+$ at 1.9 MeV, 2.25 MeV and 3.0 MeV respectively.

The differential cross-section and the polarization were calculated using formulas (4.39) and (4.44). We made assumptions similar to those made in the preceding section - namely,

1. At the energy in question, only one level with definite J and $\pi$ is significant (this enables one to use the single-level approximation for the scattering matrix);

2. The terms corresponding to incoming and outgoing particles with $l > 1$ are negligible;

3. Owing to parity conservation, the orbital momenta of the incoming and outgoing particles are the same ($l = l'$). As the ground states of $^{7}Li$ and $^{7}Be$ have $J^\pi = 3/2^-$, in a reaction passing through the $2^-$ and $3^+$ levels the channel spin is conserved (and $s' = s = 2$). Neglect of orbital angular momenta greater than I' is justified by the fact that, in the energy region 1.88-3.0 MeV, the penetrability

---

*/ It follows from the general polarization formula (4.44) that, if the levels interfere and contribute to the polarization, then each of them must be formed by a wave with a channel spin which is the same as that of at least one of the remaining levels.

of the Coulomb barrier is at least an order of magnitude greater for an s-wave than for a d-wave (for a p-wave than for an f-wave). In the same energy region, the penetrability for a p-wave is greater than the penetrability for a d-wave by a factor of at least 5.

In the case under consideration - i.e. that of the reaction $^7Li(p,n)^7Be$ - $\alpha \neq \alpha'$ and $\delta_{\alpha\alpha'} = 0$. Then $V^{J\pi} = -S^{J\pi}$

$$|V^{J\pi}|^2 = |S^{J\pi}|^2 = (f^{J\pi})^2 \sin\delta^{J\pi} \tag{7.1}$$

$$Re\, V^{*J_1\pi_1} V^{J_2\pi_2} = Re\, S^{*J_1\pi_1} S^{J_2\pi_2} = f^{J_1\pi_1} f^{J_2\pi_2} \times \sin\delta^{J_1\pi_1} \sin\delta^{J_2\pi_2} \cos(\delta^{J_2\pi_2} - \delta^{J_1\pi_1} + \varphi^{J_1\pi_1} - \varphi^{J_2\pi_2}) \tag{7.2}$$

$$Im\, V^{*J_1\pi_1} V^{J_2\pi_2} = Im\, S^{*J_1\pi_1} S^{J_2\pi_2} = f^{J_1\pi_1} f^{J_2\pi_2} \times \sin\delta^{J_1\pi_1} \sin\delta^{J_2\pi_2} \sin(\delta^{J_2\pi_2} - \delta^{J_1\pi_1} + \varphi^{J_1\pi_1} - \varphi^{J_2\pi_2}). \tag{7.3}$$

Here

$$\varphi^{J\pi} = \sigma_\ell - \sigma_0 - \Phi_n^\ell - \Phi_p^\ell \tag{7.4}$$

(where $\sigma_\ell$ is the Coulomb phase, and $\Phi_n^\ell$ and $\Phi_p^\ell$ are the phases of scattering by a solid sphere for neutrons and protons respectively),

$$f^{J\pi} = \pm \frac{2(\Gamma_n^{J\pi}\Gamma_p^{J\pi})^{1/2}}{\Gamma^{J\pi}}; \quad \delta^{J\pi} = \operatorname{arc\,tg} \frac{\Gamma^{J\pi}}{2(E_R - E_p)};$$

$$\Gamma^{J\pi} = \Gamma_n^{J\pi} + \Gamma_p^{J\pi} + \Gamma_\alpha^{J\pi}, \tag{7.5}$$

where $\Gamma_n^{J\pi}$ and $\Gamma_p^{J\pi}$ are partial widths of neutron and proton emission from a $^8Be$ compound state characterized by definite J and $\pi$; $\Gamma_\alpha^{J\pi}$ is the sum of the partial widths of decay of the $^8Be$ compound nucleus over all other open channels; $E_r$ is the resonance energy; $E_p$ is the energy of the incoming protons.

The interaction radius was calculated from the formula

$$r = 1.4\,(A^{1/3} + 1)f \tag{7.6}$$

and assumed to be equal to 4f.

The $\pm$ in the expression for $f^{J\pi}$ is there because the scattering amplitude phases are determined experimentally to within $\pi$. Here, the signs for $f^{J\pi}$ are chosen so as to obtain the correct sign for the $B_1$-coefficient with $P_1(\cos\vartheta)$ in the expansion of the differential cross-section in Legendre polynomials.

The calculations were performed using the following level parameters:

| E (MeV, lab.) | $J^\pi$ | S | Sign for $J^\pi$ | $\gamma_n^2/\gamma_p^2$ | $\gamma_n^2$ (MeV; lab.) | $\Gamma_\alpha$ (MeV) |
|---|---|---|---|---|---|---|
| 1,9 | $2^-$ | 2 | - | 5,0 | 4,3 | 0 |
| 2,25 | $3^+$ | 2 | + | 5,2 | 0,83 | 0 |
| 3,0 | $2^+$ | 2 | - | 1,0 | 0,28 | 0,57 |

For the phases of scattering by a solid sphere for neutrons near the threshold we chose the same values as would be obtained in the case of scattering by a solid sphere having a radius of 12f and then the same values as would be obtained if the interaction radius decreased smoothly by a linear law to 4f at 2.3 MeV. This was done without an adequate theoretical basis for fitting a computed curve to polarization data. It is known, however, that distant resonances can influence a phase shift through the constant diagonal terms in the R-matrix and the corresponding energy dependence of the phases may quite well be linear.

The results of the calculations are presented in Figs 14 and 15, together with experimental data taken from Ref. [14]. As can be seen from these figures, the set of parameters listed above satisfactorily describes the experimental data on the total cross-section for and the polarization of neutrons in the reaction $^7Li(p,n)^7Be$ at 50° for proton energies in the range extending from the threshold to 3 MeV. Less satisfactory agreement is observed in the case of the angular distribution of the polarization, especially for $E_p$ = 2.6 MeV. However, the experimental data are not completely reliable. For example, the measurements of the differential cross-section for the reaction $^7Li(p,n)^7Be$ for $E_p$ = 2.7 MeV presented in Ref. [17] differ from the data presented in Ref. [18] by more than 50%.

## 8. Scattering of neutrons by $^4$He nuclei

This example was first considered in detail by Lepore [5]. It is assumed that contributions to the scattering process are made simultaneously by the resonances of two odd states ($P_{3/2}$ and $P_{1/2}$) of the $^5$He compound nucleus. It is also assumed that all the contributing partial waves have total momenta of 3/2 and 1/2 - i.e. in polarization calculations based on formula (7.15), with A and B determined in accordance with expressions (5.10) and (5.11), in the elements $V_\ell^J = 1-\exp(-2i\delta_\ell)$ the phases $\delta_\ell^J$ for

the $s_{1/2}$, $p_{1/2}$, $p_{3/2}$ and $d_{3/2}$ waves introduced in expression (1.4) were assumed to be non-vanishing. The contribution of the other momenta is insignificant at energies below 10 MeV. The dependence of the polarization on neutron energy, which was calculated from the phase shifts presented in Ref. [6], is shown in Fig. 1, where the scattering angle is given for each curve (the first number indicates the angle in the centre-of-mass system of co-ordinates and the number in parentheses indicates the angle in the laboratory system). For high neutron energies, the results are in good agreement with the calculations of Levintov et al. [7]; however, around 1 MeV Levintov's results differ somewhat from those obtained by us. It can be seen from Fig. 1 that helium is an excellent polarization analyser. Owing to the considerable width of the two P states which appear here, the polarization varies relatively slowly with energy; the polarization value is very significant. At neutron energies above 0.4 MeV, by a suitable choice of scattering angle it is possible to find a polarization value exceeding 0.75. The maximum polarization angle increases from $\vartheta = 90°$ at a neutron energy of 1 MeV to $\vartheta = 135°$ for neutron energies of 4 MeV or more. Little is known about the uncertainty associated with the calculated polarization.

The differences between results obtained in determining the $p_{1/2}$-phase shift at 2.6 MeV were discussed in Ref. [8]. The value of the d-phase is still very uncertain. This is the reason for the considerable uncertainty associated with calculations of the polarization at neutron energies above 10 MeV; however, no quantitative estimates of the error have been made so far. From the available information we estimate that below 6 MeV the uncertainty associated with the polarization is 10% near the angular distribution maximum and about 20% where the polarization varies rapidly with the angle.

## 9. Elastic scattering of neutrons by $^{12}C$ nuclei

In the case of neutrons with energies up to 4 MeV and $^{12}C$ nuclei, only elastic scattering is possible. As $^{12}C$ has zero spin, the entrance and exit channel spin is 1/2. It has been reliably established that there are two $d_{3/2}$-resonances - at $E_n$ = 2.95 MeV and $E_n$ = 3.5 MeV - which interfere strongly with each other, as can be seen from total cross-section experiments [9]. The extent of such interference between "resolved" states with the same J and $\pi$ is unusual in fast neutron spectroscopy and requires the use of at least a two-level collision matrix when these states are being described, which is important for polarization at energies below 2 MeV.

From angular distribution data, Lane [10] obtained the parameters of R-function (1.3) presented in Table 1.

Table 1

R-function parameters for neutron scattering by $^{12}C$ nuclei in the case of an interaction radius r = 3.72f and with a boundary condition $b_{\ell J}$ such that $E_\lambda \approx E_{res}$ for the resonances at energies up to 4 MeV

| $\ell J$ | $\lambda = 1$ | | $\lambda = 2$ | | $R^0_{\ell J}$ | $b_{\ell J}$ |
|---|---|---|---|---|---|---|
| | $E_{\ell J}$ (MeV; c.m.s.) | $\gamma^2_{\ell J}$ (MeV) | $E_{\ell J}$ | $\gamma^2_{\ell J}$ | | |
| 0 1/2 | - 1,86 | 4,0 | - | - | 0 | - 1,035 |
| 1 1/2 | - | - | - | - | 0,1 | 0 |
| 1 3/2 | - | - | - | - | 0,25 | 0 |
| 2 3/2 | 2,734 | 0,212 | 3,372 | 1,742 | 0,107 | - 1,368 |
| 2 5/2 | - | - | 1,922 | 0,030 | - 0,558 | - 1,541 |

In Figs 2-7, we give - together with the experimental results reported in Ref. [10] - the results of calculations performed on the basis of the resonance parameters presented in Table 1 and of formulas (4.39) and (4.44), where relation (1.4) is used for V. In Figs 2-4, we present the angular dependence of the polarization of neutrons scattered by $^{12}C$ nuclei for the energy range 0.5-2 MeV. The neutron energy is given in the laboratory system of co-ordinates and the angles in the centre-of-mass system. In Figs 5-7, we present the corresponding energy dependence of the coefficients

of the expansion of the differential cross-section and the polarization in Legendre polynomials:

$$\sigma(\theta) = \frac{d\sigma}{d\Omega} = \sum_L B_L(E) P_L(\cos\theta), \tag{9.3}$$

$$P(\theta)\frac{d\sigma}{d\Omega} = \sum_L C_L(E) P_L^1(\cos\theta) \tag{9.4}$$

As can be seen from these figures, the resonance parameters selected (Table 1) satisfactorily describe all the data on the angular distribution and the polarization for energies up to 2 MeV.

## Annex 1

We present below some properties of the vector sum coefficients used in this work.

### 1. Clebsch-Gordan coefficients

Clebsch-Gordan coefficients are used here for expanding the wave function in the representation of the total momentum in wave functions in the representations of the orbital momentum and the spin:

$$G_{esJM} = \sum_{m_e m_s} (\ell S m_e m_s | JM)(i^{\ell} Y_{\ell m})\chi_{sm_s} \tag{A.1.1}$$

The squares of the Clebsch-Gordan coefficients ($|(\ell S m_\ell m_s | JM)|^2$) give a probability that, on being added, the orbital momentum $\ell$ with projection $m_\ell$ and the spin s with projection $m_s$ will yield the total momentum J and its projection M. Clebsch-Gordan coefficients possess the following symmetry, orthogonality and normalization properties:

a) $$m_s + m_\ell = M \tag{A.1.2}$$

b) $$(a\,b\,\alpha\,\beta\,|\,c\,\gamma) = (b\,a\,-\beta\,-\alpha\,|\,c\,-\gamma) = \tag{A.1.3}$$
$$= (-1)^{a+b+c}(b\,a\,\beta\,\alpha\,|\,c\,\gamma) = (-1)^{a+b-c}(a\,b\,-\alpha\,-\beta\,|\,c\,-\gamma) =$$
$$= (-1)^{a-\alpha}[(2c+1)/(2b+1)]^{1/2}(a\,c\,\alpha\,-\gamma\,|\,b\,-\beta) = (-1)^{b+\beta}[(2c+1)/(2a+1)]^{1/2}(c\,b\,-\gamma\,\beta\,|\,a\,-\alpha)$$

c) $$(a\,b\,0\,0\,|\,c\,0) = 0 \qquad (a+b+c = 2n+1)\ ; \tag{A.1.4}$$

d) $$\sum_{\alpha\beta}(a\,b\,\alpha\,\beta\,|\,c'\gamma')(a\,b\,\alpha\,\beta\,|\,c\,\gamma) = \delta_{cc'}\delta_{\gamma\gamma'}\ ; \tag{A.1.5}$$

$$\sum_{c\gamma}(a\,b\,\alpha'\beta'\,|\,c\,\gamma)(a\,b\,\alpha\,\beta\,|\,c\,\gamma) = \delta_{\alpha\alpha'}\delta_{\beta\beta'}\ ; \tag{A.1.6}$$

$$\sum_{\alpha\gamma}(a\,b'\alpha'\beta'\,|\,c\,\gamma)(a\,b\,\alpha\,\beta\,|\,c\,\gamma) = \frac{2c+1}{2a+1}\delta_{bb'}\delta_{\beta\beta'} \tag{A.1.7}$$

### 2. Racah coefficients

In analyses of the angular distribution and the polarization in nuclear reactions, use is made of Racah coefficients determined by the following relation [25]:

$$\sum_{m m_1 M}(a\,b\,M-m\,m_1\,|\,\ell\,M-m+m_1)(b\,d\,m_1\,m-m_1\,|\,f\,m)(a\,f\,M-m\,m\,|\,c\,M)\times$$
$$\times(\ell\,d\,M-m+m\,m-m_1\,|\,c\,M) = \sqrt{(2e+1)(2f+1)}\ W(a\,b\,c\,d;\,e\,f). \tag{A.1.8}$$

Racah coefficients possess the following symmetry properties:

$$W(abcd;ef) = W(badc;ef) = W(cdab;ef) = W(acbd;fe) = \\ = (-1)^{e+f-a-d} W(ebcf;ad) = (-1)^{e+f-b-c} W(aefd;bc) \tag{A.1.9}$$

Moreover, Racah coefficients satisfy the following orthonormality conditions:

$$\sum_f (2e+1)(2f+1) W(abcd;ef) W(abcd;e'f) = \delta_{ee'}; \tag{A.1.10a}$$

$$\sum_e (2e+1)(2f+1) W(abcd;ef) W(abcd;ef') = \delta_{ff'}; \tag{A.1.10b}$$

and also possess the following properties:

$$W(agfb;cd) = \sum_e (2e+1)(-1)^{a+b-c} W(abcd;ef) W(bacd;eg) \tag{A.1.11a}$$

$$\sum_e (2e+1)(-1)^{e+f+g} W(abcd;fe) W(adcb;ge) = (-1)^{a+b+c+d} W(abcd;fg), \tag{A.1.11b}$$

$$W(a\alpha b\beta;c\gamma) W(a'\alpha' b'\beta';c'\gamma) = \sum_\lambda (2\lambda+1) W(a'\lambda\alpha c;ac') \times \\ \times W(b\lambda\beta c';b'c) W(a'\lambda\gamma b;ab') \tag{A.1.12}$$

The following relations are extremely useful when one is summing over magnetic quantum numbers:

$$(ab\alpha\beta|e\alpha+\beta)(ed\alpha+\beta\delta|c\alpha+\beta+\delta) = \sum_f [(2e+1)(2f+1)]^{1/2} (bd\beta\delta|f\beta+\delta) \times \\ \times (af\alpha\beta+\delta|c\alpha+\beta+\delta) W(abcd;ef), \tag{A.1.13}$$

$$\sum_\beta (ab\alpha\beta|e\alpha+\beta)(ed\alpha+\beta\gamma-\alpha-\beta|c\gamma)(bd\beta\gamma-\alpha-\beta|f\gamma-\alpha) = \\ = [(2e+1)(2f+1)]^{1/2} (af\alpha\gamma-\alpha|c\gamma) W(abcd;ef). \tag{A.1.14}$$

## 3. Z coefficients

The final expressions for the angular distributions contain Blatt-Biedenharn coefficients defined as follows [28]:

$$Z(abcd;ef) = i^{f-a+c} [(2a+1)(2b+1)(2c+1)(2d+1)]^{1/2} \times \\ \times (ac00|f0) W(abcd;ef). \tag{A.1.15}$$

From this it is clear that Z(abcd; ef) is non-vanishing only when a + c + f is even and that Z (abcd; ef) is real. Z coefficients satisfy the following symmetry and orthogonality conditions:

$$Z(e_1 J_1 e_2 J_2; SL) = (-1)^L Z(e_2 J_2 e_1 J_1; SL). \tag{A.1.16}$$

$$\sum_b Z(abcd;ef) Z(abc'd;ef) = \delta_{cc'} (2a+1)(2d+1) \times \\ \times [(ac00|f0)^2]. \tag{A.1.17}$$

Lastly, we give values of Z when either $\ell$ or f is zero:

$$Z(abcd;0f) = \delta_{ab}\delta_{cd}(-1)^{2f} i^{f-a-c}\left[(2a+1)(2c+1)\right]^{1/2}(ac\,00|f0) \qquad \text{(A.1.18)}$$

$$Z(abcd;\ell 0) = \delta_{ac}\delta_{bd}(-1)^{b-c}(2b+1)^{1/2} \qquad \text{(A.1.19)}$$

## 4. X coefficients

X coefficients have been used by Fano and Racah in the following manner [27]:

$$X\begin{pmatrix} a & b & c \\ d & e & f \\ g & h & i \end{pmatrix} = X(abc,def,ghi) = (-1)^S \sum_z (2z+1) W(bdcg;za) \times W(dbfh;ze) W(gchf;zi), \qquad \text{(A.1.20)}$$

where

$$S = a+b+c+d+e+f+g+h+i .$$

Fano and Racah have shown that X is multiplied by $(-1)^S$ if two columns change places and that the transposition of X relative to the main diagonal leaves X unchanged. It should be noted that the elements of each row and each column should form a triangle. The following relation is useful in practical applications:

$$X(abc,dec,gg0) = (-1)^{c+g-a-e} W(abde;cg) \times \left[(2c+1)(2g+1)\right]^{-1/2} \qquad \text{(A.1.21)}$$

## Literature relating to Clebsch-Gordan coefficients, Racah coefficients and X and Z coefficients

| Source | Clebsch coefficients or 3j symbols | Racah W coefficients or 6i symbols | 9i symbols (X coefficients) | Z coefficients |
|---|---|---|---|---|
| [1] A.P. Jucis, A.A. Bandzaitis, Teorija momenta količestva dviženija v kvant. mehanike (Theory of angular momentum in quantum mechanics), Vilnius (1965) | Tables for $\begin{pmatrix} j_1 j_2 j_3 \\ m_1 m_2 m_3 \end{pmatrix}$ $j_{max} \leq 6$ $j_1+j_2+j_3 \leq 16$ | Formulas for $\begin{pmatrix} a & b & c \\ d & e & f \end{pmatrix}$ | Formulas for X coefficients | – |
| [2] A. Edmonds, Angular momentum in quantum mechanics, in "Deformacija atomnyh jader" (Deformation of atomic nuclei), Moscow (1958) | Formula for $\begin{pmatrix} j_1 j_2 j_3 \\ m_1 m_2 m_3 \end{pmatrix}$ $j_3 = 0; \frac{1}{2}; 1; \frac{3}{2}; 2$ | Formula for $\begin{pmatrix} a & b & c \\ d & e & f \end{pmatrix}$ $d = 0; \frac{1}{2}; 1; \frac{3}{2}; 2$ | – | – |
| [3] A.S. Davydov, Teorija atomnogo jadra (Theory of the atomic nucleus) | Formula for $(j_1 j_2 m_1 m_2 / jm)$ | Formula for $W(abcd; \frac{1}{2}f)$ | – | – |
| [4] A.M. Baldin et al., Kinematika jadernyh reakcij (Kinematics of nuclear reactions) | Formulas $(j_1 j_2 m_1 m_2 / jm)$ $j_2 = \frac{1}{2}; 3/2; 2$ | Tables $W(abcd, ef)$ $e = \frac{1}{2}; 1; 3/2$ $f = 0,1,2,3,4$ | Tables $X(ab\frac{1}{2}; d\,\frac{1}{2}; kkl)$ $k = 1,2,3,4$ | Tables $Z(abcd; ef)$ $e = \frac{1}{2}; 1; 3/2$ $f = 0,1,2,3,4,5$ |
| [5] Sbornik - gamma luči (Gamma rays - a collection of articles) | – | – | Formulas for $X\begin{pmatrix} \ell & \ell' & L \\ \frac{1}{2} & \frac{1}{2} & S \\ j & j' & J \end{pmatrix}$ Numerical tables $\ell \leq 4;\ \ell' = \ell;\ \ell \pm 1;\ L \leq 5$ $j, j' \leq \frac{7}{2};\ J \leq 5;\ S = 0,1$ | – |

| Source | Clebsch coefficients or 3j symbols | Racah W coefficients or 6i symbols | 9i symbols (X coefficients) | Z coefficients |
|---|---|---|---|---|
| [6] A.I. Akhiezer, V.V. Berestetsky, Kvantovaja elektrodinamika (Quantum electrodynamics) | Formulas for $(j_1 j_2 m_1 m_2 / jm)$ $j_2 = \frac{1}{2}; 1$ | Formulas for W(abcd; ef) $f = \frac{1}{2}; 1$ | - | - |
| [7] V. Heine, Group theory in quantum mechanics | Numerical tables $(j_1 j_2 m_1 m_2 \mid jm)$ $j_1 = \frac{1}{2}$ ; $\frac{1}{2} \leq j_2 \leq \frac{7}{2}$. $j_1 = 1$ ; $1 \leq j_2 \leq 3$ $j_1 = \frac{3}{2}$ ; $j_2 = \frac{3}{2}; 2$ $j_1 = 2$; $j_2 = 2$ . | - | - | - |

## Annex 2

### Polarization at isolated resonances

As indicated in section 6, the polarization in nuclear reactions occurs in the following very simple cases:

1. The reaction proceeds with appreciable intensity through two compound states with differing total momenta or parity;
2. A contribution is made to the reaction by one resonance and the interfering amplitudes of potential scattering with other J and $\pi$ (this case is confined to elastic scattering);
3. A contribution is made to the reaction by one resonance with several possible initial and final channel spins or orbital momenta.

Let us consider the last two cases in greater detail.

In accordance with expression (1.1), a matrix element of the P-matrix has the form

$$U^{J\pi}_{\alpha c s,\alpha' c' s'} = \delta_{\alpha\alpha'}\delta_{cc'}\delta_{ss'} - e^{-i\varphi_{\alpha' c' s'}}\left(\delta_{\alpha\alpha'}\delta_{cc'}\delta_{ss'} + i\frac{\Gamma^{1/2}_{\alpha' c' s'}\Gamma^{1/2}_{\alpha c s}}{(E-E_R)-i\Gamma/2}\right)e^{-i\varphi_{\alpha c s}} \qquad (A.2.1)$$

Thus,

$$U^{J\pi_1}_{\alpha' c_1' s_1'\,\alpha c_1 s_1} U^{*\,J\pi_2}_{\alpha' c_2' s_2'\,\alpha c_2 s_2} = \delta_{\alpha\alpha'}\delta_{c_1 c_1'}\delta_{c_2 c_2'}\delta_{s_1 s_1'}\delta_{s_2 s_2'}\left(1-e^{-2i\varphi_{\alpha c_1 s_1}}\right)\left(1-e^{+2i\varphi_{\alpha c_2 s_2}}\right) +$$
$$+ i\,\delta_{\alpha\alpha'}\delta_{c_1 c_1'}\delta_{s_1 s_1'}\frac{\Gamma^{1/2}_{\alpha c_2 s_2}\Gamma^{1/2}_{\alpha' c_2' s_2'}}{(E-E_2)+i\Gamma_2/2}e^{i(\varphi_{\alpha c_2 s_2}+\varphi_{\alpha' c_2' s_2'})}\left(1-e^{-2i\varphi_{\alpha c_1 s_1}}\right) + \qquad (A.2.2)$$
$$+ i\,\delta_{\alpha\alpha'}\delta_{c_2 c_2'}\delta_{s_2 s_2'}\frac{\Gamma^{1/2}_{\alpha c_1 s_1}\Gamma^{1/2}_{\alpha' c_1' s_1'}}{(E-E_1)-i\Gamma_1/2}e^{-i(\varphi_{\alpha c_1 s_1}+\varphi_{\alpha' c_1' s_1'})}\left(1-e^{2i\varphi_{\alpha c_2 s_2}}\right) +$$
$$+\left[\left(\Gamma_{\alpha c_1 s_1}\Gamma_{\alpha' c_1' s_1'}\Gamma_{\alpha c_2 s_2}\Gamma_{\alpha' c_2' s_2'}\right)^{1/2}/(E-E_2+i\Gamma_2/2)(E-E_1-i\Gamma_1/2)\right]e^{i(\varphi_{\alpha c_1 s_1}+\varphi_{\alpha' c_1' s_1'}-\varphi_{\alpha c_2 s_2}-\varphi_{\alpha' c_2' s_2'})}$$

Using expression (A.2.2), we calculate the quantities $V_1V_2^* + V_1^*V_2$ and $V_1V_2^* - V_1^*V_2$ entering into expressions for the differential cross-section and the polarization:

$$\frac{1}{2}(U_1U_2^* + U_1^*U_2) = 4\delta_{\alpha\alpha'}\delta_{\ell_1\ell_1'}\delta_{\ell_2\ell_2'}\delta_{s_1s_1'}\delta_{s_2s_2'}\sin\varphi_{\alpha\ell_1s_1}\sin\varphi_{\alpha\ell_2s_2}\times$$
$$\times\cos(\varphi_{\alpha\ell_1s_1} - \varphi_{\alpha\ell_2s_2}) + 2\delta_{\alpha\alpha'}\delta_{\ell_1\ell_1'}\delta_{s_1s_1'}\frac{\Gamma_{\alpha\ell_2s_2}^{1/2}\Gamma_{\alpha'\ell_2's'}^{1/2}}{(E-E_2)^2+\Gamma_2^2/4}\times$$
$$\times\sin\varphi_{\alpha\ell_1s_1}\left[(E_2-E)\cos(\varphi_{\alpha\ell_1s_1}-\varphi_{\alpha\ell_2s_2}-\varphi_{\alpha'\ell_2's'}) + \frac{1}{2}\Gamma_2\sin(\varphi_{\alpha\ell_1s_1}-\varphi_{\alpha\ell_2s_2}-\varphi_{\alpha'\ell_2's'})\right] + \quad (A.2.3)$$
$$+ 2\delta_{\alpha\alpha'}\delta_{\ell_2\ell_2'}\delta_{s_2s_2'}\frac{\Gamma_{\alpha\ell_1s_1}^{1/2}\Gamma_{\alpha\ell_1's'}^{1/2}}{(E-E_1)^2+\Gamma_1^2/4}\sin\varphi_{\alpha\ell_2s_2}\left[(E_1-E)\cos(\varphi_{\alpha\ell_2s_2}-\varphi_{\alpha\ell_1s_1}-\varphi_{\alpha'\ell_1's'}) + \right.$$
$$\left. + \frac{1}{2}\Gamma_1\sin(\varphi_{\alpha\ell_2s_2}-\varphi_{\alpha\ell_1s_1}-\varphi_{\alpha'\ell_1's'})\right] + \frac{1}{2}\left(\Gamma_{\alpha\ell_1s_1}\Gamma_{\alpha'\ell_1's'}\Gamma_{\alpha\ell_2s_2}\Gamma_{\alpha'\ell_2's'}\right)^{1/2}\times$$
$$\times\left[\frac{\exp i(\varphi_{\alpha\ell_2s_2}+\varphi_{\alpha'\ell_2's'}-\varphi_{\alpha\ell_1s_1}-\varphi_{\alpha'\ell_1's'})}{(E-E_2+i\Gamma_2/2)(E-E_1-i\Gamma_1/2)} + \frac{\exp i(\varphi_{\alpha\ell_1s_1}+\varphi_{\alpha'\ell_1's'}-\varphi_{\alpha\ell_2s_2}-\varphi_{\alpha'\ell_2's'})}{(E-E_2-i\Gamma_2/2)(E-E_1+i\Gamma_1/2)}\right].$$

$$\frac{1}{2}(U_1U_2^* - U_1^*U_2) = 4i\delta_{\alpha\alpha'}\delta_{\ell_1\ell_1'}\delta_{\ell_2\ell_2'}\delta_{s_1s_1'}\delta_{s_2s_2'}\sin\varphi_{\alpha\ell_1s_1}\sin\varphi_{\alpha\ell_2s_2}\times$$
$$\times\sin(\varphi_{\alpha\ell_2s_2} - \varphi_{\alpha\ell_1s_1}) + 2i\delta_{\alpha\alpha'}\delta_{\ell_1\ell_1'}\delta_{s_1s_1'}\frac{\Gamma_{\alpha\ell_1s_1}^{1/2}\Gamma_{\alpha'\ell_1's'}^{1/2}}{(E-E_2)^2+\Gamma_2^2/4}\times$$
$$\times\sin\varphi_{\alpha\ell_1s_1}\left[(E-E_2)\sin(\varphi_{\alpha\ell_1s_1}-\varphi_{\alpha\ell_2s_2}-\varphi_{\alpha'\ell_2's'}) + \right.$$
$$\left. + \frac{1}{2}\Gamma_2\cos(\varphi_{\alpha\ell_1s_1}-\varphi_{\alpha\ell_2s_2}-\varphi_{\alpha'\ell_2's'})\right] - 2i\delta_{\alpha\alpha'}\delta_{\ell_2\ell_2'}\delta_{s_2s_2'}\times$$
$$\times\frac{\Gamma_{\alpha\ell_1s_1}^{1/2}\Gamma_{\alpha'\ell_1's'}^{1/2}}{(E-E_1)^2+\Gamma_1^2/4}\sin\varphi_{\alpha\ell_2s_2}\left[(E-E_1)\sin(\varphi_{\alpha\ell_2s_2}-\varphi_{\alpha\ell_1s_1}-\varphi_{\alpha'\ell_1's'}) + \right. \quad (A.2.4)$$
$$\left. + \frac{1}{2}\Gamma_1\cos(\varphi_{\alpha\ell_2s_2}-\varphi_{\alpha\ell_1s_1}-\varphi_{\alpha'\ell_1's'})\right] + \frac{i}{2}\left(\Gamma_{\alpha\ell_1s_1}\Gamma_{\alpha'\ell_1's'}\Gamma_{\alpha\ell_2s_2}\Gamma_{\alpha'\ell_2's'}\right)^{1/2}\times$$
$$\times\left[\frac{\exp i(\varphi_{\alpha\ell_1s_1}+\varphi_{\alpha'\ell_1's'}-\varphi_{\alpha\ell_2s_2}-\varphi_{\alpha'\ell_2's'})}{(E-E_2+i\Gamma_2/2)(E-E_1-i\Gamma_1/2)} - \frac{\exp i(\varphi_{\alpha\ell_1s_1}+\varphi_{\alpha'\ell_1's'}-\varphi_{\alpha\ell_2s_2}-\varphi_{\alpha'\ell_2's'})}{(E-E_2-i\Gamma_2/2)(E-E_1+i\Gamma_1/2)}\right].$$

As can be seen from expressions (A.2.3) and (A.2.4), from the product of the V-matrices it is possible to separate out terms corresponding to purely potential scattering, resonance scattering and interference between potential and resonance scattering. After the substitution of expressions (A.2.3) and (A.2.4) into expressions (4.39) and (4.44), the sums corresponding to interference scattering can be combined. When there is only one resonance with definite $J_0\pi_0$ and $E_0$, the expressions for T(00) and T(11) are given by expressions (A.2.5) and (A.2.6). The quantities $a_L$ and $b_L$ entering into these expressions are the corresponding products of the vector sum coefficients in expressions (6.24b) and (6.29):

$$T(00)=\Big\{4\sum\delta_{\alpha\alpha'}a_L(J_1J_2\ell_1\ell_2\ell_1\ell_2SS)\sin\varphi_{\alpha\ell_1 s}\sin\varphi_{\alpha\ell_2 s}\cos(\varphi_{\alpha\ell_1 s}-\varphi_{\alpha\ell_2 s})+$$
$$+4\delta_{\alpha\alpha'}\sum a_L(J_1J_0\ell_1\ell_2\ell_1'\ell_2'SS)\sin\varphi_{\alpha\ell_1 s}\Big[(E_0-E)\cos(\varphi_{\alpha\ell_1 s}-\varphi_{\alpha\ell_2 s}-\varphi_{\alpha'\ell_1's})+\tfrac{1}{2}\Gamma\times$$
$$\times\sin(\varphi_{\alpha\ell_1 s}-\varphi_{\alpha\ell_2 s}-\varphi_{\alpha'\ell_1's})\Big]\frac{\Gamma_{\alpha\ell_1 s}\Gamma_{\alpha'\ell_2's}}{(E-E_0)^2+\Gamma^2/4}+ \qquad (A.2.5)$$
$$+\sum a_L(J_0J_0\ell_1\ell_2\ell_1'\ell_2'SS')\frac{\Gamma_{\alpha\ell_1 s}\Gamma_{\alpha'\ell_1's'}\Gamma_{\alpha\ell_2 s}\Gamma_{\alpha'\ell_2's'}}{(E-E_0)^2+\Gamma^2/4}\cos(\varphi_{\alpha\ell_1 s}+\varphi_{\alpha'\ell_1's'}-\varphi_{\alpha\ell_2 s}-\varphi_{\alpha'\ell_2's'})\Big]P_L(\cos\theta)$$

$$T(11)=\Big\{4i\delta_{\alpha\alpha'}\sum b_L(J_1J_2\ell_1\ell_2\ell_1\ell_2S'S'S')\sin\varphi_{\alpha\ell_1 s'}\sin\varphi_{\alpha\ell_2 s'}\sin(\varphi_{\alpha\ell_2 s'}-\varphi_{\alpha\ell_1 s'})+$$
$$+4i\delta_{\alpha\alpha'}\sum b_L(J_1J_0\ell_1\ell_2\ell_1'\ell_2'S'S_2S')\sin\varphi_{\alpha\ell_1 s'}\Big[(E-E_0)\sin(\varphi_{\alpha\ell_1 s'}-\varphi_{\alpha\ell_2 s_2}-\varphi_{\alpha'\ell_2's'})+$$
$$+\tfrac{1}{2}\Gamma\cos(\varphi_{\alpha\ell_1 s'}-\varphi_{\alpha\ell_2 s_2}-\varphi_{\alpha'\ell_2's'})\Big]\frac{\Gamma_{\alpha\ell_1 s_2}^{1/2}\Gamma_{\alpha'\ell_2's'}^{1/2}}{(E-E_0)^2+\Gamma^2/4} \qquad (A.2.6)$$
$$+i\sum b(J_0J_0\ell_1\ell_2\ell_1'\ell_2'S_1S_2S')\frac{(\Gamma_{\alpha\ell_1 s_1}\Gamma_{\alpha'\ell_1's'}\Gamma_{\alpha\ell_2 s_2}\Gamma_{\alpha'\ell_2's'})^{1/2}}{(E-E_0)^2+\Gamma^2/4}\times$$
$$\times\sin(\varphi_{\alpha\ell_2 s_2}+\varphi_{\alpha\ell_1's'}-\varphi_{\alpha\ell_1 s_1}-\varphi_{\alpha'\ell_1's'})\Big\}P_L^1(\cos\theta)$$

Using the fact that the potential scattering phases $\varphi_{\alpha\ell s}$ and the partial widths $\Gamma_{\alpha\ell s}$ vary only slightly in the resonance region, it is possible to follow the energy dependence of T(00), T(11) and the degree of polarization $P(\vartheta) \sim iT(11)/T(00)$.

Let us rewrite expressions (A.2.5) and (A.2.6) in the form

$$T(00)=\delta_{\alpha\alpha'}A_1+\delta_{\alpha\alpha'}\frac{A_2(E-E_0)+A_3}{(E-E_0)^2+\Gamma^2/4}+\frac{A_4}{(E-E_0)^2+\Gamma^2/4}, \qquad (A.2.7)$$

$$T(11)=\delta_{\alpha\alpha'}B_1+\delta_{\alpha\alpha'}\frac{B_2(E-E_0)+B_3}{(E-E_0)^2+\Gamma^2/4}+\frac{B_4}{(E-E_0)^2+\Gamma^2/4}, \qquad (A.2.8)$$

$$P(\theta)=\frac{\delta_{\alpha\alpha'}B_1[(E-E_0)^2+\Gamma^2/4]+\delta_{\alpha\alpha'}[B_2(E-E_0)+B_3]+B_4}{\delta_{\alpha\alpha'}A_1[(E-E_0)^2+\Gamma^2/4]+\delta_{\alpha\alpha'}[A_2(E-E_0)+A_3]+A_4} \qquad (A.2.9)$$

where $A_1$ and $B_1$ correspond to purely potential scattering, $A_3$, $A_2$, $B_2$ and $B_3$ correspond to interference between potential and resonance scattering and $A_4$ and $B_4$ correspond to purely resonance scattering. It should be noted that $A_1$, $A_2$, $A_3$, $A_4$, $B_1$, $B_2$, $B_3$ and $B_4$ are constants in the resonance region.

Expression (A.3.9) can be reduced to the form

$$P(\theta) = \frac{B_1}{A_1}\delta_{\alpha\alpha'} + \frac{(B_2 - A_2B_1/A_1)(E-E_0)\bar{\sigma}_{\alpha\alpha'} + (B_3 - B_1A_3/A_1)\bar{\sigma}_{\alpha\alpha'} + (B_4 - \delta_{\alpha\alpha'}A_4B_1/A_1)}{\left[A_1(E-E_0+A_2/2A_1)^2 + \Gamma^2/4 - A_2^2/4A_1 + A_3\right]\delta_{\alpha\alpha'} + A_4} \quad (A.2.10)$$

The first term in expression (A.2.10) gives the constant background, while the second gives the asymmetric resonance peak shifted relative to the resonance in the differential cross-section and having another width. Thus, in the case of elastic scattering ($\alpha = \alpha'$), the percentage polarization varies considerably at the resonance and has the form of an asymmetric resonance peak. In the case of inelastic scattering or of an $\alpha \neq \alpha'$ reaction, $\delta_{\alpha\alpha'} = 0$ and - as can be seen from expression (A.2.10) - the polarization is constant at the resonance:

$$P(\vartheta) \sim \frac{B_4}{A_4} \quad (A.2.11)$$

Let us now consider in greater detail the case of inelastic scattering when the potential scattering phases do not depend on the total momentum and there are one entrance - $(\alpha \ell s)$ - and two exit - $(\alpha_1 \ell_1 s_1)$ and $(\alpha_2 \ell_2 s_2)$ - channels.

In this case,

$$B_4 = \text{const}\,\frac{\Gamma_{\alpha\ell s}\left(\Gamma_{\alpha_1\ell_1 s_1}\Gamma_{\alpha_2\ell_2 s_2}\right)^{1/2}}{(E-E_0)^2 + \Gamma^2/4}\sin\left(\varphi_{\alpha_1\ell_1 s_1} - \varphi_{\alpha_2\ell_2 s_2}\right) \quad (A.2.12)$$

The resonance polarization will be significant if $\Gamma_{\alpha_1\ell_1 s_1}$ and $\Gamma_{\alpha_1\ell_2 s_2}$ are comparable and if $\varphi_{\alpha_1\ell_1 s_1} \neq \varphi_{\alpha_1\ell_2 s_2}$. From the phase inequality requirement it follows that $\ell_1 \neq \ell_2$, for the potential scattering phases depend only slightly (or not at all) on the channel spin s. It follows from the law of parity conservation that $\ell_1$ and $\ell_2$ must differ by at least a factor of two; hence, if the energy of the outgoing particles is low, it is difficult to find a case where $\Gamma_{\alpha_1\ell_1 s_1}$ and $\Gamma_{\alpha_1\ell_2 s_2}$ are comparable. Thus, the most interesting cases from the point of view of obtaining significant polarization are those where the outgoing particles have an energy which is so high that the penetrabilities for the s and d waves are of the same order of magnitude.

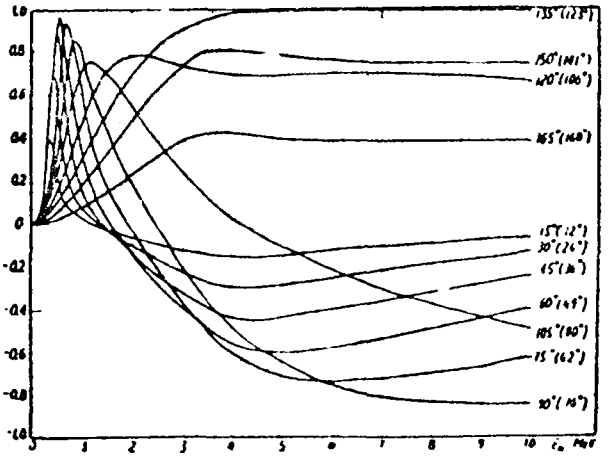

Fig. 1 Polarization in neutron scattering by $^{4}He$ at neutron energies below 10 MeV. The scattering angle is indicated for each curve (the first number indicates the angle in the centre-of-mass system of co-ordinates, while the number in parentheses indicates the angle in the laboratory system).

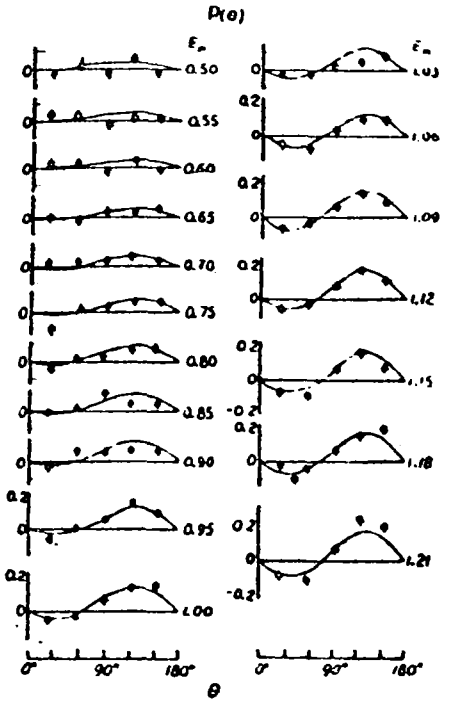


Fig. 2 Polarization of neutrons scattered by $^{12}C$. The neutron energy (in MeV) is given in the laboratory system of co-ordinates and the scattering angles in the centre-of-mass system. The continuous curve is the result of calculations based on R-matrix theory and performed using the parameters in Table 1.

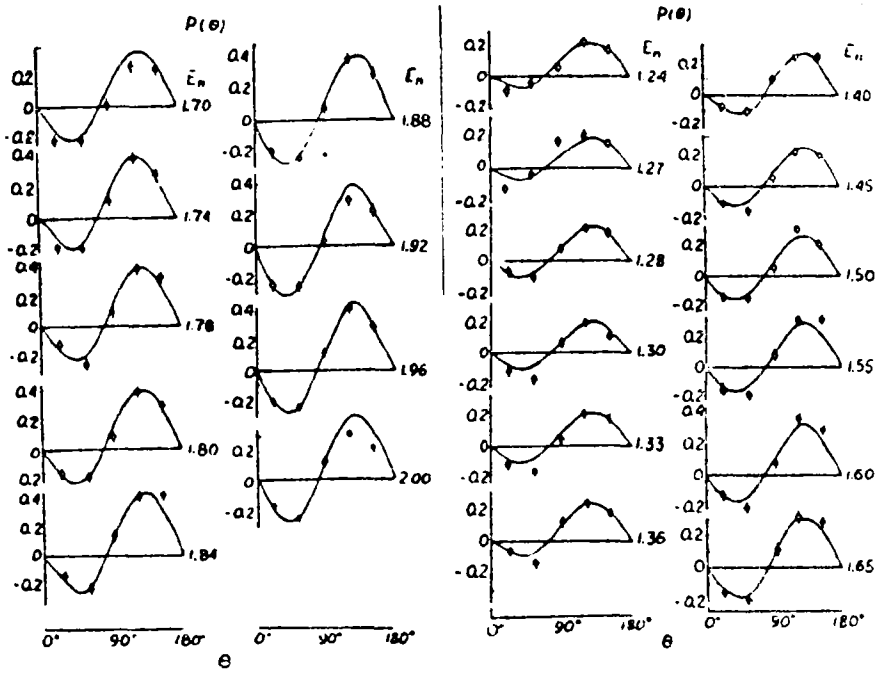


Figs 3 and 4 Polarization of neutrons scattered by $^{12}C$. The neutron energy (in MeV) is given in the laboratory system of co-ordinates and the scattering angles in the centre-of-mass system. The continuous curve is the result of calculations based on R-matrix theory and performed using the parameters in Table 1.

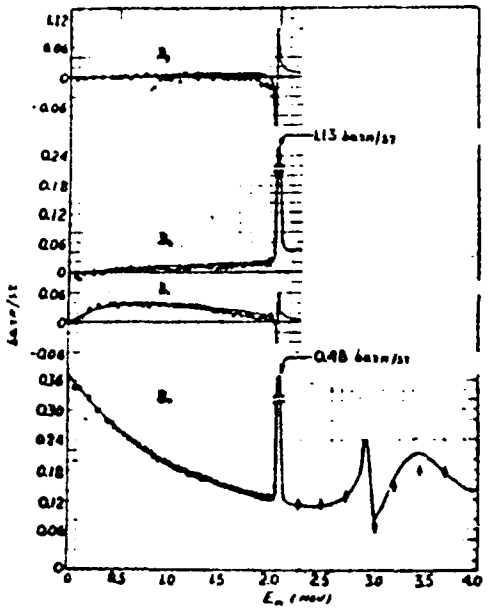


Fig. 5 Coefficients of the expansion of the differential cross-section in Legendre polynomials. The differential cross-section and the angles are given in the centre-of-mass system of co-ordinates and the neutron energy in the laboratory system. The continuous curve is the result of calculations performed using the parameters in Table 1.

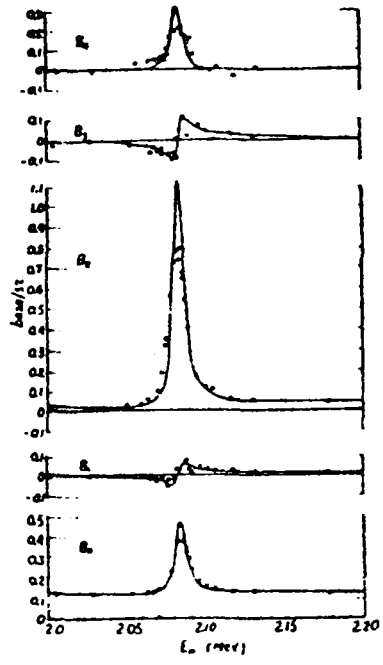

Fig. 6 Coefficients of the expansion of the differential cross-section for neutron scattering by $^{12}C$ in Legendre polynomials in the region of the resonance at 2.08 MeV. The differential cross-section and the angles are given in the centre-of-mass system of co-ordinates and the neutron energy in the laboratory system. The continuous curve is the result of calculations performed using the parameters in Table 1.

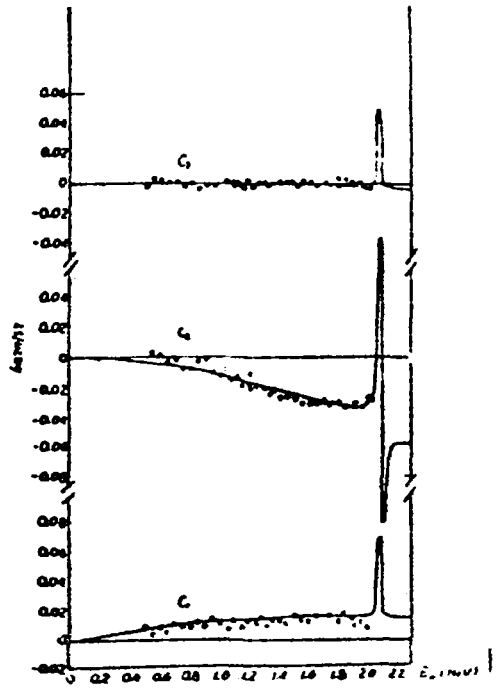

Fig. 7 Coefficients of the expansion of the cross-section for polarization in neutron scattering by $^{12}C$ in associated Legendre polynomials. The polarization cross-section and the angles are given in the centre-of-mass system of co-ordinates and the neutron energy in the laboratory system. The continuous curve is the result of calculations performed using the parameters in Table 1.

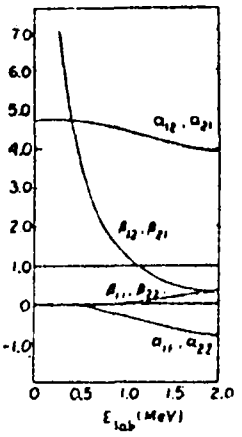


Fig. 8 The energy dependence of the phases used in calculating C.

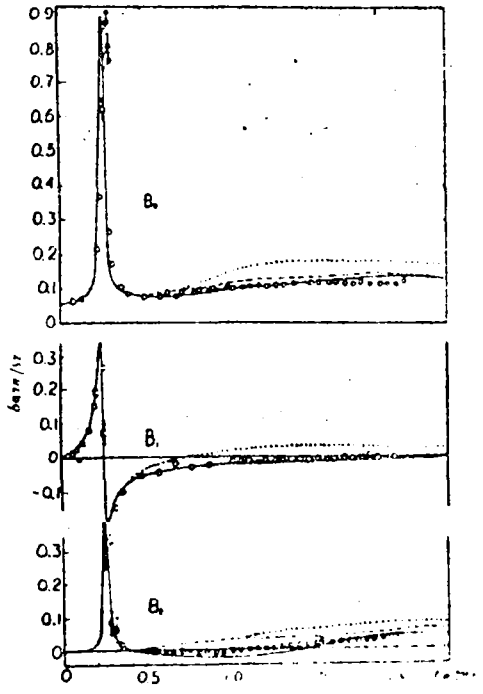


Fig. 9 Coefficients of the expansion of the differential cross-section for neutron scattering by $^{7}$Li in Legendre polynomials. The differential cross-section and the angles are given in the centre-of-mass system of co-ordinates and the neutron energy in the laboratory system. The dotted, dashed and continuous curves are the results of calculations performed using the parameter sets A, B and C respectively. The values of $B_L$ with $L \geq 3$ are small and are not presented here.

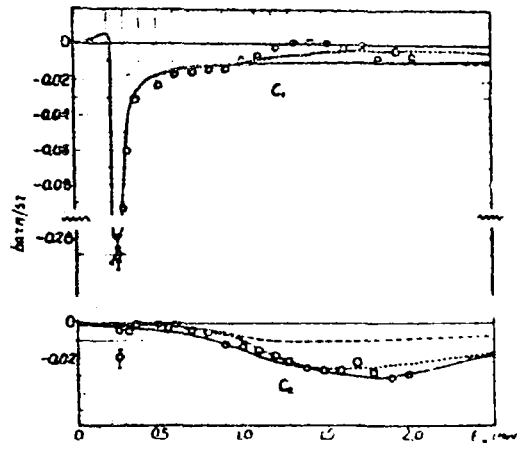

Fig. 10 Coefficients of the expansion of the cross-section for the polarization of neutrons scattered by $^{7}Li$ in associated Legendre polynomials. The polarization cross-section and the angles are given in the centre-of-mass system of co-ordinates and the neutron energy in the laboratory system. The dotted, dashed and continuous curves are the results of calculations performed using the parameter sets A, B and C respectively. Values of $C_L$ with $L \geq 3$ are small and are not presented here.

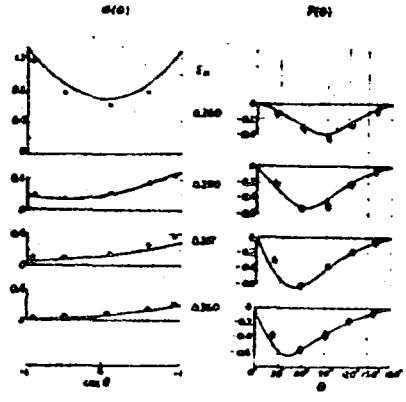

Fig. 11 Angular distribution $\sigma(\vartheta)$ and polarization $P(\vartheta)$ of neutrons in scattering by $^{7}Li$. The angles are given in the centre-of-mass system of co-ordinates and the neutron energy (in MeV) in the laboratory system. The continuous curves are the results of calculations performed using parameter set C.

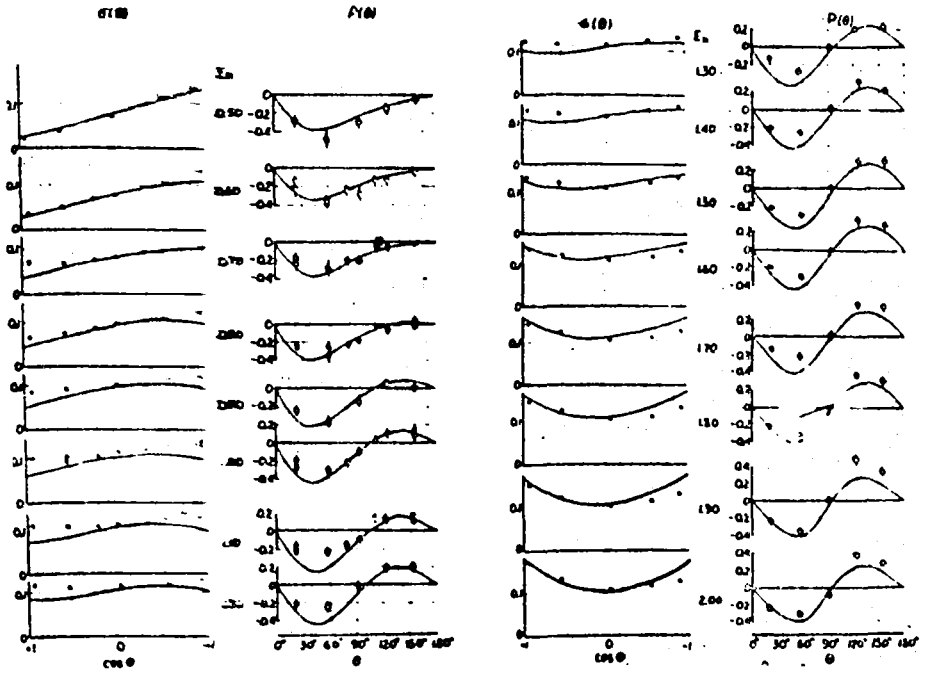

Figs 12 and 13 Angular distribution $\sigma(\vartheta)$ and polarization $P(\vartheta)$ of neutrons in scattering by $^{7}Li$. The angles are given in the centre-of-mass system of co-ordinates and the neutron energy (in MeV) in the laboratory system. The continuous curves are the results of calculations performed using parameter set C.

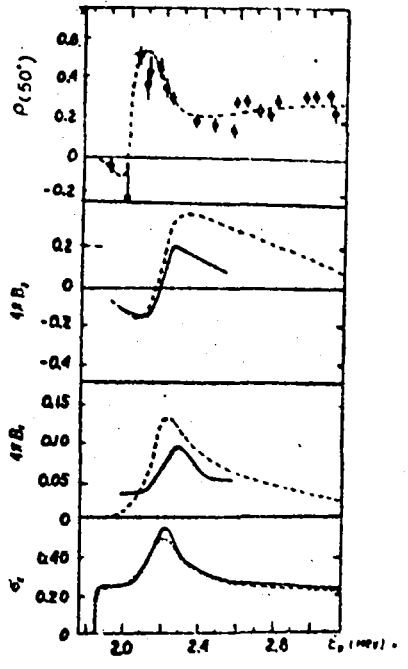

Fig. 14 Cross-section for the reaction $^{7}Li(p,n)^{7}Be$ and the polarization of neutrons from this reaction, calculated using the parameter set indicated in the text. The angles are given in the centre-of-mass system of co-ordinates and the proton energy in the laboratory system.

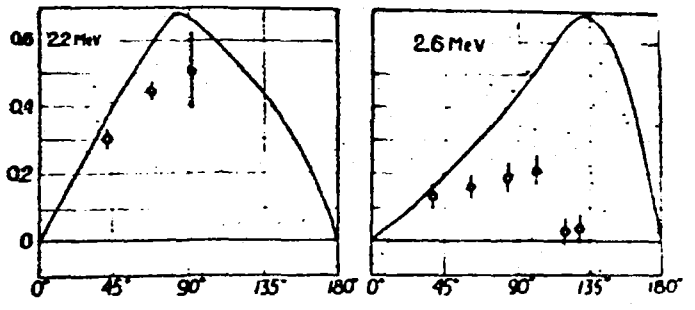


Fig. 15 Angular distribution of the polarization of neutrons from the reaction $^{7}Li(p,n)^{7}Be$ calculated using the parameter set indicated in the text. The angles are given in the centre-of-mass system and the proton energy in the laboratory system.

REFERENCES


[1] HUMBLET, J. and ROSENFELD, B.L., Nuclear Physics, 26 519 (1961).

[2] BLATT, J.M. and BIEDENHARN, L.C., Rev. Mod. Phys., 24 258 (1951).

[3] SATCHLER, G.R., Nuclear Physics, 8 65 (1958).

[4] SIMON, A., Phys. Rev., 92 1050 (1953).

[5] LEPORE, J.V., Phys. Rev., 79 137 (1950).

[6] SEAGRAVE, J.D., Phys. Rev., 92 1222 (1953).

[7] LEVINTOV et al., Nuclear Physics, 3 221 (1957).

[8] WILLARD, H.B. et al., in Fizika bystryh nejtronov (Physics of fast neutrons), Vol. 2, Atomizdat, Moscow (1966) 162.

[9] BOCHELMÁN et al., Phys. Rev., 84 69 (1951).

[10] LANE, R.O. et al., Phys. Rev., 188 1618 (1969).

[11] ELWYN, A.J. and LANE, R.O., Nuclear Physics, 31 78 (1962).

[12] LANE, R.O. et al., Phys. Rev., B136 B1710 (1964).

[13] MACKLIN, R.L. and GIBBONS, J.H., Phys. Rev., 109 105 (1958).

[14] AUSTIN et al., Nuclear Physics, 22 451 (1961).

[15] MINZATU, I. et al., Nuclear Physics, 40 347 (1963).

[16] BUCCINO, S.G. et al., Nuclear Physics, 53 375 (1964).

[17] GABBARD, F., et al., Phys. Rev., 114 201 (1959).

[18] TASCHER, R. and HEMMENDINGER, A., Phys. Rev., 74 373 (1948).

[19] GALONSKY A. et al., Phys. Rev. Letters 2 349 (1959).

[20] GOLDFARB, L.J., Nuclear Physics, 12 657 (1959).

[21] BROWN, L., CHRIST, H.A., RUDIN, H., Nuclear Physics, 79 459 (1966).

[22] McINTURE, L.C. and HAEBERLI, W., Nuclear Physics, A91 369 (1967).

[23] CONDON, E.U. and SHORTLEY, G.H., The theory of atomic spectra, Cambridge University Press (1967).

[24] LANE, A. and THOMAS, R., Teorija jadernyh reakcij pri nizkih energijah (Theory of nuclear reactions at low energies), a Russian translation published by Inostrannaja Literatura, Moscow, (1960).

[25] DAVYDOV, A.S., Teorija atomnogo jadra (Theory of the atomic nucleus), Fizmatgiz, Moscow (1958).

[26] ROSE, M.E., Elementary theory of angular momentum, Wiley, New York, 1957.

[27] FANO, U.. National Bureau of Standards Report, No. 1214 (1952).

[28] BALDIN, A.M. et al., Kinematika jadernyh reakcij (Kinematics of nuclear reactions), Atomizdat, Moscow (1968).

[29] WELTON, T.A., in Fizika bystryh nejtronov (Physics of fast neutrons), Vol. 2, Atomizdat, Moscow (1966) 239.

(Vol. 9, pp 146-175)

# MUF - A PROGRAMME FOR THE MULTILEVEL CALCULATION OF THE CROSS-SECTIONS OF NON-FISSIONABLE NUCLEI FROM RESONANCE PARAMETERS

L.P. Abagyan, M.N. Nikolaev, V.V. Sinitsa

## Introduction

In the region of resolved resonances, the energy dependence of cross-sections can be reproduced on the basis of known resonance parameters. In the case of isolated resonances, when the widths of the levels are less than the distances between them ($\Gamma \ll D$), the neutron cross-sections are satisfactorily described by the single-level Breit-Wigner formula underlying the URAN programme [1,2]. The URAN programme is intended for calculating the cross-sections of heavy non-fissionable nuclei, for which the condition $\Gamma \ll D$ is usually satisfied. The cross-sections of such nuclei are greatly influenced by the Doppler effect, so that the temperature of the medium is taken into account when the cross-sections are calculated by the URAN programme. The interference of potential and resonance scattering is also taken into account. For light nuclei and nuclei of intermediate atomic weight (in fact, for all nuclei at sufficiently high energies), the isolated resonance condition may break down. In such cases, in cross-section calculations it becomes necessary to take into account the effect of inter-resonance interference.

In this paper, we describe the MUF (Mnoga-Urovnevaja Formula = Multi-Level Formula) programme, which enables one to calculate the energy dependence of the cross-sections of non-fissionable nuclei with allowance for the effects of inter-resonance interference and interference between resonance and potential scattering. In the MUF programme, as in the URAN programme, there is provision for calculating mean-group cross-sections, self-shielding coefficients and transmission functions. In cross-section calculations, the MUF programme does not make it possible to take into account the temperature of the medium, so that it can be used for calculating only the cross-sections of light nuclei and nuclei of intermediate weight, for which the Doppler effect is negligible (in the temperature range of practical importance, the resonance widths for these nuclei greatly exceed the Doppler width).

## Description of the formula for calculating the energy dependence of the cross-sections

The MUF programme is based on a multilevel formula derived by A.A. Lukyanov [3] within the framework of the Wigner-Eisenbud formalism with a number of assumptions. For each compound nucleus level system ($\nu$) characterized by definite total momentum ($J$) and parity ($\pi$) values, the following assumptions are made:

1. In view of the large number of independent radiation channels, the radiation width may be written

$$\Gamma_{\gamma,\lambda\mu} = \bar{\Gamma}_\gamma \cdot \delta_{\lambda\mu} \qquad (1)$$

where $\lambda\mu$ represents resonances from the system $\nu$ and $\bar{\Gamma}_\gamma$ is the mean radiation width;

2. For a neutron width $\Gamma_n$, the single-channel approximation - whereby only specific orbital momentum ($\ell$) and channel spin ($j$) values correspond to each of the independent compound nucleus level systems - is valid.

As a rule, these assumptions hold good for various non-fissionable nuclei in the energy region where there is no inelastic neutron scattering and where the contribution of waves with high orbital momenta ($\ell \geq 2$) is insignificant.

With these assumptions, the collision matrix element $u^{\nu}_{nn}$ may be represented in the form

$$U^{\nu}_{nn}(E) = e^{-2i\varphi_n} \cdot \frac{1 + i X^{\nu}(E)}{1 - i X^{\nu}(E)} \quad , \qquad (2)$$

where

$$X^{\nu}(E) = \frac{i}{2} \sum_{\lambda(\nu)} \frac{\Gamma_{n,\lambda}}{E_\lambda - E - i\frac{\Gamma_\lambda}{2}} \qquad (3)$$

$E_\lambda$ being the energy of the $\lambda$-th level from the system $\nu$ (the sum is taken over all levels ($\lambda$)).

The total cross-section ($\sigma$) and the capture cross-section ($\sigma_c$) are expressed in terms of collision matrix elements in the following manner:

$$\sigma(E) = 2\pi\lambda^2 \sum_{\nu} g_\nu \cdot Re\left[1 - U^{\nu}_{nn}(E)\right] , \tag{4.1}$$

$$\sigma_c(E) = \pi\lambda^2 \sum_{\nu} g_\nu \left(1 - |U^{\nu}_{nn}(E)|^2\right) . \tag{4.2}$$

Here $\lambda$ is the neutron wavelength and $g_\nu$ the statistical weight of a state with given $J_\nu$.

By substituting expressions (2) and (3) into expressions (4.1) and (4.2), it is possible to obtain the following expressions for the cross-sections:

$$\sigma(E) = 4\pi\lambda^2 \sum_{\nu} g_\nu \sin^2\varphi_\nu + 4\pi\lambda^2 \sum_{\nu} g_\nu \frac{(B_{1,\nu} + B^2_{1,\nu} + B^2_{2,\nu})\cos 2\varphi_\nu - B_{2,\nu}\sin 2\varphi_\nu}{(1+B_{1,\nu})^2 + B^2_{2,\nu}} \tag{5.1}$$

$$\sigma_c(E) = 4\pi\lambda^2 \sum_{\nu} g_\nu \frac{B_{1,\nu}}{(1+B_{1,\nu})^2 + B^2_{2,\nu}} \tag{5.2}$$

$$\sigma_s(E) = \sigma(E) - \sigma_c(E) , \tag{5.3}$$

where

$$B_{1,\nu} = su1 = \sum_{\lambda(\nu)} \frac{\Gamma_{n,\lambda}/\Gamma_\gamma}{1 + \left(2\frac{E_\lambda - E}{\Gamma_\gamma}\right)^2} \tag{6.1}$$

$$B_{2,\nu} = su2 = \sum_{\lambda(\nu)} \frac{\Gamma_{n,\lambda}/\Gamma_\gamma \left(2\frac{E_\lambda - E}{\Gamma_\gamma}\right)}{1 + \left(2\frac{E_\lambda - E}{\Gamma_\gamma}\right)^2} \tag{6.2}$$

If it is assumed that $\varphi_\nu$ is the phase of scattering by a reflecting sphere, then

$$\varphi_{s(l=0)} = x , \tag{7.1}$$

$$\varphi_{p(l=1)} = x - arctg\, x , \tag{7.2}$$

$$\varphi_{d(l=2)} = x - arctg\, \frac{3x}{3 - x^2} , \tag{7.3}$$

$$x = kR \tag{8}$$

Here k is the wave number of a neutron outside a nucleus; it is associated with the kinetic energy of the neutron outside the nucleus by the relation

$$k = 0{,}2197\left(\frac{A+1}{A}\right)\ 10^{10}\sqrt{E(\mathrm{eV})} \qquad (9)$$

where A is the mass of the nucleus in neutron mass units and R is the interaction radius. Weisskopf [4] has stated that R depends on atomic weight as follows:

$$R \approx rad\,(A^{1/3} + 0{,}55)\,(cm)\,; \quad rad \sim 1{,}3 \div 1{,}5 \cdot 10^{-13} \qquad (10)$$

In the MUF programme, the parameter rad is introduced together with other input data. In some specific cases, rad can be determined more precisely on the basis of total cross-section or potential scattering cross-section measurements already performed.

The energy dependence of the neutron widths is computed from the formulas

$$\Gamma_n(E) = \Gamma_n(E_\lambda)\,\frac{v_\ell(E)}{v_\ell(E_\lambda)}\,\sqrt{\frac{E}{E_\lambda}}\ , \qquad (11)$$

$$v_0 = 1\,, \quad v_1 = \frac{x^2}{1+x^2}\,, \quad v_2 = \frac{x^4}{9+3x^2+x^4}\,, \quad x = kR \qquad (12)$$

The introduction of the quantity $\varphi_\ell$ (formulas (7.1)-(7.3)) enables us to calculate the potential scattering cross-section:

$$\sigma_p(E) = 4\pi\lambda^2\sum_\nu g_\nu \sin^2\varphi_\nu = 4\pi\lambda^2\sum_\ell (2\ell+1)\sin^2\varphi_\ell\,. \qquad (13)$$

There is also provision in the MUF programme for introducing the non-resonance part of the total cross-section ($\sigma_p$) as a function of energy. The array of specified potential scattering cross-sections is designated as SPOT and the array of energies at which they are specified as ESP. At the calculated energy points, the values of $\sigma_p$ are determined by linear interpolation.

In calculations of the cross-sections of a mixture of isotopes, the level system ($\nu$) is also characterized by $A_\nu$ - the atomic weight of the isotope to which it belongs.

The cross-section calculation formulas (5.1)-(5.3) have an advantage over other multilevel formulas, for when using them to restore the energy dependence of the cross-sections, there is no need to specify any additional parameters characterizing the multilevel state. In formulas (5.1)-(5.3), the cross-sections are functions of the single-level resonance parameters which are used in calculations based on the Breit-Wigner formula. It is this set of parameters which, as a rule, is determined by experimentalists when analysing data obtained near each resonance (by the "method of squares" or the "method of shape").

In Ref. [5], Garrison presents curves of the total cross-section of two interfering resonances calculated using multilevel formulas. The positions of the resonances were fixed (1000 eV and 1010 eV), while the widths varied within a wide range (1 eV-50 eV). It was assumed that there was no capture. These data were used as a basis for total cross-section calculations by the MUF programme which made it possible to reproduce completely the shape of the total cross-section curves. In Fig. 1 we present the results of the total cross-section calculations using the MUF programme (continuous curves). The results of cross-section calculations performed with the URAN programme are represented by broken curves. It can be seen from the Figure that the URAN programme can be used for restoring the energy dependence of the total cross-section only if $\Gamma/D \leq 0.1$.

## Description of the MUF programme

The programme is written in ALGOL-60. It is translated into M-20 computer language by a TA-2 translator. The comments below relate to some of the blocks and compound statements constituting the MUF programme.

1. Next energy point selection statement (VYTOČKA). This governs the size of the next energy step. For the i-th resonance, the first step is $\Gamma_i/32$; it then doubles, provided that the total cross-section at two neighbouring points differs by less than 5%. Doubling of the step proceeds until dE does not exceed $\Gamma_i$. The step then becomes constant and equal to $\Gamma_i$, but only if the total number of points on the resonance wing in question does not exceed 100 (otherwise, the step is selected in such a way that the number of points on the resonance wing is 100).

2. Determination of inter-resonance points. This is somewhat modified in relation to the URAN programme [1,2]. For each i-th resonance, the inter-resonance energy is determined on the right ($E_{i-1,i}$) and on the left ($E_{i,i+1}$) of the resonance:

$$E_{i-1,i} = \frac{E^{\circ}_{i-1}\Gamma_i g_i + E^{\circ}_i \Gamma_{i-1} g_{i-1}}{\Gamma_{i-1} g_{i-1} + \Gamma_i g_i} \qquad (14)$$

In those cases where

$$E_{i-2,i-1} \leq EN < E_{i-1,i} \ , \qquad (15)$$

the energy region from EN to $E_{i-1,i}$ was regarded in the URAN programme as the "left wing" of the i-th resonance (i.e. the cross-section calculations were performed from the i-th resonance peak to an energy of EN). Similarly, when

$$E_{i+1,i+2} \geq EV > E_{i,i+1} \ , \qquad (16)$$

the energy region from $E_{i,i+1}$ to EV was regarded as the "right wing" of the i-th resonance. As was shown in Ref. [2], with this approach to the selection of inter-resonance points it is not always possible to achieve the required precision in integrating the energy dependence of the cross-sections.

Accordingly, alterations were introduced into the inter-resonance energy selection statement. For $EN < E_{i-1,i}$, the energy region $EN-E_{i-1,i}$ is calculated by means of the "VYTOČKA" algorithm from EN to the right with an initial energy step $\Gamma_{i-1}/32$. For $EV > E_{i,i+1}$, the energy region $E_{i,i+1}-E_V$ is calculated by means of the "VYTOČKA" algorithm from EV to the left with an initial energy step $\Gamma_{i+1}/32$. In the remaining cases, the calculations are performed from the i-resonance peak energy $E^{o}_i$, with a step of $\Gamma_i/32$, first for the left and then for the right wing of the resonance.

This way of selecting inter-resonance points enables one to describe in detail the energy dependence of the cross-sections in the case where the resonance lies near the boundary of the group and outside the group interval. The algorithm enables one to calculate the group cross-sections in the case where the energy interval of the group falls into the region between the resonance peaks.

Owing to the advantages of this way of determining the inter-resonance energies, the algorithm in question has also been introduced into the URAN programme.

3. Calculation of resonance integrals. In the group, such calculations are performed using the formula

$$J_R^t = Avr \cdot \Delta U = \sum_i \frac{\pi}{2} \frac{\sigma_{mi}\Gamma_i}{|E_{oi}|},$$

$$J_R^c = Avc \cdot \Delta U = \sum_i \frac{\pi}{2} \frac{\sigma_{mi}(\Gamma_i - \Gamma_{oi})}{|E_{oi}|}, \qquad (17)$$

where $$J_R^s = Avs \cdot \Delta U = J_R^t - J_R^c,$$

$$\sigma_{mi} = 4\pi\lambda^2 g \cdot \frac{\Gamma_{ni}}{\Gamma} \qquad (18)$$

is the cross-section at the resonance peak. Those levels (i) are summed whose energies $E_{oi}$ satisfy the inequality $EN < E_{oi} \leq EV$.

4. Calculation of quantities averaged over the energy group (SUM block). In the MUF programme there is provision for obtaining:

(a) unblocked cross-sections -

$$\langle\sigma\rangle = At = \frac{1}{\Delta U}\int_{\Delta U}\sigma E^2 dE = \frac{1}{\Delta U}\sum_i\sum_{k=kN}^{kN-1}(\sigma[E_k]E_k^2 + \sigma[E_{k+1}]E_{k+1}^2)\frac{dE_k}{2},$$

$$\langle\sigma_c\rangle = Ac = \frac{1}{\Delta U}\int_{\Delta U}\sigma_c E^2 dE = \frac{1}{\Delta U}\sum_i\sum_{k=kN}^{kN-1}(\sigma_c[E_k]E_k^2 + \sigma_c[E_{k+1}]E_{k+1}^2)\frac{dE_k}{2}, \qquad (19)$$

$$\langle\sigma_s\rangle = As = \frac{1}{\Delta U}\int_{\Delta U}(\sigma-\sigma_c)E^2 dE = \frac{1}{\Delta U}\sum_i\sum_{k=kN}^{kN-1}[(\sigma[E_k]-\sigma_c[E_k])E_k^2 + (\sigma[E_{k+1}]-\sigma_c[E_{k+1}])E_{k+1}^2]\frac{dE_k}{2}.$$

(b) blocked cross-sections and self-shielding coefficients -

$$\bar{\sigma} = \frac{\left\langle\frac{1}{\sigma+\sigma_o}\right\rangle}{\left\langle\frac{1}{(\sigma+\sigma_o)^2}\right\rangle} - \sigma_o, \qquad \bar{\sigma}_c = \frac{\left\langle\frac{\sigma_c}{\sigma+\sigma_o}\right\rangle}{\left\langle\frac{1}{\sigma+\sigma_o}\right\rangle},$$

$$\bar{\sigma}_e = \frac{\left\langle\frac{\sigma-\sigma_c}{\sigma+\sigma_o}\right\rangle}{\left\langle\frac{1}{\sigma+\sigma_o}\right\rangle}, \qquad \bar{\sigma}_{e2} = \frac{\left\langle\frac{\sigma-\sigma_c}{(\sigma+\sigma_o)^2}\right\rangle}{\left\langle\frac{1}{(\sigma+\sigma_o)^2}\right\rangle}, \qquad (20)$$

$$f_\sigma = \frac{\bar{\sigma}}{\langle\sigma\rangle}, \qquad f_c = \frac{\bar{\sigma}_c}{\langle\sigma_c\rangle},$$

$$f_e = \frac{\bar{\sigma}_e}{\langle\sigma_s\rangle}, \qquad f_{e2} = \frac{\bar{\sigma}_{e2}}{\langle\sigma_s\rangle}; \qquad (21)$$

(c) transmission functions

$$Tt(t) = \frac{1}{\Delta u}\int e^{-\sigma(E)t}E^2dE = \frac{1}{\Delta u}\sum_{i}\sum_{K=KN}^{KM-1}(e^{-\sigma[E_K]t}E_K^2 + e^{-\sigma[E_{K+1}]t}E_{K+1}^2)\frac{dE_K}{2},$$

$$T_c(t) = \frac{1}{\Delta u\langle\sigma_c\rangle}\int\sigma_c(E)e^{-\sigma(E)t}E^2dE = \frac{1}{\Delta u\langle\sigma_c\rangle}\sum_{i}\sum_{K=KN}^{KM-1}(\sigma_c[E_K]e^{-\sigma[E_K]t}E_K^2 + \sigma_c[E_{K+1}]e^{-\sigma[E_{K+1}]t}E_{K+1}^2)\frac{dE_K}{2}, \quad (22)$$

$$T_s(t) = \frac{1}{\Delta u\langle\sigma_s\rangle}\int[\sigma(E) - \sigma_c(E)]e^{-\sigma(E)t}E^2dE =$$

$$= \frac{1}{\Delta u\langle\sigma_s\rangle}\sum_{i}\sum_{K=KN}^{KM-1}[(\sigma[E_K] - \sigma_c[E_K])e^{-\sigma[E_K]t}E_K^2 + (\sigma[E_{K+1}] - \sigma_c[E_{K+1}])e^{-\sigma[E_{K+1}]t}E_{K+1}^2)]\frac{dE_K}{2}$$

The set of thicknesses $\{t_i\}$ for calculating the transmission functions can be calculated by the programme using the following relations:

$$t_2 = \frac{C}{J_R^t/\Delta u + \sigma_p(E^*,\ EN \le E^* \le EV)}, \quad t_1 = 0.75t_2;\ t_{i+1} = 2t_{i-2},\ i = 3,4,\ldots,50. \quad (23)$$

In the programme, we take the coefficient C to be $2^{-15}$. There is also provision for introducing the set of thicknesses on punched cards. The array of specified thicknesses is denoted by TOL.

## Examples of cross-section calculations using the MUF programme

Total cross-section calculations were performed for the elements Ti, V and Mn. These elements were chosen because, in the energy ranges considered, the condition $\Gamma/D < 0.1$ breaks down for some resonances. As a result, inter-resonance interference is very prominent in the total cross-section curves and the energy dependence of the cross-sections cannot be restored using the URAN programme.

In the cross-section calculations using the MUF programme, the resonance parameters recommended in Ref. [6] were first taken as a basis.

In Table 1 we present the resonance parameters of titanium.

Table 1

Resonance parameters of $_{22}Ti$ [6]

| E (keV) | $\Gamma_n$ (eV) | A | B |
|---|---|---|---|
| 10.51 | 60 | 47 | 0.08 |
| 12.12 | 60 | 47 | 0.08 |
| 12.82 | 80 | 47 | 0.08 |
| 16.40 | 185 | 47 | 0.08 |
| 17.34 | 7500 | 48 | 0.73 |
| 18.1 | 154 | 49 | 0.06 |
| 20.8 | 122 | 49 | 0.06 |
| 22.1 | 400 | 49 | 0.06 |
| 22.2 | 500 | 49 | 0.06 |
| 26.9 | 410 | 49 | 0.06 |
| 27.0 | 700 | 47 | 0.08 |
| 29.1 | 79 | 47 | 0.08 |
| 29.2 | 160 | 49 | 0.06 |
| 31.2 | 925 | 49 | 0.06 |
| 32.3 | 500 | 47 | 0.08 |
| 35.8 | 142 | 49 | 0.06 |
| 36.1 | 202 | 47 | 0.08 |
| 37.0 | 200 | 47 | 0.08 |
| 37.0 | 1100 | 48 | 0.73 |
| 37.9 | 1560 | 49 | 0.06 |
| 39.1 | 370 | 47 | 0.08 |

In Fig. 2 we show the calculated curve of the energy dependence of the total cross-section of titanium in the energy range 15-30 keV. The experimental results of Garg et al. (open dots) are taken from Ref. [6].

The resonance parameters for vanadium were taken from Ref. [7]. We succeeded in describing the energy dependence of the total cross-sections only after varying the neutron widths and resonance positions several times. In Table 2 we present the initial and modified resonance parameters of vanadium.

Table 2

Resonance parameters of $_{23}V$ [7]

| E (keV) | $\Gamma_n$ (eV) | J |
|---|---|---|
| 4.17 (4.16) | 508 (450) | 4 |
| 6.89 (6.84) | 1280 (1100) | 3 |
| 11.81 (11.3) | 5500 (4300) | 3 |
| 16.60 (16.4) | 350 (300) | 4 |
| 17.40 (17.3) | 350 (200) | 4 |
| 21.65 (21.6) | 790 (390) | 3 |
| 29.45 (29.6) | 191 (150) | 4 |
| 39.30 | 570 | 3 |
| 48.15 | 150 | 4 |
| 49.55 | 630 | 3 |
| 51.95 | 115 | 4 |
| 53.0 | 980 | 3 |
| 62.9 | 3800 | 3 |

The cross-section of vanadium was considered in the energy range 2-30 keV. The results of calculations of the total cross-section of vanadium based on the initial (broken line) and modified (continuous line) resonance parameters are presented in Fig. 3. The experimental points were taken from Ref. [6].

The cross-section of manganese was considered in the energy range 0.1-10 keV. In order to describe the total cross-section curve, the neutron widths of two levels had to be modified somewhat relative to those recommended in Ref. [6]. The resonance parameters of manganese taken by us are given in Table 3.

Table 3

Resonance parameters of $_{25}Mn$ [6]

| E (keV) | $\Gamma_n$ (eV) | J |
|---|---|---|
| -2.83 | 26.9 | 2 |
| -0.078 | 0.14 | 3 |
| 0.337 | 22 | 2 |
| I.098 | I4.6 | 3 |
| 2.375 | 400 | 3 |
| 7.I70 | 425 (440) | 2 |
| 8.870 | 404 (385) | 3 |
| I7.8 | I5.0 | 2 |
| I8.0 | 45.0 | 3 |
| 2I.0 | 860 | 3 |
| 23.7 | 380 | 2 |
| 25.9 | 7.0 | 3 |
| 26.4 | I20 | 2 |
| 27.0 | 380 | 3 |

The numbers in brackets are the modified neutron width values. In Fig. 4 we present the results of manganese total cross-section calculations.

In the cases considered, we succeeded in describing satisfactorily the energy dependences of the cross-sections. For this we had to vary the resonance parameters somewhat by hand. A programme for the automatic fitting of resonance parameters, written on the basis of the given multi-level formula, will have to be devised.

Besides the detailed energy dependence of the cross-sections, the MUF programme permits us to calculate transmission functions, resonance self-shielding coefficients and mean-group cross-sections. Some of these quantities are presented by way of illustration in Tables 4 and 5 and in Fig. 5.

It did not take more than 10-15 minutes to calculate any of the variants on the M-220 computer.

Table 4

Resonance self-screening factors and mean-group cross-sections of $_{23}V$

| Group No. (BNAB) | Boundaries of groups (keV) | ER | Mean-group cross-sections (barn) | | Resonance self-shielding factors of cross-sections for $\sigma_o$ (barn) | | | | | |
|---|---|---|---|---|---|---|---|---|---|---|
| | | | | | | = 0 | 10 | $10^2$ | $10^3$ | $10^4$ |
| II | I0 - 2I,5 | 0,7656 | $\langle\sigma\rangle$ | 56,94 | FT | 0,2356 | 0,4237 | 0,7722 | 0,9656 | 0,9934 |
| | | | $\langle\sigma_c\rangle$ | 0,028 | FC | 0,7586 | 0,797I | 0,9I82 | 0,9873 | 0,9986 |
| | | | $\langle\sigma_s\rangle$ | 56,9I | FS | 0,5558 | 0,68I8 | 0,883I | 0,9827 | 0,9982 |
| I2 | 4,65 - I0 | 0,7658 | $\langle\sigma\rangle$ | 69,8I | FT | 0,I222 | 0,2492 | 0,6624 | 0,94II | 0,9935 |
| | | | $\langle\sigma_c\rangle$ | 0,056 | FC | 0,6935 | 0,755I | 0,8870 | 0,9795 | 0,9978 |
| | | | $\langle\sigma_s\rangle$ | 69,76 | FS | 0,3708 | 0,5400 | 0,8205 | 0,9702 | 0,9933 |
| I3 | 2,15 - 4,65 | 0,77I8 | $\langle\sigma\rangle$ | 78,74 | FT | 0,I753 | 0,2048 | 0,3700 | 0,79I9 | 0,9730 |
| | | | $\langle\sigma_c\rangle$ | 0,I3 | FC | 0,289I | 0,349I | 0,5784 | 0,8908 | 0,9867 |
| | | | $\langle\sigma_s\rangle$ | 78,6I | FS | 0,2750 | 0,3339 | 0,5664 | 0,8880 | 0,9864 |

Table 5

Resonance self-screening factors and mean-group cross-sections of $_{25}Mn$

| Group No. (BNAB) | Boundaries of groups (keV) | ER | Mean-group cross-sections (barn) | | Resonance self-shielding factors of cross-sections for $\sigma_o$ (barn) | | | | | |
|---|---|---|---|---|---|---|---|---|---|---|
| | | | | | | = 0 | 10 | $10^2$ | $10^3$ | $10^4$ |
| I2 | 4,65 - I0 | 0,7660 | $\langle\sigma\rangle$ | 36,I2 | FT | 0,I435 | 0,2234 | 0,5397 | 0,9013 | 0,9888 |
| | | | $\langle\sigma_c\rangle$ | 0,039 | FC | 0,3263 | 0,4476 | 0,7334 | 0,9509 | 0,9946 |
| | | | $\langle\sigma_s\rangle$ | 36,08 | FS | 0,2592 | 0,4013 | 0,7183 | 0,9489 | 0,9944 |
| I3 | 2,I5 - 4,65 | 0,77I5 | $\langle\sigma\rangle$ | I67,7 | FT | 0,09089 | 0,1143 | 0,2399 | 0,6734 | 0,9519 |
| | | | $\langle\sigma_c\rangle$ | 0,I8 | FC | 0,I5I4 | 0,1995 | 0,4087 | 0,8949 | 0,9737 |
| | | | $\langle\sigma_s\rangle$ | I67,5 | FS | 0,I869 | 0,2377 | 0,4453 | 0,8190 | 0,9756 |

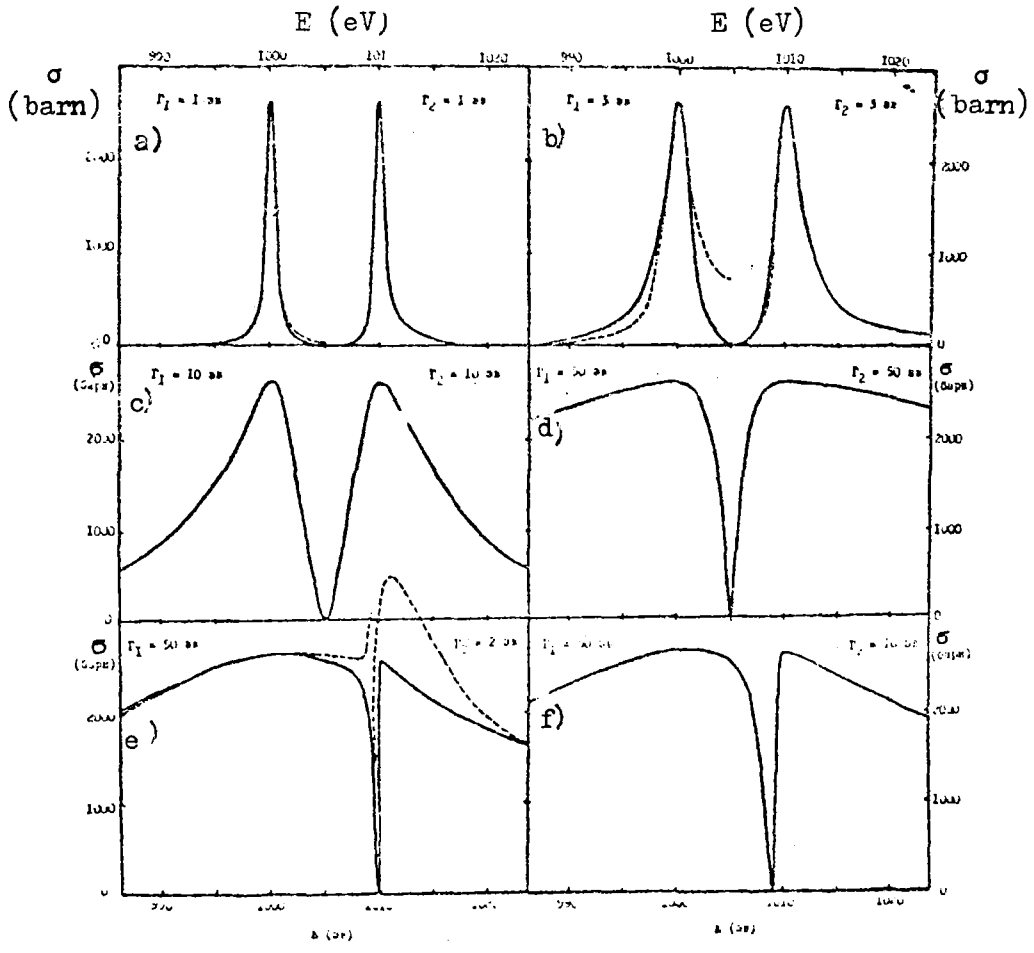


Fig. 1 Results of calculations of the total cross-sections of two interfering resonances with energies $E_1$ = 1 keV and $E_2$ = 1.01 keV. Continuous curves - calculations performed using the MUF programme; broken curves - calculations performed using the URAN programme.

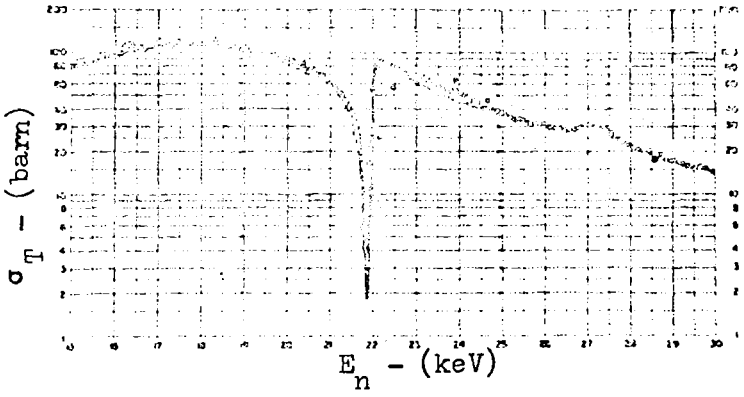


Fig. 2 Total cross-section of titanium

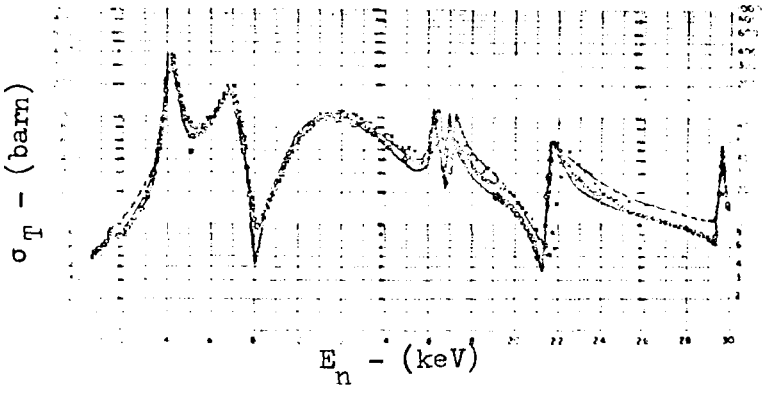


Fig. 3 Total cross-section of vanadium

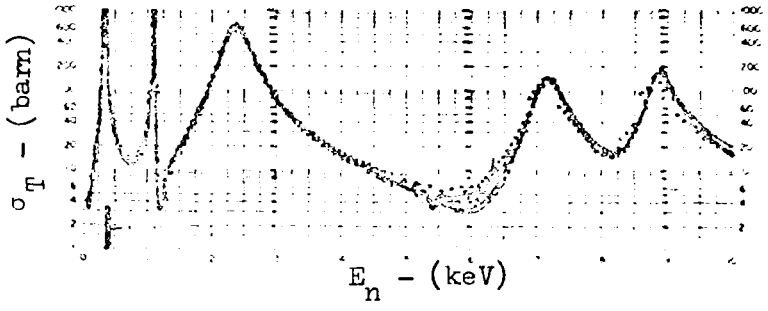


Fig. 4 Total cross-section of manganese

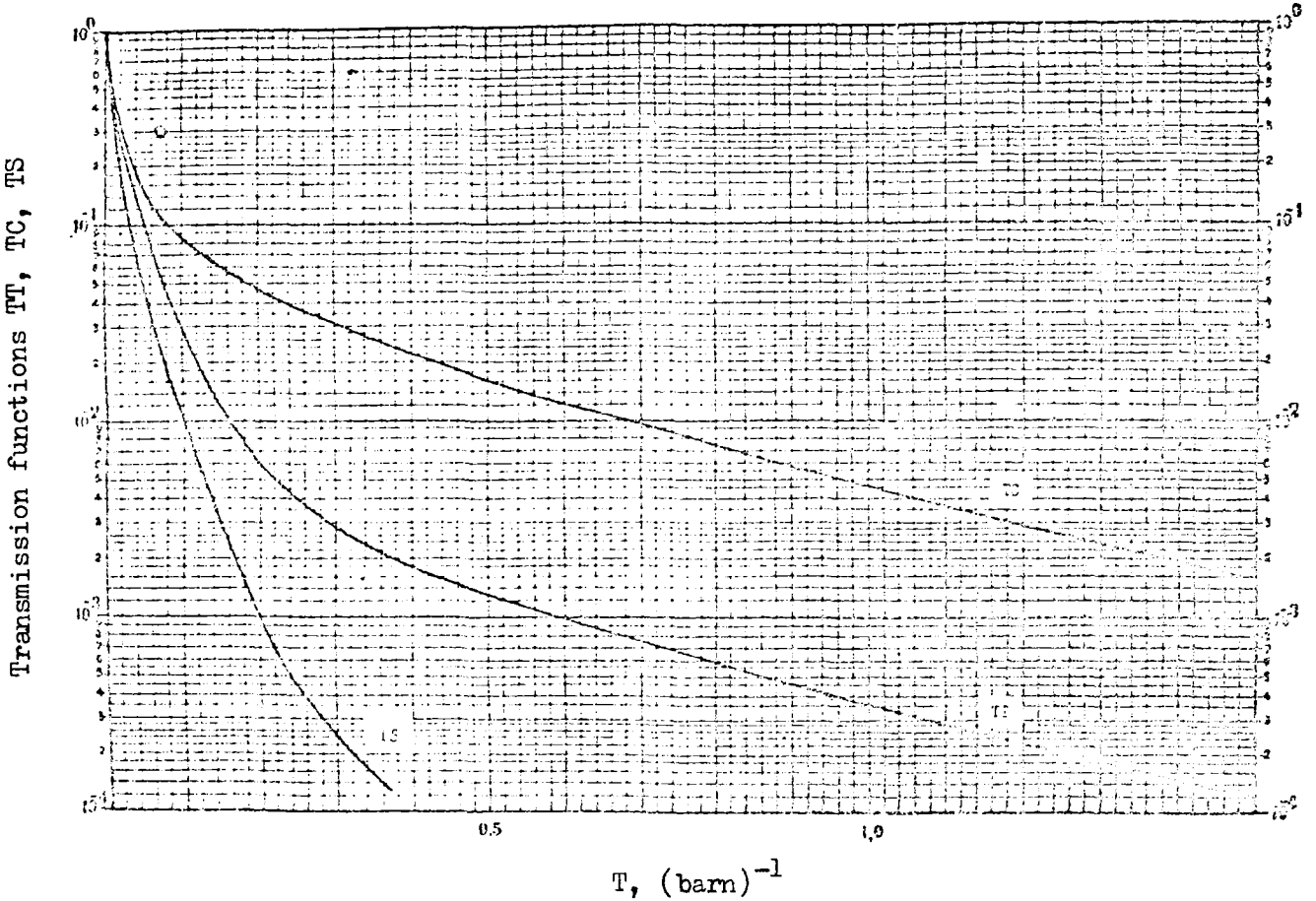


Fig. 5 Transmission functions TT, TC and TS as functions of thickness T in the energy range 15-30 keV for $_{22}$Ti

# ANNEX

## Text of MUF programme in ALGOL-60

```
001:  BEGIN REAL EN,EV,AT,AT1,AC,AC1,AS,AVR,AVC,AVS,
002:  R,AB1,BI1,BI2,ER,ER1,RAD;
003:  INTEGER NB,MM,DM,SM,NB1,NB2,I,J,K,KN,KM,
004:  M,D,S,ASM,NU,NUM,ISP,P,PM,Q,KB;
005:  COD('R10-2',KB);
006:  F9:COD('R10-2',AB1,R,NB,MM,DM,SM,PM,NUM,RAD);
007:  BEGIN ARRAY EG[1:ABS(DM)],E0,GAN,GAG,KAR0[1:ABS(NB)],
008:  TIL[1:ABS(SM)],E,SIT,SIC[-100:100],CKT,SKT,
009:  SKT2[1:ABS(SM)],RKT[1:ABS(SM),1:ABS(MM)],
010:  SP,AB,G,SU1,SU2[1:ABS(NUM)];
011:  COMMENT DO 'EG'26'E0''GAN''GAG''KAR0'100'TIL'7
012:  'CKT''SKT''SKT2'7'RKT'42'SP''AB''G''SU1''SU2'50;
013:  BEGIN INTEGER ARRAY MNU[1:ABS(NB)],L[1:ABS(NUM)];
014:  COMMENT DO 'MNU'100'L'50;
015:  COD('R10-2',EG,E0,GAN,GAG,MNU,AB,G,L,TIL);
016:  FOR NU:=1 STEP 1 UNTIL ABS(NUM) DO BEGIN
017:  SP[NU]:=AB[NU];AB[NU]:=ABS(AB[NU]) END ;D:=1;
018:  F5:P:=0; FOR NU:=D+1 STEP 1 UNTIL ABS(NUM) DO
019:  BEGIN IF SP[NU]≠0 THEN BEGIN
020:  IF AB[NU]≠AB[D] THEN BEGIN P:=P+1;
021:  IF P=1 THEN M:=NU END ELSE SP[NU]:=0 END END ;D:=M;
022:  IF P>0 THEN GOTO F5;
023:  COD('P2-10',AB1,NB,NUM,MM,SM,R);
024:  P:=0, FOR NU:=1 STEP 1 UNTIL ABS(NUM) DO
025:  IF SP[NU]<0 THEN P:=P+1;
026:  IF PM<0 THEN PM:=-50;
```

```
027:   BEGIN ARRAY EX,EO[-1:1],ESP[1:10],SPOT[1:P,1:10],
028:  TOL,TT,TC,TS[1: IF PM<0 THEN 50 ELSE PM];
029:   COMMENT DO 'SPOT'30'TOL''TT''TC''TS'50;
030:   IF P<>0 THEN INOUT('R10-2',ESP,SPOT);
031:   IF PM>0 THEN COD('R10-2',TOL);
032:  BI1:=2.197@-4*RAD; FOR I:=1 STEP 1 UNTIL ABS(NB) DO
033:   BEGIN NU:=NNU[I];P:=ENTIER(AB[NU]);
034:  KARO[I]:=BI1*SQRT(ABS(EO[I]))*(.55+P*.3333)
035:  /(1+1/P);AB1:=KARO[I]↑2;
036:   IF L[NU]=1 THEN KARO[I]:=KARO[I]*AB1/(1+AB1);
037:   IF L[NU]=2 THEN
038:  KARO[I]:=KARO[I]*AB1↑2/(9+3*AB1+AB1↑2) END ;
039:  NB2:=1;O[1]:=EG[1];
040:   FOR D:=1 STEP 1 UNTIL ABS(DM)-1 DO
041:   BEGIN EN:=EG[D];AVR:=AVC:=AVS:=AT:=AC:=AS:=ER:=0;
042:   IF DM>0 THEN BEGIN ASM:=ABS(SM);
043:   FOR S:=1 STEP 1 UNTIL ASM DO BEGIN
044:  CKT[S]:=SKT[S]:=SKT2[S]:=0;
045:   FOR M:=1 STEP 1 UNTIL ABS(MM) DO
046:  RKT[S,M]:=0 END END ;
047:   FOR P:=1 STEP 1 UNTIL ABS(PM) DO
048:  TT[P]:=TC[P]:=TS[P]:=0;
049:  P:=NB2-1;EX[0]:=-1;
050:   FOR P:=P+1 WHILE EO[P]<EG[D+1] DO BEGIN
051:   IF P>ABS(NB) THEN GOTO F3;
052:   IF EO[P]>EN THEN BEGIN NU:=NNU[P];
053:  ISP:=ENTIER(AB[NU]);BI1:=(AB[NU]-ISP)*10;
054:  BI2:=BI1*G[NU]*GAN[P]/EO[P]↑2;AVR:=AVR+BI2;
055:  AVC:=AVC+BI2/(1+GAN[P]/GAG[P]) END END ;
```

```
056:  F3:NB1:=NB2; FOR I:=NB2,I+1 WHILE EV<EG[D+1] DO
057:   BEGIN REAL GN,GA,SU,SIT1,KAR,SP0,SP1;
058:  BI1:=(AB[MNU[I]]-ENTIER(AB[MNU[I]]))*10;
059:  D[-1]:=D[1]; IF I<ABS(NB) THEN BEGIN
060:  GA:=GAN[I]*GAG[I];GN:=GAN[I+1]*GAG[I+1];
061:  BI2:=(AB[MNU[I+1]]-ENTIER(AB[MNU[I+1]]))*10;
062:  EV:=(E0[I+1]*GA*BI1+E0[I]*GN*BI2)/
063:  (GA*BI1+GN*BI2) END ELSE EV:=EG[D+1];
064:   IF EV>EG[D+1] THEN EV:=EG[D+1];
065:   IF EV<D[1] THEN BEGIN NB2:=NB2+1; GOTO F3 END ;
066:  D[1]:=EV;NB2:=1;K:=KN:=0;KM:=1;E[0]:=E0[1];Q:=-1;
067:   IF D[-1]>E[0] THEN BEGIN E[0]:=D[-1];Q:=1 END ;
068:   IF D[1]<E[0] THEN BEGIN E[0]:=D[1];KM:=0 END ;
069:  F1: FOR NU:=1 STEP 1 UNTIL ABS(NUM) DO
070:   BEGIN SU1[NU]:=SU2[NU]:=0 END ;
071:  BI1:=2.197@-4*RAD*SQRT(E[K]);
072:   FOR J:=1 STEP 1 UNTIL ABS(NB) DO
073:   BEGIN NU:=MNU[J];P:=ENTIER(AB[NU]);
074:  KAR:=BI1*(.55+P↑.33333)/(1+1/P);AB1:=KAR↑2;
075:   IF L[NU]=1 THEN KAR:=AB1/(1+AB1)*KAR;
076:   IF L[NU]=2 THEN KAR:=AB1↑2/(9+3*AB1+AB1↑2)*KAR;
077:  GN:=GAN[J]*KAR/KAR0[J];KAR:=(E0[J]-E[K])*2/GAG[J];
078:  SU:=GN/(GAG[J]*(1+KAR↑2));
079:  SU1[MNU[J]]:=SU+SU1[MNU[J]];
080:  SU2[MNU[J]]:=SU*KAR+SU2[MNU[J]] END ;
```

```
081:  SIT[K]:=SIC[K]:=0;ISP:=1;B12:=2009m3/E[K];
082:   FOR NU:=1 STEP 1 UNTIL ABS(NUM) DO
083:   BEGIN P:=ENTIER(AB[NU]);
084:  AB1:=(AB[NU]-P)*10;SIT1:=B12*AB1*(1+1/P)↑2;
085:  KAR:=B11*(.55+P↑.33333)/(1+1/P);
086:  SPO:=KAR-ARCTAN(KAR);SPI:=KAR-ARCTAN(3*KAR/(3-KAR↑2));
087:   IF SP[NU]>0 THEN
088:  SP[NU]:=SIT1*(SIN(KAR)↑2+3*SIN(SPO)↑2+5*SIN(SPI)↑2);
089:   IF SP[NU]<0 THEN BEGIN SP[NU]:=0;
090:   FOR P:=2 STEP 1 UNTIL 10 DO BEGIN
091:   IF ESP[P]≥E[K] THEN BEGIN
092:  SP[NU]:=((ESP[P]-E[K])*SPOT[ISP,P-1]
093:  *(E[K]-ESP[P-1])*SPOT[ISP,P])
094:  /(ESP[P-1]-ESP[P])*AB1*SP[NU] END END ;
095:  ISP:=ISP+1 END ;
096:   IF L[NU]=1 THEN KAR:=SPO;
097:   IF L[NU]=2 THEN KAR:=SPI;
098:  KAR:=2*KAR;SIT1:=SIT1*G[NU];
099:  SIT1:=SIT1/((1+SU1[NU])↑2+SU2[NU]↑2);
100:  SIT[K]:=SIT[K]+SIT1*((SU1[NU]+SU1[NU]↑2+
101:  SU2[NU]↑2)*COS(KAR)-SU2[NU]*SIN(KAR));
102:  SIC[K]:=SIC[K]+SIT1*SU1[NU] END ;
103:  SPO:=0; FOR NU:=1 STEP 1 UNTIL ABS(NUM) DO
104:  SPO:=ABS(SP[NU])+SPO;SIT[K]:=SIT[K]+SPO;
105:   IF EX[0]<0 THEN BEGIN
106:  EX[0]:=4.0982m6/LN(EG[D+1]/EG[D]);
107:  AVR:=AVR+EX[0];AVC:=AVC+EX[0];AVS:=AVR-AVC;
108:  COD('P2-10',AVR,AVC,AVS);EX[0]:=1/(3276A*AVR+SPO) END ;
```

```
109:   IF K≠0 THEN BEGIN REAL ER2,AT2,AC2,DE,
110:  TOT1,TOT2,SS1,SS2,TT1,TT2;
111:   IF ABS(K)=1 THEN BEGIN
112:  ER1:=E[0]↑R;AT1:=SIT[0]•ER1;AC1:=SIC[0]•ER1;
113:   IF PM<0 THEN BEGIN
114:  EX[-1]:=EXP(-SIT[0]•EX[0]•.75);
115:  EX[1]:=EXP(-SIT[0]•EX[0]);TOL[1]:=EX[-1]•ER1;
116:  TOL[2]:=EX[1]•ER1;S:=-1;
117:   FOR P:=3 STEP 1 UNTIL 50 DO BEGIN
118:  TOL[P]:=TOL[P-2]•EX[S];EX[S]:=EX[S]↑2;S:=-S
119:   END END END ;
120:  DE:=(E[K]-E[K-Q])•G/2;ER2:=E[K]↑R;
121:  AT2:=SIT[K]•ER2;AC2:=SIC[K]•ER2;
122:  AT:=(AT1+AT2)•DE+AT;AC:=(AC1+AC2)•DE+AC;
123:  AS:=(AT1-AC1+AT2-AC2)•DE+AS;ER:=(ER1+ER2)•DE+ER;
124:   IF PM<0 THEN BEGIN
125:  EX[-1]:=EXP(-SIT[K]•EX[0]•.75);
126:  EX[1]:=EXP(-SIT[K]•EX[0]);S:=-1;
127:   FOR P:=1 STEP 1 UNTIL 50 DO BEGIN
128:  TT[P]:=TT[P]+(TOL[P]•EX[S]•ER2)•DE;
129:  TC[P]:=TC[P]+(TOL[P]•SIC[K-Q]•EX[S]•SIC[K]•ER2)•DE;
130:  TS[P]:=TS[P]+(TOL[P]•(SIT[K-Q]-SIC[K-Q])•
131:  EX[S]•(SIT[K]-SIC[K])•ER2)•DE;TOL[P]:=EX[S]•ER2;
132:  EX[S]:=EX[S]↑2;S:=-S END END ;
```

```
133:   IF PM>0 THEN BEGIN
134:   FOR P:=1 STEP 1 UNTIL PM DO BEGIN
135:  TT1:=EXP(-SIT[K-Q]*TOL[P])*ER1;
136:  TT2:=EXP(-SIT[K]*TOL[P])*ER2;
137:  TT[P]:=(TT1*TT2)*DE+TT[P];
138:  TC[P]:=(SIC[K-Q]*TT1+SIC[K]*TT2)*DE+TC[P];
139:  TS[P]:=((SIT[K-Q]-SIC[K-Q])*TT1+
140:  (SIT[K]-SIC[K])*TT2)*DE+TS[P] END END ;
141:   IF DM>0 THEN BEGIN
142:   FOR S:=1 STEP 1 UNTIL ASM DO BEGIN
143:  TOT1:=SIT[K-Q]*TIL[S];TOT2:=SIT[K]*TIL[S];
144:  SS1:=(AT1-AC1)/TOT1;SS2:=(AT2-AC2)/TOT2;
145:  CKT[S]:=(AC1/TOT1+AC2/TOT2)*DE+CKT[S];
146:  SKT[S]:=(SS1+SS2)*DE+SKT[S];
147:  SKT2[S]:=(SS1/TOT1+SS2/TOT2)*DE+SKT2[S];
148:  SS1:=SS2:=1;
149:  ISP:=ABS(MM); IF TOT1+TOT2<MM-3 THEN ISP:=2;
150:   FOR M:=1 STEP 1 UNTIL ISP DO
151:   BEGIN SS1:=SS1/TOT1;SS2:=SS2/TOT2;
152:  RKT[S,M]:=(ER1*SS1+ER2*SS2)*DE+RKT[S,M] END
153:   END END ;ER1:=ER2;AT1:=AT2;AC1:=AC2 END ;
```

```
154:  F:K:=K+Q; IF ABS(K)=1 THEN BEGIN
155:  D[0]:=GA/32; IF (Q*E[0]+C[0])>D[Q]*Q THEN
156:   BEGIN E[K]:=D[Q]; GOTO F1 END ;
157:  E[K]:=E[C]+D[0]*Q; GOTO F1 END ;
158:   IF ABS(SIT[K-2*Q]/SIT[K-Q]-1)<.1 THEN
159:   BEGIN IF 2*D[C]<(D[Q]-E[K-Q])*Q THEN
160:   BEGIN D[C]:=2*D[C]; IF C[C]>GA THEN
161:   BEGIN IF Q*(D[Q]-E[K-Q])/GA<(100-ABS(K)) THEN
162:  D[0]:=GA ELSE C[C]:=Q*(C[C]-E[K-Q])/(100-ABS(K))
163:   END END END ;
164:   IF (Q*E[K-Q]+D[C])<D[Q]*Q THEN
165:   BEGIN E[K]:=E[K-Q]+Q*D[C]; GOTO F; END ;
166:   IF E[K-Q]≠D[Q] THEN BEGIN F[K]:=D[Q]; GOTO F1 END ;
167:   IF Q<0 THEN BEGIN Q:=1;KM:=K+1;
168:   IF KM>0 THEN BEGIN
169:  K:=0; GOTO F END ;K:=1 END ;KM:=K-1;
170:   IF NB<0 THEN
171:   BEGIN INTEGER BO; ARRAY BON[KN:KM];
172:   COMMENT DC 'BON'20];
173:   FOR BO:=KN STEP 1 UNTIL KM DO BON[BO]:=E[BO];
174:  COD('P2-10',BON);
175:   FOR BO:=KN STEP 1 UNTIL KM DO BON[BO]:=SIT[BC];
176:  COD('P2-10',BON);
177:   FOR BO:=KN STEP 1 UNTIL KM DO BON[BO]:=SIC[BC];
178:  COD('P2-10',BON) END END ;
```

```
179:   BEGIN ARRAY BOT[1:10];
180:  BOT[1]:=EN;BOT[2]:=EV;BOT[3]:=ER;BOT[4]:=LN(EV/EN);
181:  BOT[5]:=AT/ER;BOT[7]:=AC/ER;BOT[9]:=AS/ER;
182:  BOT[6]:=BOT[8]:=BOT[10]:=0;
183:   IF PM<0 THEN BEGIN TOL[1]:=EX[0]*.75;TOL[2]:=EX[0];
184:   FOR P:=3 STEP 1 UNTIL 50 DO
185:  TOL[P]:=2*TOL[P-2] END ;
186:   IF PM>0 THEN BEGIN
187:   FOR P:=1 STEP 1 UNTIL ABS(PM) DO BEGIN
188:  TT[P]:=TT[P]/ER;TC[P]:=TC[P]/AC;
189:  TS[P]:=TS[P]/AS END ;
190:  COD('P2-10',BOT,TOL,TT,TC,TS) END ;
191:   IF DM>0 THEN BEGIN
192:   ARRAY CB,SB,SB2,TRB,FC,FS,FS2,FT[1:ASM];
193:   COMMENT DO 'CB''SB''SB2''TRB''FC''FS''FS2''FT'7;
194:   FOR S:=1 STEP 1 UNTIL ASM DO
195:   BEGIN CB[S]:=CKT[S]/RKT[S,1];
196:  SB[S]:=SKT[S]/RKT[S,1];
197:  SB2[S]:=SKT2[S]/RKT[S,2];
198:  TRB[S]:=RKT[S,1]/RKT[S,2]-TIL[S];
199:  FT[S]:=TRB[S]/BOT[5];FC[S]:=CB[S]/BOT[7];
000:  FS[S]:=SB[S]/BOT[9];FS2[S]:=SB2[S]/BOT[9] END ;
001:  BOT[6]:=FT[1]*BOT[5];
002:  BOT[8]:=FC[1]*BOT[7];
003:  BOT[10]:=FS[1]*BOT[9];
004:  COD('P2-10',BOT,TIL,FC,FS,FS2,FT,RKT) END END ;
005:   END ;COD('P2-10',EG,E0,GAM,GAC,HNU,AB,G,L,RAD)
006:   END END ;KB:=KB-1;
007:   IF KB>0 THEN GOTO F9
008:   END END ;
```

REFERENCES

[1] ABAGYAN, L.P., NIKOLAEV, M.N., PETROVA, L.V., URAN-programma rasčeta sečenij i koefficientov gomogennoj rezonansnoj samoekranirovki v oblasti razrešennyh rezonansov (The URAN programme for calculating cross-sections and homogeneous resonance self-shielding coefficients in the region of resolved resonances), Bulletin of the Information Centre for Nuclear Data, issue III, Atomizdat, Moscow (1966) 418.

[2] ABAGYAN, L.P., NIKOLAEV, M.N., PETROVA, L.V., Rasčet sečenij urana-238 po programme URAN (Calculation of uranium-238 cross-sections by means of the URAN programme), Bulletin of the Information Centre for Nuclear Data, issue IV, Atomizdat, Moscow (1967) 392.

[3] LUKYANOV, A.A., Približennaja mnogourovnevaja model nejtronnyh sečenij v rezonansnoj oblasti (Approximate multilevel model of neutron cross-sections in the resonance region), preprint FEI-124 published by the Institute of Physics and Power Engineering, Obninsk (1968).

[4] WEISSKOPF, V.F., The theoretical prediction of the neutron cross-sections of non-fissionable elements for energies up to 10 MeV, paper P/830 presented at First International Conference on the Peaceful Uses of Atomic Energy, Geneva (1955).

[5] GARRISON, J.D., A study of teo-level interference in neutron cross-sections, Ann. of Phys. 50 (1968) 355.

[6] GOLDBERG, M.D., MUGHABGHAB, S.F., MAGURNO, B.A., MAY, V.M., Neutron cross-sections, vol. 11 A Z=21 to 40, BNL-325, Second Editions, Supplement No. 2 (1966).

[7] ROHR, G., FRIEDLAND, E., A study of neutron resonances of vanadium and manganese, Nucl. Phys. A104, 1 (1967).